

### Summary.

The importance of the study of the reaction kinetics of transition metal complexes with gases in solution is discussed. Apparatus designed for following the kinetics of gas uptake, changes in absorption spectra and pH of the solution is described. Possible improvements are suggested.

Four transition metal complex / gas systems were selected for kinetic studies on the grounds of their potential use as biological model systems or in the generation of industrially useful homogeneous catalysts.

The uptake of oxygen by aqueous solutions containing 1, 2-diaminoethane and various cobalt (II) salts is shown to be rapid. The reagents interact in the stoichiometric ratios of 1 : 5 : 2 respectively to give  $[(en)_2Co\mu O_2\mu en Co(en)_2]^{4+}$ . This compound slowly equilibrates with  $[(en)_2Co\mu O_2\mu OH Co(en)_2]^{3+}$  while it may be oxidised to  $[(en)_2Co\mu O_2\mu en Co(en)_2]^{5+}$ . These compounds were examined by physical techniques. Solutions of the  $\mu$ -peroxo species were shown to react with gaseous carbon dioxide to yield  $[Co(en)_2CO_3]^+$ .

The reaction between oxygen and manganese (II) complexes of N, N' - disalicylaldehyde - 1, 3 - propanediimine was studied in various solvents. The reagent complexes and their various oxygen adducts were examined by physical techniques and are believed to be oligomeric or polymeric.

The kinetics of the reduction of  $[Rh^{III}(L)_2Cl_2]^+$  cations (where L is bipyridyl, phenanthroline or their substituted derivatives) in alkaline ethanolic solution at 60°C under a hydrogen atmosphere

were investigated by following the rate of  $[\text{Rh}^{\text{I}}(\text{L})_2]^+$  production spectrophotometrically and the rate of 1 : 1 hydrogen uptake.

An autocatalytic mechanism with hydrogen gas acting as reducing agent, is suggested.

The rhodoxime (III) complexes  $\text{H} [\text{Rh}^{\text{III}}(\text{DMG})_2\text{Cl}_2]$  and  $[\text{Rh}^{\text{III}}(\text{DMG})_2 \text{P Ph}_3 \text{Cl}]$  and their reduction products were investigated by physical techniques. The kinetics of the reduction of  $\text{H} [\text{Rh}^{\text{III}}(\text{DMG})_2\text{Cl}_2]$  in alkaline ethanolic solution under a nitrogen atmosphere were investigated by following the rate of  $\text{H} [\text{Rh}^{\text{I}}(\text{DMG})_2]$  production spectrophotometrically. The reaction mechanism proved to be autocatalytic.

This work was carried out between 1968 and 1971

at the University of Aston in Birmingham .

It has been done independently and

has not been submitted for any other degree.

*F. D. Oliver*

F. D. OLIVER.

Acknowledgments.

I wish to express my sincere thanks to Dr. J.D. Miller for his supervision.

I should also like to thank Dr. W. R. McWhinnie and Dr. A. W. Downs for many helpful discussions.

My thanks go also to Mr. W. E. Sabin for making the glassware, to Mr. E. J. Hartland for the preparation of N. M. R. spectra, to Mr. L. Parker for his metalwork, to Mr. M. C. Perry for the preparation of infra-red spectra, to Mrs. V. M. Clenton and Mrs. P. M. Evans for their help with ultra-violet spectroscopy, to Mr. M. J. Houghton for the preparation of mass spectra and to Mrs. B. Taylor for performing the elemental analyses.

I am most grateful to Miss. P. J. Oliver for typing the manuscript.

Finally, I am indebted to the University of Aston for a research assistantship.

Contents.

		Page Number
Chapter I	Introduction .	1 - 14
Chapter II	Experimental .	15 - 45
Chapter III	The Uptake of Gaseous Oxygen by Aqueous Solutions Containing Cobalt Ions and Diaminoethane .	46 - 64
Chapter IV	A Study of the Reaction between Oxygen and Manganese (II) Complexes of N, N'-Disalicylaldehyde - 1, 3 - Propanediimine ,	65 - 81
Chapter V	The Kinetics of the Autocatalytic Reduction of cis- Dichlorobis-(2, 2' bipyridyl) Rhodium (III) Nitrate Dihydrate in Alkaline Ethanolic Solution under a Hydrogen Atmosphere.	82 - 109
Chapter VI	The Kinetics of the Autocatalytic Reduction of Monohydrogen Dichlorobis (dimethylglyoximato) Rhodium (III) in Alkaline Ethanolic Solution under a Nitrogen Atmosphere .	110 - 128
Chapter VII	Conclusion .	129 - 136
Appendix 1	Conductivity Data .	137
Appendix 2	Rate Data for the Kinetics of Conversion of (B) to (C).	138 - 139
Appendix 3	Temperature Dependence of the Rate of Reduction of cis-Dichlorobis-(bipyridyl) Rhodium(III) Nitrate Dihydrate in 25% Ethanol / Water.	140
Appendix 4	Hydroxide Dependence of the Rate of Reduction of cis-Dichlorobis-(bipyridyl) Rhodium(III) Nitrate Dihydrate in 25% Ethanol / Water .	141
Appendix 5	Ionic Strength Dependence of the Rate of Reduction of cis-Dichlorobis-(bipyridyl) Rhodium(III) Nitrate Dihydrate in 25% Ethanol / Water .	142
Appendix 6	Ethanol Dependence of the Rate of Reduction of cis-Dichlorobis-(bipyridyl) Rhodium(III) Nitrate Dihydrate in 25% Ethanol / Water.	143

Appendix 7	Temperature Dependence of the Rate of Reduction of trans-Monohydrogen Dichlorobis(dimethylglyoximate)Rhodium(III) in 25% Ethanol / Water.	144
Appendix 8	Hydroxide Dependence of the Rate of Reduction of trans-Monohydrogen Dichlorobis(dimethylglyoximate)Rhodium(III) in 25% Ethanol / Water.	145
Appendix 9	ZRH SIMPLIFY	146
Appendix 10	ZRH KINETICS	147
Bibliography		148 - 156

### Figures.

Figure 1(a)	Some Homogeneous Reactions of Olefins Catalysed by Transition Metal Complexes.	2
1(b)	Coordination Numbers of some Transition Metal Complexes.	2
Figure 2	Species of Related Configurations and Reactivities in Organic and Coordination Chemistry.	4
Figure 3	Generalised Reaction Scheme for the Uptake of Oxygen by Transition Metal Complexes.	7
Figure 4	Apparatus for Following the Kinetics of Gas Absorption or Evolution.	15
Figure 5	Micro Hydrogenation Apparatus HR - 100.	17
Figure 6	Macro Hydrogenation Apparatus HR - 160.	18
Figure 7	Reaction Vessel.	20
Figure 8(a) and 8(b)	Apparatus for Following the Kinetics of Reduction of Rhodium (III) Complexes by Spectrophotometry.	22 - 23
Figure 9	Automatic Titration System.	25
Figure 10	Apparatus for the Isolation of Air Sensitive Complexes.	35
Figure 11	Graph of Molar Conductivity against Square Root of Concentration.	50
Figure 12	E. S. R. Spectrum of $[(en)_2Co \mu O_2 \mu enCo(en)_2]^{5+}$ .	52

Figure 13(a) and 13(b)	60 MHz N. M. R. Spectra with T.M.S. as External Standard.	54 - 55
Figure 14	Graph Showing the Relative Ratios and Stoichiometry of Oxygen Uptake of Mixtures containing Co : en : OH ratios of 1:2.5:0.5 and 1 : 2 : 0.5.	57
Figure 15	Graph of $\log_{10} \left\{ \frac{1}{(1 + K) \frac{Bt}{B_0} - 1} \right\}$ against Time .	59
Figure 16	Graph of pH against ml of 0.0195 N NaOH <sub>aq</sub> added.	61
Figure 17	Ultra Violet and Visible Spectra in Solution .	67
Figure 18	Diffuse Reflectance Spectra of solids between 45,000 and 10,000 cm <sup>-1</sup> .	68
Figure 19(a)	Arrangement of Ligand when one Ligand Molecule Bridges Two Metal Ions .	70
19(b)	Possible Structure of a Polymeric Oxygenated Product .	70
Figure 20	Relationship, Empirical Formulae and Symbols used for Products Discussed in Chapter IV.	72
Figure 21(a)	Infra-Red Spectra of salpn, Mn(salpn)H <sub>2</sub> O and Oxygen Adducts C, D, H and E (Nujol Müll).	74
21(b)	Infra-Red Spectra of Benzene, Pyridine and Mn Py <sub>2</sub> Cl <sub>2</sub> .	75
Figure 22(a)	Ultra Violet Spectra of $[\text{Rh}^{\text{III}}(\text{bipy})_2\text{Cl}_2]^+$ salts .	
22(b)	Absorption Maxima in the Visible of Various Rhodium(I) Complexes and Corresponding Extinction Coefficients .	84
Figure 23	Specimen Graph of Optical Density at 557 nm Against Time in Minutes Showing Computer Fits .	86
Figure 24	Graphical Differentiation of a Typical Rate Plot for the Autocatalytic Reduction of cis-Dichloro-bis (2, 2' bipyridyl) Rhodium(III) Nitrate Dihydrate .	88
Figure 25	Graph of $\log_{10} k_{\text{obs}}$ against $\frac{1}{T}$ .	90
Figure 26	Graph of $\frac{[\text{OH}^-]}{k_{\text{obs}}}$ against $[\text{OH}^-]$ .	92

Figure 27	Graph of $\log_{10} k_{\text{obs}}$ against $I^{\frac{1}{2}}$ .	94
Figure 28	Graph of $\log_{10} k_{\text{obs}}$ against $\log_{10} [\text{EtOH}]$ .	96
Figure 29	Graph of % Reaction Against Time Obtained by Following the Increase in Optical Density at 458 nm and 575 nm.	115
Figure 30	Specimen Graph of Optical Density at 575 nm Against Time in Minutes Showing Computer Fit.	117
Figure 31	Graphical Differentiation of a Typical Rate Plot for the Autocatalytic Reduction of Monohydrogen Dichlorobis (dimethylglyoximato) Rhodium(III).	119
Figure 32	Graph of $\log_{10} k_{\text{obs}}$ against $\frac{1}{T}$ .	121
Figure 33	Graph of $\log_{10} k_{\text{obs}}$ against $-\log_{10} [\text{OH}^-]$ .	123
Figure 34	Improved Reaction Vessel for the Spectrophotometric System.	131

Abbreviations.

acac	acetylacetonate.
amp	2-(aminomethyl)pyridine.
A. R.	analytical reagent grade.
bae	N, N'-ethylenebis (acetylacetonateiminato).
bipy	2, 2'-bipyridyl.
depe	1, 2 -bisdiethylphosphinoethane.
D	dimethyl glyoxime dianion.
dien	diethylenetriamine.
diphos	bis(diphenyl phosphino)ethane.
DMG } DH }	dimethyl glyoxime monoanion .
(DO)(DOH)pn	diacetyl monoxime imino-diacetyl-monoximato imino propane.
E. D. T. A.	ethylenediamine tetracetate.
en	ethylenediamine .
E. S. R.	Electron Spin Resonance.
Et	ethyl .
hist	histamine.
I. R.	infra-red.
L	ligand.
Me	methyl.
N. M. R.	Nuclear Magnetic Resonance.
Ph	phenyl.
phen	1, 10 - phenanthroline.
py	pyridine.
R	alkyl or aryl group.
salen	N, N' - ethylenebis(salicylideneiminato).

7, 7'-(CH <sub>3</sub> ) <sub>2</sub> -salen	N, N' ethylenebis(7, 7'-dimethyl-salicylideneiminato).
saloph	o-phenylene-bis(salicylideneiminato).
salpn	N, N'-( $\gamma$ , $\gamma'$ di-n-propylamine) bis (salicylideneiminato).
T.H.F.	tetrahydrofuran.
trien	triethylenetetramine.
X	halogen or pseudohalogen.

Symbols.

$\epsilon$	molar extinction coefficient (litre mole <sup>-1</sup> cm <sup>-1</sup> )
$\bar{e}$	electron .
$E^0$	redox potential.
$\bar{\nu}$	wave number (cm <sup>-1</sup> )
$\mu$	ionic strength.
$\mu_{\text{eff}}$	effective magnetic moment in Bohr magnetons.
$\chi_g$	gram magnetic susceptibility.
$\chi_M$	molar magnetic susceptibility.
$\chi_M^{\text{corr}}$	$\chi_M$ corrected for the diamagnetism of the ligands.

The Reaction Kinetics of Transition Metal Complexes with Gases  
in Solution.

Chapter I.  
Introduction.

A significant recent development in the field of homogeneous catalysis is the use of transition metal complexes to activate inert saturated molecules or to add to unsaturated molecules (1, 2, 3). These molecules may be saturated diatomic gases such as oxygen, hydrogen and nitrogen, unsaturated gases such as the lower alkenes and alkynes, carbon monoxide and nitric oxide or more complex saturated or unsaturated aliphatic or aromatic molecule derivatives. In most cases, coordination to the transition metal ion promotes reaction.

For example, the hydrogenation of olefins is catalysed by complexes of ruthenium, (4) cobalt, (5) rhodium, (6) iridium, (7) platinum (8) and other metals. The hydroformylation of olefins is catalysed by complexes of cobalt or rhodium; (Oxo Process) (9, 10) that of acetylenes by nickel carbonyl (Reppe Process) (11). Rhodium complexes (12) catalyse the dimerisation of ethylene and the polymerisation of dienes is catalysed by complexes of iron (13, 14) and rhodium (15). The isomerisation of olefins is catalysed by complexes of rhodium, (16, 17) palladium, (18) cobalt, (19) platinum (20) and other metals. In the Wacker Process, palladium chloride catalyses the oxidation of olefins to aldehydes, ketones and vinyl esters (21, 22). The hydration of acetylenes is catalysed by ruthenium trichloride (23) and rhodium trichloride (24) (see Figure 1(a)).

More recently, the conversion of alkyl isocyanides to isocyanates by oxygen, catalysed by nickel complexes, (25) the

Figure 1(a) (from reference (1) ).  
Some homogeneous reactions of olefins catalysed by transition metal complexes.

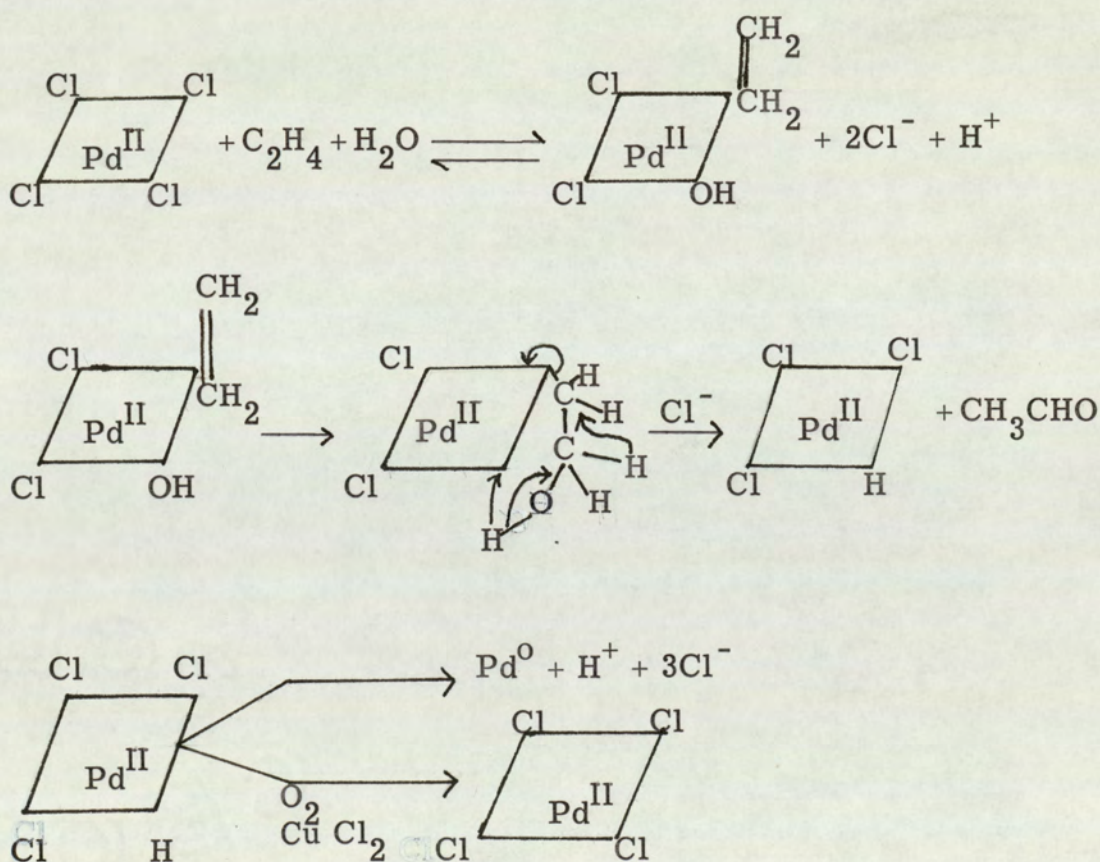
Reaction	Typical catalysts (L = PPh <sub>3</sub> )					
	Ru <sup>II</sup> d <sup>6</sup>	Co <sup>II</sup> d <sup>7</sup>	Fe <sup>0</sup>	Rh <sup>I</sup>	Ir <sup>I</sup> d <sup>8</sup>	Pt <sup>II</sup>
Hydrogenation	RuCl <sub>6</sub> <sup>4-</sup>	Co(CN) <sub>5</sub> <sup>3-</sup>	Fe(CO) <sub>5</sub>	RhClL <sub>3</sub>	IrI(CO)L <sub>2</sub>	Pt <sup>II</sup>
Hydroformylation	aRuCl <sub>2</sub> L <sub>4</sub>		CoH(CO) <sub>4</sub>	RhCl(CO)L <sub>2</sub>		aPt(SnCl <sub>3</sub> ) <sub>5</sub> <sup>3-</sup>
Double-bond migration			FeH(CO) <sub>4</sub> <sup>-</sup>	RhCl <sub>3</sub> (olefin) <sup>2-</sup>	PdCl <sub>4</sub> <sup>2-</sup>	aPt(SnCl <sub>3</sub> ) <sub>5</sub> <sup>3-</sup>
Dimerisation				RhCl <sub>2</sub> (C <sub>2</sub> H <sub>4</sub> ) <sub>2</sub> <sup>+</sup>	PdCl <sub>4</sub> <sup>2-</sup>	
Oxidation						
( <sup>a</sup> Active form of catalyst uncertain).						

Figure 1(b) Coordination Numbers of Some Transition Metal Complexes (from reference (1) ).

Coordination number	Examples	Electron configuration	Total number of valence electrons
8	Mo(CN) <sub>8</sub> <sup>3-</sup> , Mo(CN) <sub>8</sub> <sup>4-</sup>	d <sup>1</sup> , d <sup>2</sup>	17, 18
6	M(CN) <sub>6</sub> <sup>3-</sup> (M = Cr, Mn, Fe, Co)	d <sup>3</sup> , d <sup>4</sup> , d <sup>5</sup> , d <sup>6</sup>	15 - 18
5	Co(CN) <sub>5</sub> <sup>3-</sup> , Ni(CN) <sub>5</sub> <sup>3-</sup>	d <sup>7</sup> , d <sup>8</sup>	17, 18
4 (Square planar)	Ni(CN) <sub>4</sub> <sup>2-</sup>	d <sup>8</sup>	16
4 (Tetrahedral)	Cu(CN) <sub>4</sub> <sup>3-</sup> , Ni(CO) <sub>4</sub>	d <sup>10</sup>	18
2	Ag(CN) <sub>2</sub> <sup>-</sup> , Au(CN) <sub>2</sub> <sup>-</sup>	d <sup>10</sup>	14

hydrogenation of nitrobenzene to aniline, catalysed by cobalamins and borohydride (26) and the conversion of aliphatic and aralkyl amines to nitriles by molecular oxygen catalysed by ruthenium complexes (27) have been reported.

Several of these processes, for example the Oxo, Wacker and Reppe reactions have achieved considerable industrial importance. The study of the reaction kinetics and mechanisms operating in this field of catalysis is therefore of industrial interest (28, 29). Detailed kinetic, equilibrium and isotopic-tracer studies support the following mechanism for the Wacker Process (1, 21, 22).



The general principles which seem to underlie the catalytic activity of transition metal complexes are as follows. Most catalytic reactions involve transition metals at the right hand end of each transition series, notably Fe, Ru, Os, Co, Rh, Ir,

Figure 2. (From Reference (1) ).

Species of related configurations and reactivities in organic and coordination chemistry.

ORGANIC SPECIES		TRANSITION METAL COUNTERPART				
Species	C.N	N.B.E.	Characteristic reactions	C.N.	N.B.E.Examples	Reactions
Saturated molecule (R <sub>3</sub> C-X)	4	0	Substitution	6	RhCl <sub>6</sub> <sup>3-</sup>	RhCl <sub>6</sub> <sup>3-</sup> + H <sub>2</sub> O → RhCl <sub>5</sub> OH <sub>2</sub> <sup>2-</sup> + Cl <sup>-</sup> RhCl <sub>6</sub> <sup>3-</sup> + H <sub>2</sub> → RhHCl <sub>5</sub> <sup>3-</sup> + HCl
Free radical (R <sub>3</sub> C·)	3	1	Dimerisation			2Co(CN) <sub>5</sub> <sup>3-</sup> ⇌ Co <sub>2</sub> (CN) <sub>10</sub> <sup>6-</sup>
Carbene (R <sub>2</sub> C:)	2	2	Addition	4	IrI(CO)(PPh <sub>3</sub> ) <sub>2</sub>	Co(CN) <sub>5</sub> <sup>3-</sup> + CH <sub>3</sub> I → Co(CN) <sub>5</sub> I <sup>3-</sup> + CH <sub>3</sub> · 2Co(CN) <sub>5</sub> <sup>3-</sup> + CH ≡ CH → [(NC) <sub>5</sub> CoCH = CHCo(CN) <sub>5</sub> ] <sup>6-</sup>
Carbanion (R <sub>3</sub> C <sup>-</sup> )	3	2	Addition of Nucleophile	5	Mn(CO) <sub>5</sub> <sup>-</sup>	Mn(CO) <sub>5</sub> <sup>-</sup> + H <sup>+</sup> → Mn(CO) <sub>5</sub> H
Carbocation (R <sub>3</sub> C <sup>+</sup> )	3	0	Addition of Electrophile	5	Mn(CO) <sub>5</sub> <sup>-</sup>	Mn(CO) <sub>5</sub> <sup>-</sup> + H <sup>+</sup> → Mn(CO) <sub>5</sub> H
Carbocation (R <sub>3</sub> C <sup>+</sup> )	3	0	Addition of Nucleophile	5	Co(CN) <sub>5</sub> <sup>2-</sup>	Co(CN) <sub>5</sub> <sup>2-</sup> + I <sup>-</sup> → Co(CN) <sub>5</sub> I <sup>3-</sup>
Carbocation (R <sub>3</sub> C <sup>+</sup> )	3	0	Addition of Electrophile	5	Mn(CO) <sub>5</sub> <sup>-</sup>	Mn(CO) <sub>5</sub> <sup>-</sup> + H <sup>+</sup> → Mn(CO) <sub>5</sub> H

(C.N. = Coordination number .

N.B.E. = Nonbonding electrons.)

Ni, Pd, Pt. Such metal atoms have  $d^6$  to  $d^{10}$  configurations, predominantly  $d^8$  and are usually spin-paired. Since the stable coordination numbers of spin-paired transition metal complexes show, to a certain extent, an inverse dependence on the number of  $d$  electrons on the metal, subject to the '18 electron rule,' the complexes of the right hand side transition metals are more often able to accept additional ligands and increase their coordination number. ( See Figure 1(b) ).

This type of electronic configuration and coordination results in complexes with reactivities analogous to the reactive intermediates of organic chemistry. For example, five coordinate  $d^7$  transition metal complexes behave like  $R_3C^\cdot$  species and undergo analogous radical reactions; dimerisation, abstraction and addition. Four coordinate  $d^8$  species resemble  $R_2C:$  carbenes and undergo addition and insertion reactions. Five coordinate  $d^6$  complexes behave like  $R_3C^+$  carbonium ions and readily add to nucleophiles whereas five coordinate  $d^8$  species act as  $R_3C^-$  carbanions and add to electrophiles. ( See Figure 2 . )

Such complexes can therefore stabilise reactive intermediates by coordination, promote rearrangements of a coordinated gas molecule by alteration of their coordination number and assemble the reaction components within their coordination shells ( template and oligomerisation reactions. ) The complexes of the left hand side transition metals, which are "harder" and exist in higher oxidation states catalyse acid-base and redox reactions.

A second reason for the importance of kinetic studies in this field is the fact that certain transition metal complexes

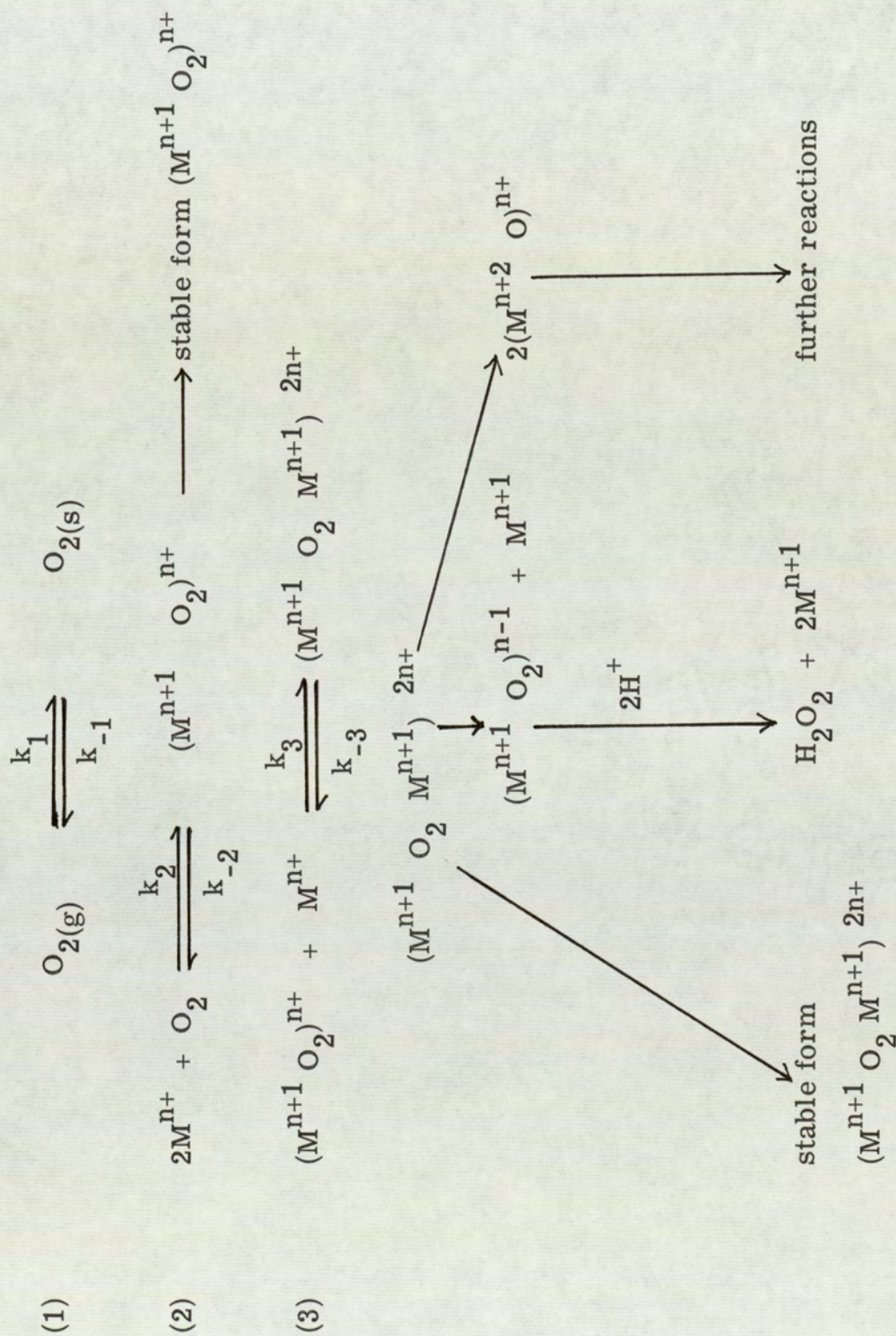
act as simple models for complex biological metallo-enzymes and proteins in their reactions with gases in solution.

For example, the biological oxygen carriers, whose prototype is haemoglobin, have complex structures consisting of protein and a transition metal-containing prosthetic group or groups. The reaction mechanisms of synthetic oxygen carriers, (30, 31) for example the cobalt complexes of amines, dipeptides, amino acids and Schiff bases (32, 33), Vaska's complex, (34) iron (II) and nickel (II) dimethylglyoxime complexes and the ruthenium (III) / E.D.T.A. complex in alkali, (35) are more easily investigated and help in understanding the biological process. In fact, studies on the reaction kinetics of oxygen uptake by various transition metal complexes (36) enable generalised reaction schemes such as that in Figure 3 to be postulated. The left hand route in Figure 3 is shown by certain  $\text{Co}^{\text{II}}$  complexes;  $(\text{M}^{\text{n}+1}\text{O}_2\text{M}^{\text{n}+1})^{2\text{n}+}$  and in some cases  $(\text{M}^{\text{n}+1}\text{O}_2)^{\text{n}+}$  may be isolated as stable forms, depending on the coordinating ligand. The central route is feasible for  $\text{Fe}^{3+}$  and  $\text{Pu}^{3+}$  in strong acid. When  $\text{M} = [\text{U}^{16}\text{OH}]^{3+}$  and  $^{18}\text{O}_2$  uptake occurs in  $^{16}\text{OH}_2$ , the product  $\text{U}^{16}\text{O}^{18}\text{O}^{2+}$  but no  $^{18}\text{OH}_2$  is obtained. This demonstrates  $^{18}\text{O}-^{18}\text{O}$  bond fission by the right hand side route. Similarly, when  $\text{M} = \text{Cr}^{2+}$ , O - O bond fission occurs to form  $[\text{Cr}^{\text{IV}}\text{O}]^{2+}$  which undergoes further reactions forming  $[\text{CrOCr}]^{4+}$  and chain species.

The bonding in transition metal complexes with molecular oxygen arises from overlap of an empty metal orbital of suitable energy and symmetry with a filled oxygen  $\pi$  bonding orbital forming a  $\sigma$  bond. Electron density is back donated into the  $\pi^*$  orbitals of oxygen from a non-bonding metal d orbital.

Study of the synthetic oxygen carriers has shown the conditions necessary for reversible oxygen bonding. Firstly,

Figure 3. (See Reference (36) ).



the transition metal ion must be capable of existence in two oxidation states so that a redox equilibrium is established. Secondly, the redox potential of the oxidised form must be positive so that oxygen uptake occurs, but within a certain range controlled by the ligands and the nature of the transition metal. Too strong a donation of electrons by the ligands results in irreversible oxidation of the transition metal ion, for example  $\text{Co}^{\text{II}}(\text{en})_3$ . On the other hand, the presence of oxygenic groups such as E.D.T.A. reduces the readiness to form stable adducts with oxygen.

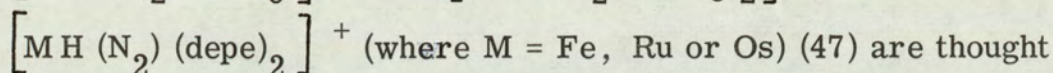
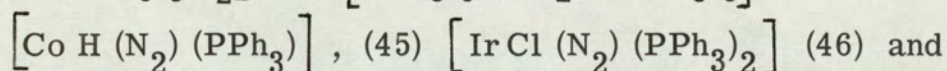
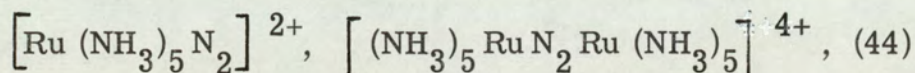
Fallab (36) states that the transition metal ion must be coordinated to at least three nitrogen ligand atoms to promote combination with oxygen. The extent of back-bonding to oxygen is determined by the degree of orbital overlap, largely controlled by the nature of the transition metal. For example, in complexes of type  $[\text{M}(\text{O}_2)(\text{diphos})_2]\text{PF}_6$  (37) where M is rhodium or iridium, the higher d orbital energy of rhodium compared to iridium results in less back donation to oxygen in the rhodium complex. The rhodium complex combines reversibly with molecular oxygen whereas the iridium complex is irreversibly oxidised (37).

Study of the reaction kinetics of transition metal complexes with nitrogen is of relevance to the elucidation of the mechanism of biological nitrogen fixation and in developing potential catalytic systems to supersede the Haber Process (38, 39).

Many attempts have been made to fix nitrogen by using transition metal complexes and powerful organometallic reducing agents in aprotic solvents. Nitrogen coordinated to the transition metal site is reduced to nitride, by donation of 6 electrons into the lowest vacant antibonding orbitals, then hydrolysed to give low yields of ammonia non-catalytically. For example, Vol'pin and Shur used the bis-cyclopentadienyl titanium dichloride / ethylmagnesium bromide system in ether under nitrogen (40, 41).

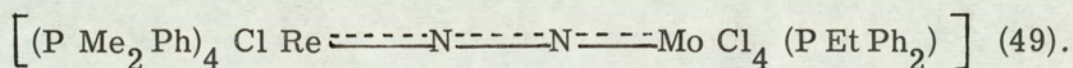
Van Tamelen and co-workers passed nitrogen through the strongly reducing system obtained by the reduction of diisobutoxy titanium dichloride with metallic potassium in dry tetrahydrofuran. The issuing nitrogen contained a low concentration of ammonia (42, 43).

The stable complexes of molecular nitrogen for example



are thought to be more valid as models for the biological nitrogenase, an Fe and Mo containing metalloenzyme. The iron or molybdenum active site of the protein is thought to pick up molecular nitrogen. Synergic bonding to nitrogen by a drift of electrons from nitrogen's weakly bonding  $3\sigma_g$  orbitals and back donation of d orbital electrons from the metal into the antibonding  $\pi^*$  orbitals of nitrogen weakens the nitrogen to nitrogen bond rendering it electrically asymmetric, thereby promoting hydrogenation to ammonia by the reducing agents existing in vivo. Originally, the reducing agent was thought to be a molybdenum or iron hydride species.

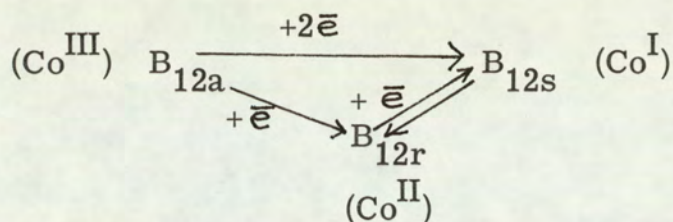
However, in view of the difficulty of reducing these stable molecular nitrogen complexes, which contain relatively strong metal nitrogen bonds, although the nitrogen nitrogen bond strength is decreased, current research is becoming centred on the nitrogen complexes of the left hand side transition metals. These metals, being "harder" and existing in higher oxidation states, readily accept electrons from nitrogen's  $3\sigma_g$  orbitals but show less back-bonding tendency. This results in weaker metal to nitrogen bonds and less stable nitrogen complexes from which the nitrogen should be more readily removed on reduction, for example the complex trans  $\left[ \text{Mo} (\text{diphos})_2 (\text{N}_2)_2 \right]$  (48). More notable binuclear complexes include :-



In this model complex, the low spin closed shell Re (I) (thought to be analogous to enzymic Fe (II)) pushes electrons from its  $t_{2g}$  orbitals into the antibonding  $\pi^*$  orbitals of the dinitrogen ligand. The open shell Mo (IV) (left hand side transition metal) withdraws bonding  $\pi$  electrons from dinitrogen into its  $t_{2g}$  orbitals. The stretching frequency of  $\text{N} \equiv \text{N}$  is reduced from  $2331 \text{ cm}^{-1}$  in the gas to  $1922 \text{ cm}^{-1}$  in the simple rhenium complex to  $1680 \text{ cm}^{-1}$  in the molybdenum complex. An analogous dimolybdenum  $\mu$ -dinitrogen complex is formed from  $[\text{Mo}^{\text{I}}\text{Cl}(\text{N}_2)(\text{diphos})_2]$  and  $[\text{Mo}^{\text{IV}}\text{Cl}_4(\text{THF})_2]$  (50) and shows greatly reduced  $\text{N} \equiv \text{N}$  stretching frequencies at  $1770 \text{ cm}^{-1}$  and  $1720 \text{ cm}^{-1}$ . Therefore, the function of the molybdenum in the metalloenzyme may be to further weaken the nitrogen nitrogen bond strength in a  $\mu$ -dinitrogen complex, thereby promoting reduction by biologically strong but chemically weak reducing agents in vivo.

Mechanistic studies have shown that one of the few cases in which model complexes duplicate the reactions and reactivities of complex natural products are the cobaloxime (51) and to a lesser extent rhodoxime (52) analogues of vitamin  $\text{B}_{12}$  coenzyme (53). Therefore kinetic studies on the oxidation, reduction and methylation of the simple cobaloxime model complexes can be used to provide mechanistic information about the biological processes catalysed by vitamin  $\text{B}_{12}$  coenzyme.

The cobalt atom of vitamin  $\text{B}_{12}$  coenzyme is capable of existence in three different formal oxidation states (54), and can also have different coordination numbers.



Vitamin  $\text{B}_{12\text{a}}$  as cobinamide or cobalamin, unlike typical cobalt (III) complexes, readily becomes five coordinate and behaves in a manner similar to that of classical carbonium ions. In this condition, rapid electron acceptance to generate vitamin  $\text{B}_{12\text{r}}$  ( $d^7$  five coordinate) occurs. Vitamin  $\text{B}_{12\text{r}}$  shows radical behaviour in reversible 1 : 1 oxygen uptake in solution although steric inhibition prevents dimerisation in the solid state. One electron reduction of vitamin  $\text{B}_{12\text{r}}$  yields vitamin  $\text{B}_{12\text{s}}$  ( $d^8$  five coordinate) which behaves in a manner similar to that of classical carbanions. The high nucleophilicity, due to a ligand modified  $d_{z^2}$  orbital localised perpendicular to the plane of the molecule, which is further increased relative to cobinamide by the 5, 6-benzimidazole cobalamin macrocyclic loop coordinated to  $\text{Co}(\text{I})$ , is thought to account for the enormous selectivity of this two electron reductant for methyl carbonium ions. Vitamin  $\text{B}_{12\text{s}}$  acts as a methyl group acceptor and a catalyst for carbon skeleton rearrangements, for example the conversion of succinyl coenzyme A to methyl malonyl coenzyme A.

The cobaloximes exist in three analogous states and undergo similar reactions. However, cobaloximes and rhodoximes (II) (55) being less sterically hindered than  $\text{B}_{12\text{r}}$  are dimeric in the solid state forming 1 : 2 adducts with oxygen (56, 57). They are alkylated by a radical mechanism (58) whereas vitamin  $\text{B}_{12\text{r}}$  is not itself alkylated. Cobaloximes (I) are identical in their kinetics of alkylation to vitamin  $\text{B}_{12\text{s}}$ . In both cases, an  $\text{S}_{\text{N}}2$  mechanism operates (59). The similarity in alkylation rate arises because the maximum in the potential energy profile of

the  $S_N2$  transition state is largely dominated by the bond breaking step and steric effects are only important after bond breakage. The nucleophilicity and reaction rate of cobaloximes (I) is increased by electron donor axial and equatorial ligands and decreased by  $\pi$  electron acceptors. The analogous rhodoxime (I) complexes have lower nucleophilicity than cobaloximes (I) owing to the greater size of the  $4d_{z^2}$  orbital or  $4d_{z^2} / 5p_z$  hybrid compared to analogous cobalt orbitals. Though the rate profiles are similar, rhodoximes (I) undergo slower  $S_N2$  reactions. Cobaloximes and rhodoximes (I) also catalyse (52, 60) carbon skeleton rearrangements in unsaturated molecules.

The similarity in the nature of the axial bonds involving cobalt in vitamin  $B_{12}$  and cobaloxime model compounds has been demonstrated by Hückel's Molecular Orbital calculations (61). Furthermore, the aerobic photodealkylation of alkyl cobalamins (62) alkyl cobaloximes and rhodoximes (61) has been shown to occur by the same mechanism. That is, the absorption of a quantum of light causes a  $\pi \rightarrow \pi^*$  electronic transition in corrinoids or a charge transfer transition in cobaloximes and induces homolytic cleavage of the alkyl cobalt bond. Steric factors have little effect on the photolysis rate. In fact, the cobalt alkyl bonds in cobaloximes are slightly less labile than those in alkyl cobalamins. Rhodium alkyl bonds are much less photosensitive.

Several studies have been done on the interactions between equatorial and axial ligands transmitted through the cobaloxime metal ion (cis and trans effects). These kinetic and mechanistic studies are important since the factors governing the physicochemical properties and analogies between vitamin  $B_{12}$  complexes and the model molecules are fundamental to understanding the mechanisms of biochemical reactions.

Variation of an axial ligand with the same equatorial ligand has ground state, thermodynamic and kinetic effects (53, 63, 64).

As the axial ligand becomes more electron donating, the trans metal-ligand bond length increases and the equilibrium constant for a given substitution reaction in the trans position decreases. As the electron density on the corrin ring is increased, the N. M. R. absorption of the  $C_{10}$  proton is shifted to higher field and the energy of the first  $\pi \rightarrow \pi^*$  electronic transition is decreased. The bond lengths between cobalt and the equatorial nitrogen atoms are also altered. Thus electronic and conformational changes are exerted by the cis effect.

Studies on the effects of variation of the equatorial tetradentate ligand of cobaloximes with the same axial ligands are also important in comparisons with vitamin  $B_{12}$  complexes (65, 66). A. Bigotto and co-workers (66) have shown that  $E^0$  values for  $Co^{III}/Co^{II}$  and  $Co^{II}/Co^I$ , the nucleophilicity of the  $Co^I$  complex, the tendency to give complexes with high coordination number increase in the order

$$Co\ Bae < 7, 7'-(CH_3)_2-Co\ salen < Co\ salen < Co\ saloph < Co\ (DH)_2 < Co\ (DO)(DOH)pn$$

(see table of abbreviations ix, x). This is the order of decreasing electron donation from the equatorial ligand to cobalt. The tendency to form 1:2 oxygen adducts, the E. S. R. hyperfine splitting constants and wavelength of the charge transfer transition of the superoxo complexes also increase in this order (56). In the nucleophilicity table vitamin  $B_{12s}$  lies between  $[Co^I\ salen]^-$  and  $[Co\ (DH)_2]^-$ .

Recent evidence (67) has justified the use of cobaloximes in the study of vitamin  $B_{12}$  dependent enzymic processes. Methyl cobaloximes have been shown to compete with corrins for the same binding site on the enzyme catalysing reductive cobalt methyl bond cleavage to generate methane. The specific activities of the methyl cobaloximes is proportional to the ease of displacement of the axial base on coordination to the enzyme. Salicylaldoximes are only active non-enzymatically using dithioerythritol for reductive demethylation. Methyl aquo rhodoxime is a weak inhibitor of enzymatic methane evolution and has only one fifth of the reactivity of the analogous

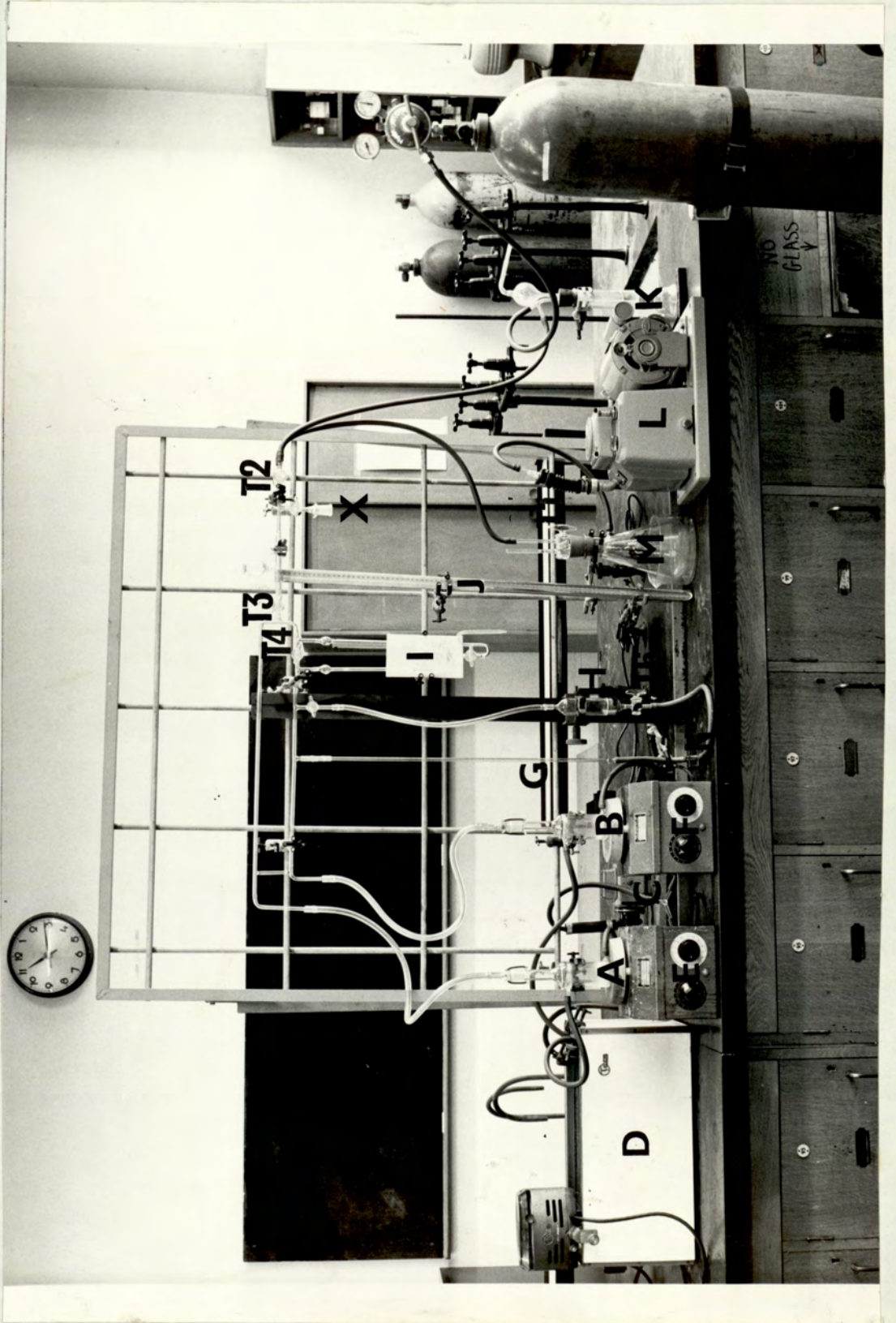
cobaloxime in the non-enzymatic reaction with dithioerythritol, a consequence of the greater rhodium methyl bond strength.

From this introduction it can be seen that the study of the reaction kinetics of transition metal complexes with gases in solution is of importance in elucidating the mechanisms of industrially and biochemically important homogeneous reactions.

A necessary prerequisite of this research was the design of apparatus suitable for investigating the kinetics and mechanisms of these reactions. A system to follow the kinetics of gas uptake as a function of gas partial pressure, temperature, concentration of the transition metal complex and other reactants was required. Since many reactions between transition metal complexes and gases proceed with changes in visible and ultra-violet absorption spectra, pH of the solution etc. systems following changes in these parameters were also needed. Many of the transition metal complexes involved as starting or end products of reactions with gases are highly reactive. To overcome this problem, methods of studying reactions occurring immediately after generation of the complex, of isolating air sensitive complexes and of gas purification were required.

The transition metal complex / gas systems chosen for kinetic studies were selected on the basis of their potential use as model systems for biological oxygen carriers, the enzyme catalysing nitrogen fixation or vitamin B<sub>12</sub> coenzyme. Systems generating potentially useful homogeneous catalysts under mild conditions were also selected for mechanistic studies. For example, complexes related to the rhodium (I) and (II) species produced are known as homogeneous hydrosilation (68) and hydrogenation catalysts (26, 69, 70). Thus, a wide range of inter-related problems, covering a wide variety of reagent types, was examined.

Figure 4. Apparatus for Following the Kinetics of Gas Absorption or Evolution.



## Chapter II. Experimental.

### 1. Apparatus for Kinetic Studies.

#### a. Kinetics of Gas Uptake. (See Figure 4).

The apparatus was designed as an improvement on the Gallenkamp Micro H. R. 100 (See Figure 5) and Macro H. R. 160 (See Figure 6) hydrogenation systems for measuring gas evolution or absorption at constant pressure. It incorporates the following features and modifications. The reaction vessel (B) and control flask (A), which contains a solvent blank to correct for gas absorption by the solvent, are equal in volume. Equal lengths of polythene and capillary tubing (including half the burette volume in the reaction vessel limb) connect them to the two limbs of manometer (I). Thus, temperature fluctuations in the "dead space" should produce equal volume changes in the two manometer limbs when  $T_4$  is closed. The two flasks are thermostatted to  $\pm 0.1^\circ\text{C}$  by pumping water by circulating pump (C) (Charles Austen Pump Model C16/300) from a Tecam water bath (D) thermostatted by Tecam Temp. Unit, through their encircling water jackets. Efficient agitation to ensure good contact between the solution and gaseous phases in (A) and (B) is achieved by using a Griffin Flask Shaker SD 110 or Voss variable speed magnetic stirrer units (E) and (F); (A) and (B) contain magnetic beads in the latter case. The 10 ml mercury containing gas burette (G) is calibrated in 0.02 ml portions. The mercury reservoir (H) can be continuously racked up or down to maintain constant pressure as gas is absorbed or evolved by the transition metal complex in (B). The butyl phthalate manometer (I) registers small pressure differences between the (A) and (B) limbs ( $T_4$  closed) which are compensated by movement of the mercury reservoir (H) thereby altering the volume of the reaction vessel limb and maintaining constant pressure in the two limbs. At pressures other than atmospheric, the mercury manometer (J)

Figure 5. Micro Hydrogenation Apparatus

H R - 100 .

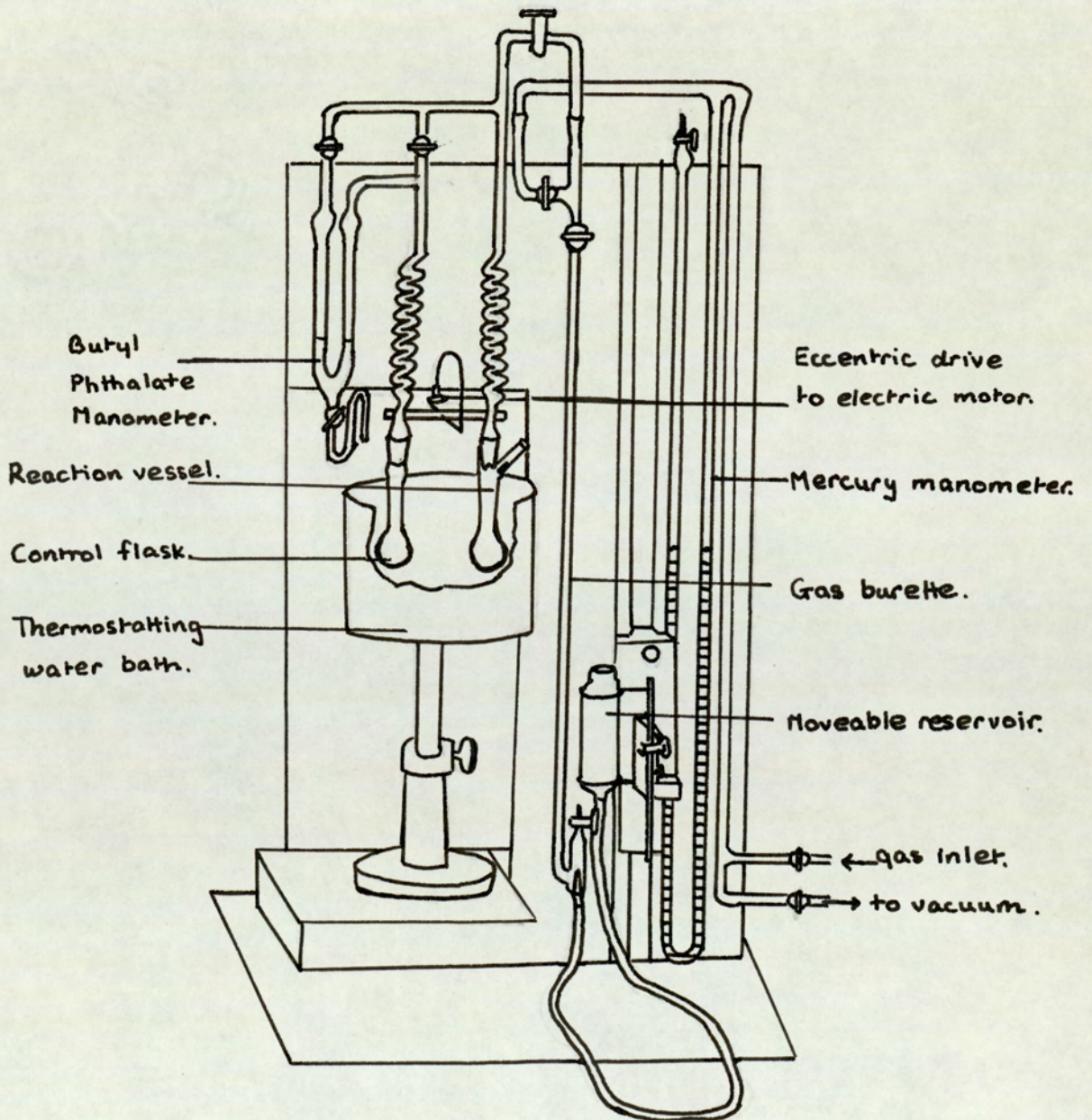
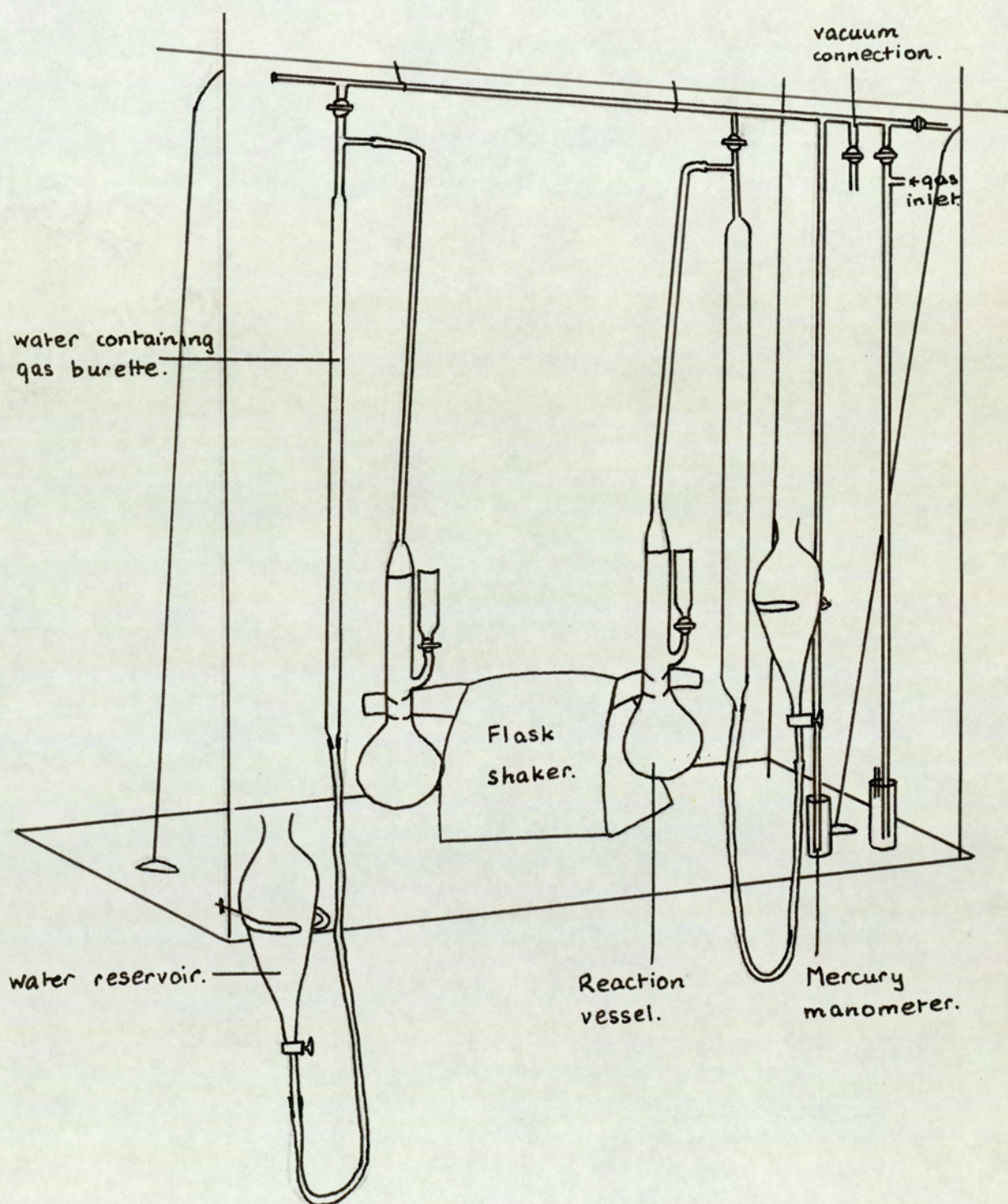


Figure 6. Macro Hydrogenation Apparatus H.R. 160.

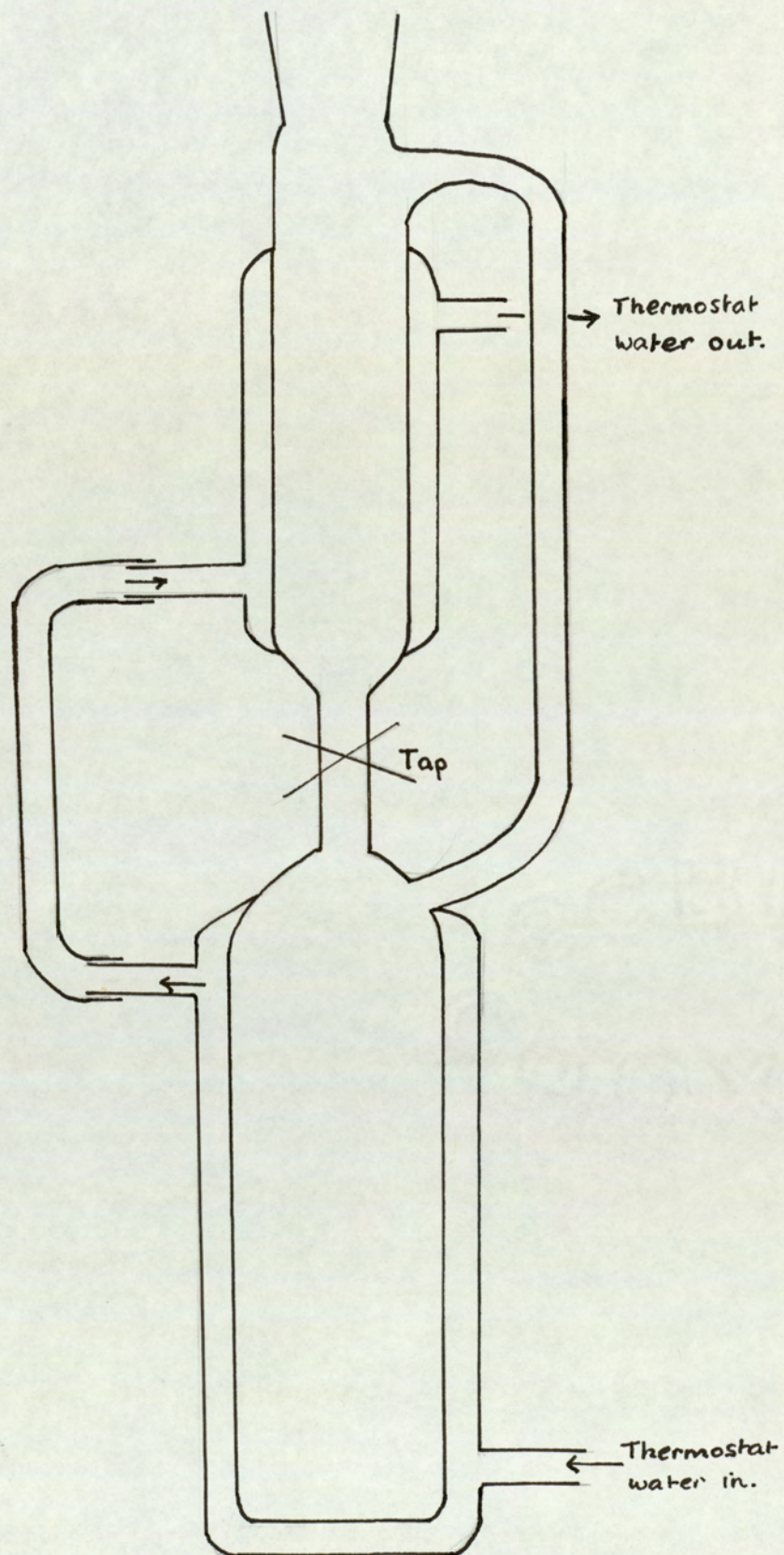


measures the pressure of gas in the closed system, the measured pressures being corrected by the vapour pressure of the solvent used. For work at atmospheric pressure the barometer is read. The mercury splashback valve (K) prevents admission of gas from the gas cylinder at pressures much greater than one atmosphere and also prevents entry of air. Evacuation of gas from the system is achieved by an N.G.N. rotary pump (L) via an ice cooled vapour trap (M). An accurate means of initiating the reaction is provided by releasing the magnetic cup containing the solid reagent, held in the neck of the reaction vessel by a bar magnet. Ideally, the magnetic cup should also act as a stirring bead (71). Alternatively, using the second design of reaction vessel, (see Figure 7) the reaction is initiated by turning the tap to mix a small volume of liquid in the upper compartment, for example, a solution of a transition metal ion or a transition metal complex, with the lower compartment solution containing for example, the ligand or reactants needed to generate the gas absorbing species.

#### Mode of Operation.

The reaction vessel and control flask are rigorously cleaned with aqua regia (to remove any solid catalytic rhodium species) and distilled water and filled with equal volumes of solvent. All taps are regreased using Apiezon M. The two flasks are equilibrated at the chosen temperature for at least 30 minutes by water pumped from the thermostat bath. A known weight of the reagent transition metal complex, preferably that which absorbs approximately 10 ml of gas, is held by bar magnet in the neck of the reaction flask. The system is closed and the solutions are stirred or shaken and carefully degassed by evacuation. In this cycle, the three way taps  $T_1$  and  $T_2$  are open to the pump,  $T_3$   $T_4$   $T_6$  are open,  $T_5$  and the screw clip (N) closed. For observation of the kinetics of gas absorption at atmospheric pressure the mercury reservoir is kept low down. Repeated

Figure 7. Reaction Vessel.



degassing and flushing with the reaction gas is carried out,  $T_1$  and  $T_2$  being open to the gas cylinder in the flushing cycle. Finally, the closed system is filled with an atmosphere of gas. The screw clip is opened and the mercury level adjusted to a suitable value in the gas burette. The levels in the two limbs of (J) are readjusted to be equal in height by gas admission or evacuation. Finally  $T_2$ ,  $T_3$  and  $T_4$  are closed. The initial burette reading is taken. The solid in the reaction vessel is added to the solution, simultaneously the stop watch is started. Differences in the gas volume absorbed by the transition metal complex solution in the reaction vessel and the equal volume of solvent blank in the control flask are registered by the butyl phthalate manometer. Pressure is kept constant i.e. atmospheric by upwards movement of the mercury reservoir and gas burette level readings are taken as a function of time.

For work at pressures other than atmospheric, that is the 200 to 900 mm mercury range, dependent on temperature and solvent vapour pressure, the mercury gas burette and reservoir are connected to the closed gas system in the reaction vessel limb of (I) by flexible polythene tubing. The system is degassed and filled with the required partial pressure of gas with taps  $T_5$  and  $T_6$  open. Tap  $T_5$  is closed before initiating the reaction. The volume of gas absorbed by the transition metal complex at the initial partial pressure of gas chosen is measured as a function of time.

b. Kinetics of the Reduction of Rhodium (III) Complexes  
by Spectrophotometry (See Figure 8).

The apparatus consists of two identical reaction vessels  $A_1$  and  $A_2$  with upper (volume approximately 40 ml) and lower (volume approximately 300 ml) compartments thermostatted by

Figure 8(a). Apparatus for Following the Kinetics of Reduction of Rhodium(III) Complexes by Spectrophotometry.

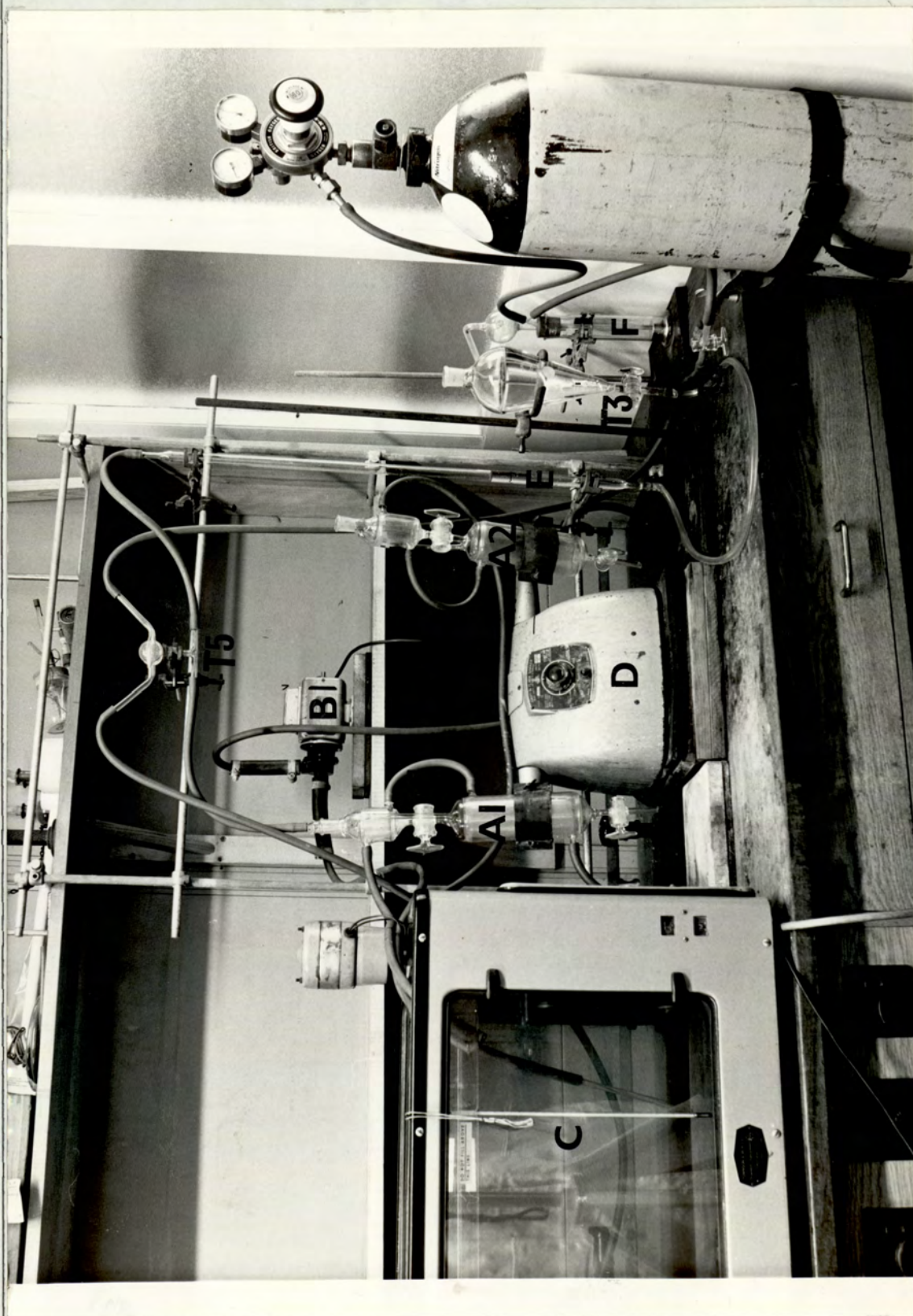
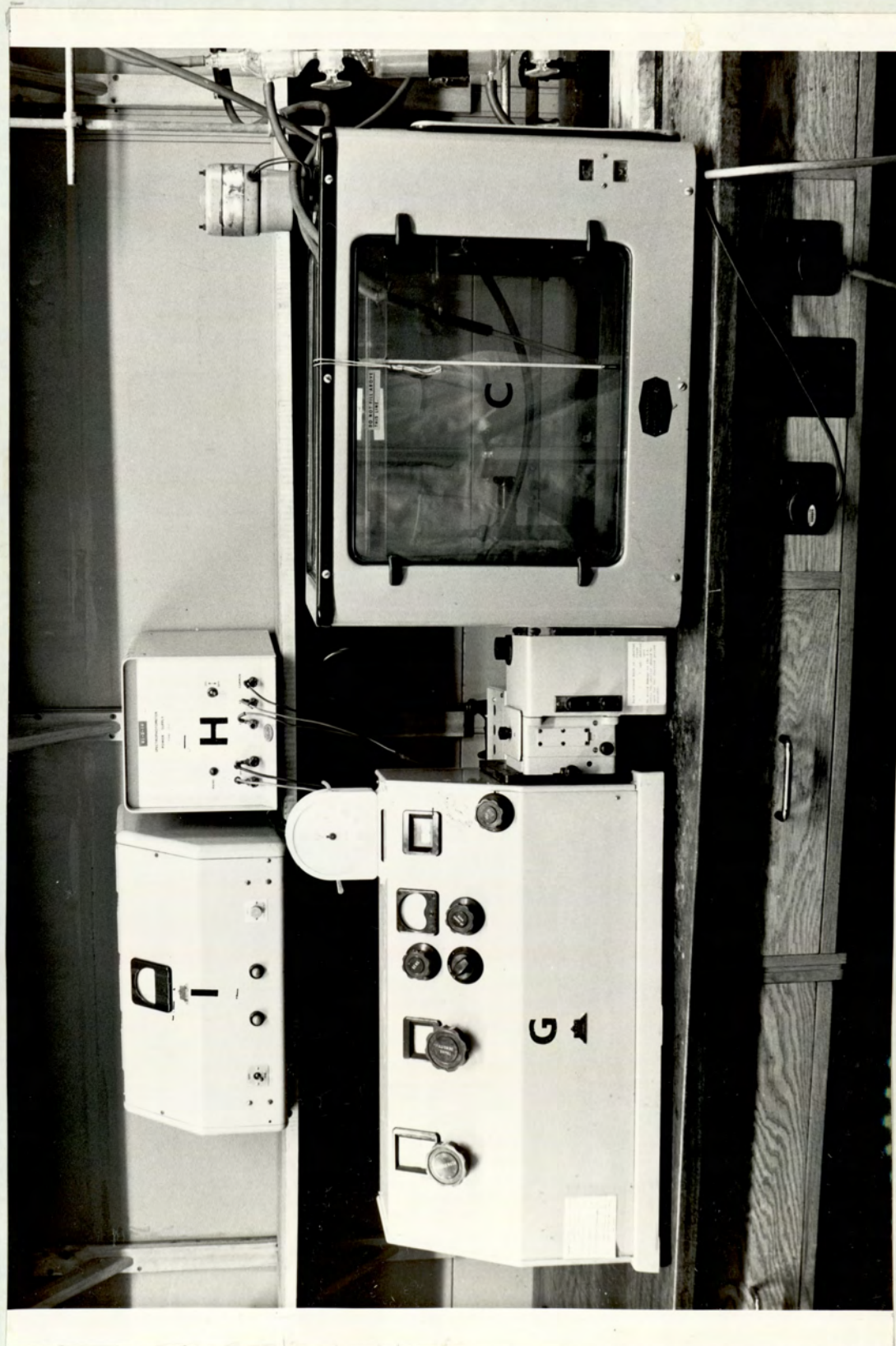


Figure 8(b). Apparatus for Following the Kinetics of the Reduction of Rhodium(III) Complexes by Spectrophotometry.

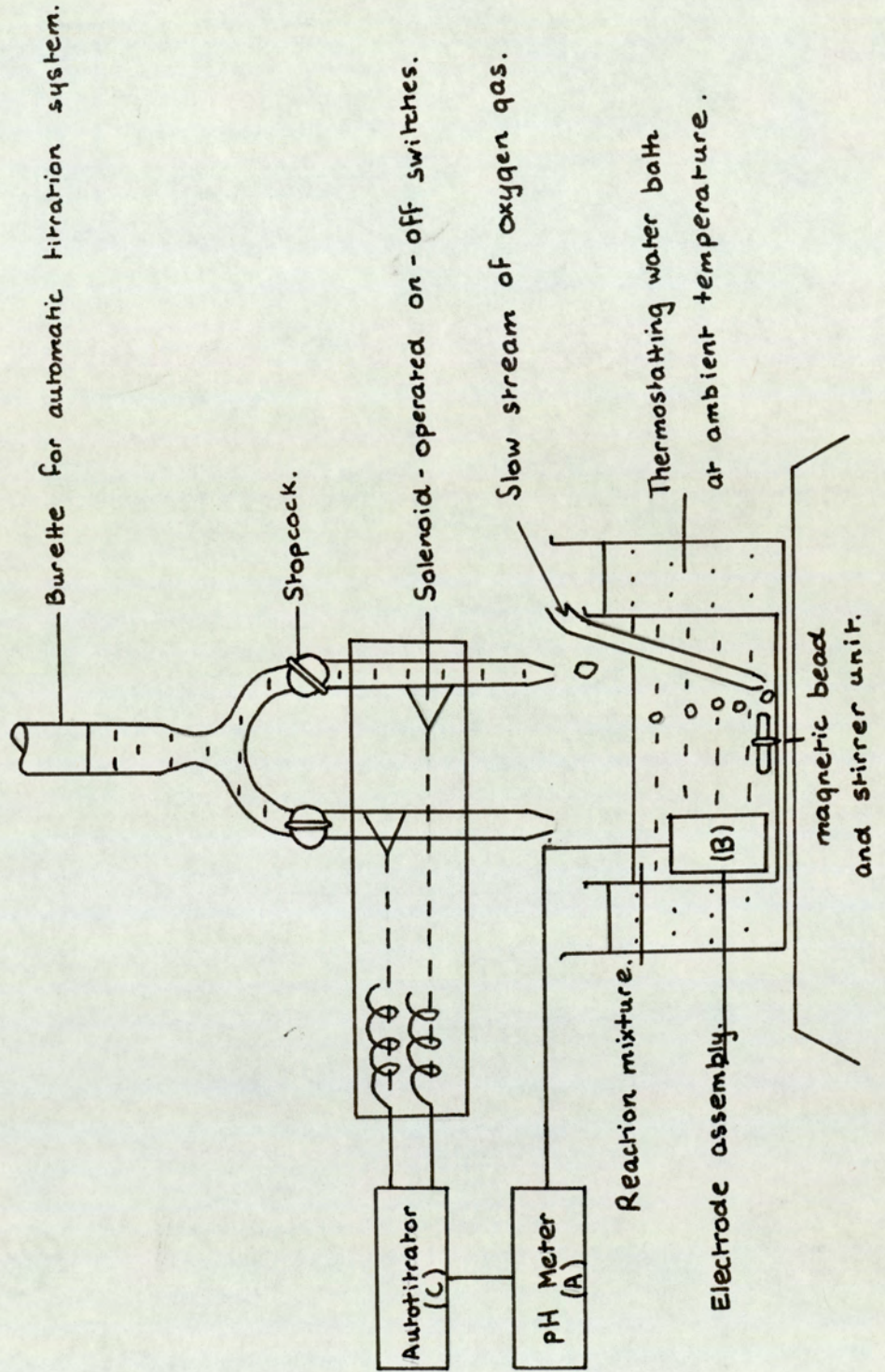


water pumped through their water jackets by circulating pump (B) (Charles Austen Pump Model C16/300) from the Townson-Mercer thermostatted water bath (C). The fluid in the vessels is agitated by Griffin flask shaker (D). (E) is a water containing 100 ml gas burette with adjustable reservoir. Evacuation is by water pump and admission of gas is via the mercury splashback (F) and gas cylinder. The Unicam S.P. 500 spectrophotometer (G) has a thermostatted cell compartment. It is fitted with a power supply type 115 D (H) and a power unit for the hydrogen lamp (I). 0.5 cm and 1.0 cm path length spectrophotometer cells are used to sample the reaction mixture.

#### Mode of Operation.

The reaction vessels and cell are cleaned with aqua regia, or ceric ion and perchloric acid (to remove solid catalytic rhodium species) distilled water, acetone and chloroform to remove grease. The reaction vessels were periodically re-annealed. The taps  $T_1$  and  $T_2$  are carefully regreased using Apiezon M. One reaction vessel is used for a kinetic run whilst the contents of the second are equilibrated. For investigation of the kinetics of the reduction of the complexes  $[\text{Rh}^{\text{III}}(\text{bipy})_2\text{Cl}_2] \text{NO}_3 \cdot 2\text{H}_2\text{O}$  and  $\text{H} [\text{Rh}^{\text{III}}(\text{DMG})_2\text{Cl}_2]$ , the lower compartment contained the required concentration of the rhodium (III) species in aqueous ethanolic solution, whilst the upper compartment contained sodium hydroxide solution at the requisite concentration. If necessary, A.R. aqueous sodium nitrate solution is used to maintain constant ionic strength. The two solutions are equilibrated for at least thirty minutes to water bath temperature ( $60^\circ$  or  $50^\circ\text{C}$ ) then degassed by evacuation ( $T_3$ ,  $T_4$  closed,  $T_5$  open to the pump, reaction vessel and gas burette) and flushed with gas (hydrogen or nitrogen) ( $T_4$  open,  $T_5$  open to gas cylinder, reaction vessel and gas burette). The evacuation / flushing sequence is repeated several times and finally the system

Figure 9. Automatic Titration System.



is filled with an atmosphere of gas.  $T_3$  is opened and the water levels in the gas burette and reservoir are adjusted to be equal.  $T_5$  is closed to all outlets.  $T_1$  is opened, the stop watch started and shaking commenced. At suitable time intervals, samples of the resulting reaction mixture are run off into the spectrophotometer cell. The optical density at the absorption maximum of the rhodium(I) species is measured against a solvent blank. The water reservoir is moved upwards to compensate for sample removal from the reaction vessel.

c. Kinetics of the Hydrolysis of  $\mu$ -Peroxo- $\mu$ -Diaminoethano-tetrakisdiamino ethane dicobalt (III) Cation (B) to the Analogous  $\mu$ -Peroxo- $\mu$ -Hydroxo Species (C) by following the pH Change.  
(See Figure 9).

The apparatus consists of an E.I.L. pH meter (A) connected to an electrode assembly of glass electrode, calomel electrode and temperature control (B) and to a Pye Autotitrator Controller (Catalogue number 11603) (C). The reaction vessel containing a magnetic bead is thermostatted at ambient temperature by a water bath. Stirring is achieved by a Voss magnetic stirrer unit.

Mode of Operation.

Preliminary experiments showed that solid samples of (B) redissolved in water gave no pH change or small pH increase and low equilibrium constants, depending on the extent of hydrolysis occurring in the time of oxygenation and rotary evaporation. Therefore, complex (B) was generated in situ to follow the kinetics of its conversion to (C). The pH meter scale was adjusted using calibrant solutions of pH 7.0 and 9.27. The electrode assembly was inserted into 40 ml of 1.19 M cobaltous perchlorate and 50 ml of distilled water in a beaker surrounded by a trough of thermostating water at the known

ambient temperature. The solution was stirred magnetically at constant rate and oxygen gas was bubbled through in a slow stream. The system was allowed to equilibrate for about thirty minutes. The formation of (B) was initiated by adding 48.1ml of 2.48 M ethylenediamine solution from a burette. The pH rose initially to 8.5 to 8.7 then slowly fell. Formation of (B) was assumed complete, that is 0.0238 moles, when the pH reached its lowest value and remained temporarily constant at pH 8.2. The stop watch was started. The autotitrator was adjusted to maintain the solution at pH 8.2 by slow addition of 1.62 M perchloric acid via the slow channel. Readings of time and burette level were taken immediately after the autotitrator had ceased addition of a portion of perchloric acid.

Comparison of the results of three runs suggested an accuracy of 10%. The errors result largely from inadequate thermostating. Exposure to the atmosphere could result in carbon dioxide uptake. A correction for the arbitrary zero time was applied by plotting  $\log_{10} (BR_{\infty} - BR_t)$  against time. Extrapolation of the straight line to zero time gave the corrected  $BR_{\infty}$  reading. Corrected values of  $BR_{\infty}$  and the equilibrium constant were then calculated. The infinity burette reading is very important since its magnitude controls that of the calculated equilibrium constant (K) and forward reaction rate ( $k_f$ ). The autotitrator tends to underestimate  $BR_{\infty}$  that is, if set to maintain pH 8.2 a rise to pH 8.30 to 8.35 is needed to trigger off perchloric acid addition. Therefore K and  $k_f$  tend to be too low. The rate of perchloric acid addition must be carefully adjusted, since slow addition of acid is essential to avoid overshooting but addition must be fast enough to obtain sufficient time and burette readings during the reaction time. A systematic error is introduced since the rate of addition slows down as the head of acid decreases. Therefore the pH at the end point of addition tends to increase with time. The earlier  $BR_t$  readings

tend to be too high and the later ones too low. This factor accounts for the apparent decreasing gradient of  $\log_{10} (BR_{\infty} - BR_t)$  versus time plots.

## 2. Physical Techniques and Apparatus.

Physical studies were carried out with a Pye Unicam SP 700 ultra-violet and visible spectrophotometer, which could be fitted with an SP 735 diffuse reflectance attachment, a Perkin Elmer model 137 ultra-violet spectrophotometer, Perkin Elmer 225 and 457 infra red spectrometers, a Perkin Elmer R 10 N.M.R. spectrometer and an A E I MS9 Mass spectrometer. E.S.R. studies were carried out using a Hilger Watts E.S.R. 3 spectrometer.

The time base was calibrated in gauss using Fremy's salt formula

$\text{ON}(\text{SO}_3\text{K})_2$  which gives a 1 : 1 : 1 triplet signal of peak separation  $13.00 \pm 0.07$  gauss. From this calibration the peak separation in the unknown was calculated. The magnetic field strength at the centre of the signal ( $H_1$ ) was calculated by comparison with that determined for D. P. P. H. ( $\alpha, \alpha'$ -diphenyl- $\beta$ -picryl hyrazyl) ( $H_2$ ) by N. M. R. probe. Knowing  $g_2 = 2.0036$  for D. P. P. H.,  $g_1$  for the unknown was calculated from the relationship  $H_1 g_1 = H_2 g_2$ .

Magnetic susceptibilities were determined by Guoy balance. For diamagnetic or weakly paramagnetic compounds A.R.  $\text{CuSO}_4 \cdot 5\text{H}_2\text{O}$  ( $Xg = 5.92 \times 10^{-6}$ , one unpaired electron per Cu atom) and  $[\text{Ni}(\text{en})_3]\text{S}_2\text{O}_3$  ( $Xg^{25^\circ\text{C}} = (10.82 \mp 0.1) \times 10^{-6}$  two unpaired electrons per Ni atom) were used as calibrants. A wide bore N. M. R. tube tightly packed with the finely ground calibrant or unknown, using a metal rod, was used to obtain a maximum weight change. For strongly paramagnetic complexes  $[\text{Hg}(\text{CoSCN})_4]$  ( $Xg^{20^\circ\text{C}} = 16.44 \times 10^{-6} \mp 0.5\%$  three unpaired electrons per Co atom) was used as calibrant. A heavier Guoy tube containing less sample was used to prevent sticking to the poles of the electromagnet. Temperature corrections were applied to the susceptibility of the standard. Molar magnetic susceptibilities calculated for the unknown were corrected for the diamagnetism of the ligands (72).

Molar conductivities were measured by Wayne Kerr Universal

Bridge B 221. The cell was calibrated using  $5 \times 10^{-3}$  to  $5 \times 10^{-4}$  M A.R. sodium chloride solutions. From the measured conductances and known molar conductivities (73) the cell constant was calculated. The conductances and hence molar conductivities of  $5 \times 10^{-3}$  to  $5 \times 10^{-4}$  M freshly prepared solutions of the unknowns in conductivity water were measured at the known ambient temperature. Graphs of molar conductivity against square root of concentration were plotted and compared with those obtained for known 1 : 1, 1 : 2, 1 : 3, 1 : 4 and 1 : 5 electrolytes.

The Mechrolab Vapour Pressure Osmometer Model 301 A was used in molecular weight determination. The chloroform solvent was purified (74) by shaking two to three times with a small volume (say 5%) concentrated sulphuric acid, washed thoroughly with distilled water, dried over anhydrous calcium chloride and distilled (boiling point  $60.5^{\circ}\text{C}$  at 757 mm Hg cf.  $61^{\circ}\text{C}$  at 760 mm Hg). The pure chloroform, free from alcohol stabiliser was kept in full bottles in the dark to avoid photochemical phosgene formation. Pyridine was dried by refluxing over caustic potash pellets and distilled with careful exclusion of water (boiling point  $115.5^{\circ}\text{C}$  at 760 mm Hg). In both cases, benzil solutions of similar concentrations to the unknown were used in calibration. In the case of pyridine, the waiting time was twelve minutes, for chloroform only two minutes. A graph of  $\Delta R$ , (a measure of the temperature difference between the solvent and solution drops, caused by the lowering of solvent vapour pressure by the solute), against concentration was plotted. From the observed  $\Delta R$  values of the unknown, the molar concentration was calculated. From the initial weight of complex used the molecular weight was obtained.

Thermogravimetric analysis was performed using 10 mg samples

of the solid under a nitrogen atmosphere in a Dupont 950 Thermogravimetric Analyser over the temperature range 50°C to 500°C with a heating rate of 5°C per minute.

### 3. Preparation of Complexes.

Rhodium trichloride trihydrate was loaned by Johnson Matthey. A large cylinder of carbon monoxide and samples of crude bipyridyl, pure 4, 4'-dimethyl-, 4, 4'-dichloro-, 5, 5'-dimethyl-bipyridyl were supplied by Imperial Chemical Industries.

1.  $\mu$ -Superoxo- $\mu$ -diaminoethano-tetrakisdiaminoethane dicobalt (III) Nitrate. (A). (75) (The alphabetical symbols are those used in Chapter III).

Preliminary methods of preparation, for example dissolving the corresponding  $\mu$ -peroxo complex in water and oxidising with concentrated nitric acid and ceric ion, or equimolar hydrogen peroxide and potassium peroxydisulphate, or concentrated sulphuric acid and potassium permanganate by the titration method (76) were unsuccessful. The resultant brown-green solutions appear to be  $\mu$ -peroxo,  $\mu$ -superoxo complex mixtures, which cannot be separated by chromatography, decompose to  $\mu$ -peroxo complex and oxidant on rotary evaporation or exposure to air and eventually produce copious crystals of deprotonated diaminoethane and the  $[\text{Co}(\text{en})_2(\text{CO}_3)]^+$  complex by carbon dioxide uptake.

Therefore, the peroxo complex was generated in situ, avoiding acid conditions, which promote protonation of the peroxo bridge and slow down oxidation (75) (red colouration observed) and cause loss of the bridging ethylenediamine ligand. A minimum volume of water solvent was used to favour precipitation. Exposure to air and high temperature was avoided.  $\text{Co}^{\text{II}}$  and  $\text{Ce}^{\text{IV}}$  ions were present as nitrates to avoid precipitation of the  $\mu$ -superoxo complex with a mixture of anions.

Diaminoethane hydrate (8.1 ml) was added to a concentrated

aqueous solution of  $\text{Co}(\text{NO}_3)_2 \cdot 6\text{H}_2\text{O}$  (11.6g in 50 ml water) and the solution was shaken under an oxygen atmosphere until gas uptake was complete. The solution was then poured into an ice cooled concentrated solution of  $(\text{NH}_4)_2 [\text{Ce}(\text{NO}_3)_6]$  (0.97g in 100 ml water). The mixture was stirred for eighty minutes at  $0^\circ$  to  $10^\circ\text{C}$ . The olive green precipitate was washed with cold ethanol, then acetone until the washings were colourless. It was dried in vacuo.

found C15.9%; H5.9%; Co15.6%; N28.6%.

$[\text{Co}_2(\text{en})_5(\text{O}_2)](\text{NO}_3)_5$  requires  
C15.8%; H5.3%; Co15.5%; N27.6%.

2.  $\mu$ -Peroxo- $\mu$ -diaminoethano-tetrakisdiaminoethanedicobalt (III) Perchlorate Monohydrate. (B)

The above preparation was repeated until gas uptake was complete, except that cobalt(II)perchlorate was used. The solution was then evaporated down to a volume of 5 ml under reduced pressure, below  $40^\circ\text{C}$ . The tarry brown mass was washed with small quantities of ice cold water and then dried in vacuo.

found C14.7%; H4.8%; Co13.6%; N16.2%;  $\text{O}_2$  3.1%;  $\text{ClO}_4$  45.3%.

$[\text{Co}_2(\text{en})_5(\text{O}_2)](\text{ClO}_4)_4 \cdot \text{H}_2\text{O}$  requires  
C13.9%; H4.9%; Co13.6%; N16.2%;  $\text{O}_2$  3.7%;  $\text{ClO}_4$  45.9%.

The percentage oxygen in this complex was determined from the volume of gas evolved on treatment with 2.0 M perchloric acid.

3.  $\mu$ -Peroxo- $\mu$ -hydroxo-tetrakisdiaminoethanedicobalt (III) Perchlorate Monohydrate (C).

This complex was prepared as in (2) using 50% aqueous ethanol in place of water as the solvent for  $\text{Co}(\text{ClO}_4)_2 \cdot 6\text{H}_2\text{O}$ . The solution was set aside overnight under oxygen and gave black crystals.

These were recrystallised from 50% aqueous ethanol and dried in vacuo.

found C12.9%; H4.9%; Co16.2%; N15.4%; ClO<sub>4</sub> 40.5%.  
 calculated for  $[\text{Co}_2(\text{en})_4(\text{O}_2)(\text{OH})](\text{ClO}_4)_3 \cdot \text{H}_2\text{O}$   
 C13.3%; H4.7%; Co16.3%; N15.5%; ClO<sub>4</sub> 41.2%.

Perchlorate in the above two complexes was estimated by cation and anion exchange resins.

#### 4. Carbonatobis diaminoethane cobalt (III) perchlorate Hemihydrate.

Approximately 0.2 M solutions of complexes (B) or (C) were shaken under an atmosphere of carbon dioxide until gas uptake was complete (three days). The pink crystalline products were washed with water and dried in vacuo.

found C16.7%; H4.8%; Co17.0%; N16.1%.  
 calculated for  $[\text{Co}(\text{en})_2(\text{CO}_3)]\text{ClO}_4 \cdot \frac{1}{2}\text{H}_2\text{O}$   
 C17.3%; H4.9%; Co17.0%; N16.1%.

#### 5. Disalicylaldehyde - 1, 3-propanediimine.

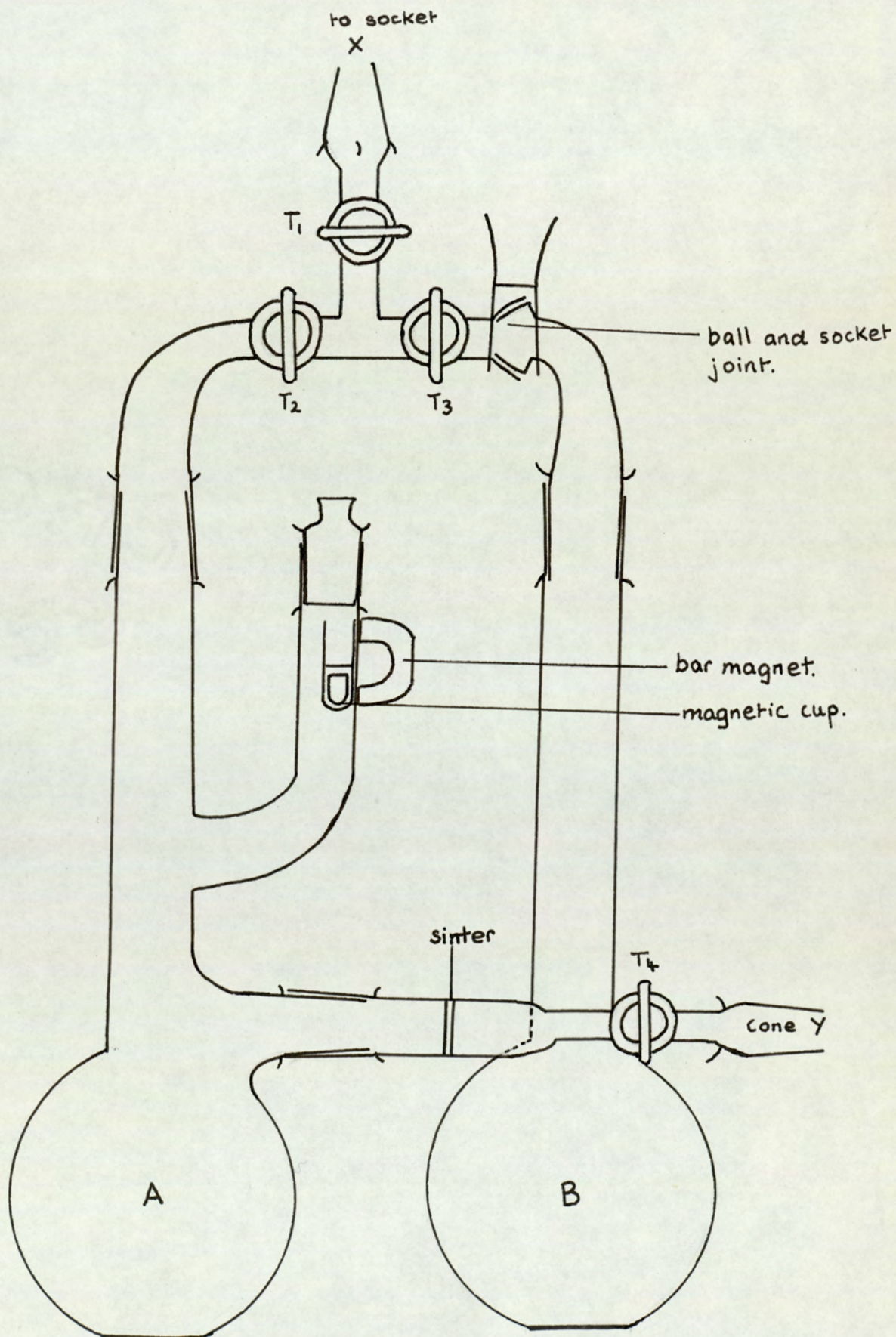
The ligand was prepared from salicylaldehyde and 1, 3-diaminopropane (ratio 2 : 1) in the standard manner (77). When recrystallised from ethanol, the melting point was 53°C (literature 53°C).

found C72.3%; H6.45%; N9.93%.  
 calculated for C<sub>17</sub> H<sub>18</sub> N<sub>2</sub> O<sub>2</sub>  
 C72.3%; H6.43%; N9.93%.

#### 6. N, N'-Disalicylaldehyde-1, 3-propanediimine-manganese (II) Monohydrate. (A). (The alphabetical symbols are those used in Chapter IV).

This complex was prepared by the literature method (78) 14.1g of the pure Schiff base were dissolved in 500 ml hot 70% ethanol / water. 12.6 g of Mn(NO<sub>3</sub>)<sub>2</sub> · 4H<sub>2</sub>O dissolved in 50 ml hot 70% ethanol / water were added keeping the temperature below 50°C.

Figure 10. Apparatus for the Isolation of Air Sensitive Complexes.



The mixture became dark brown and a yellow curdy precipitate gradually formed on cooling. The coagulated precipitate was rapidly filtered on a Hirsch funnel, successive layers being washed with distilled water to remove the surface green coating formed by aerial oxidation. The filtrate was dark green - brown (79). The bright yellow precipitate was dried in vacuo. Yield 20%.  
found C57.1%; H5.25%; Mn15.6%; N7.89%.

calculated for  $C_{17}H_{18}MnN_2O_3$   
C57.8%; H5.15%; Mn15.6%; N7.93%.

The manganese content was determined by destroying the ligand with concentrated nitric and phosphoric acids, oxidising to permanganate by potassium periodate and estimating permanganate spectrophotometrically (80). Gravimetric determinations by conversion to  $MnNH_4PO_4 \cdot H_2O$  (81) proved less reliable.

7. N, N' - Disalicylaldehyde - 1, 3 - propanediimine - manganese (II)  
(82) (Anhydrous) (B).

Preliminary experiments showed that this complex was extremely air sensitive. Even when the complex was filtered in a dry box fitted with copper tubing gas supply lines and purged with white spot nitrogen, further purified to less than 0.1 ppm oxygen by passage over activated B. T. S. catalyst (from Badische Anilin and Soda - Fabrik A G ) oxidation occurred.

The apparatus in Figure 10 was designed to prevent contact of the complex with air. It is connected to socket X on the gas uptake apparatus (see Figure 4). Vessel A contained 50 ml A. R. pyridine and 0.4 g of  $[Mn(salpn)H_2O]$  in the magnetic cup. Vessel B contained 200 ml of n-heptane. The two solvents were individually degassed by heating and stirring under vacuum and flushed with white spot nitrogen purified as above. The crude  $[Mn(salpn)H_2O]$  was added to the warm pyridine and dissolved on stirring. With

$T_1$  closed,  $T_2$  and  $T_3$  open approximately 30 ml of n-heptane was poured into the pyridine solution of  $[\text{Mn}(\text{salpn})\text{H}_2\text{O}]$ . The vessel A was removed and the contents cooled on an ice salt mixture for one hour. A conical flask with a side arm connected to the vacuum was fitted onto cone Y and the bright yellow crystals formed were filtered through the sinter under vacuum. When no traces of solvent remained in vessel A, the complex was dried under vacuum at  $80^\circ\text{C}$  for several hours by surrounding the sinter with an isotape connected to a variac and ammeter for temperature control. This process removed pyridine of recrystallisation. C H N figures could not be obtained for this complex as immediate oxidation occurred in air.

The reaction flask A was also used to prove that  $[\text{Mn}(\text{salpn})\text{H}_2\text{O}]$  in benzene suspension does not absorb nitrogen nor carbon monoxide. Flask A was filled with 300 ml of A.R. benzene, and connected to the vacuum line via socket X. The magnetic cup was filled with 0.05g  $[\text{Mn}(\text{salpn})\text{H}_2\text{O}]$ . The benzene was degassed by prolonged heating under vacuum until the volume was reduced to approximately one sixth of the initial volume. The reaction vessel was cooled to room temperature and filled with an atmosphere of nitrogen or carbon monoxide, deoxygenated by passage over activated B. T. S. catalyst. The limbs of the mercury manometer were adjusted to be equal in height. Finally, the yellow  $[\text{Mn}(\text{salpn})\text{H}_2\text{O}]$  complex was added to the benzene solvent and the mixture stirred. After several days, no yellow to brown colour change and no observable rise in the left hand limb of the mercury manometer occurred (other than that due to increase in barometric pressure). That is no oxidation occurred. On admission of oxygen, immediate gas uptake occurred to form the brown oxidised product (C).

8. Oxygen Adducts (C) and (D) derived from (A) (See Chapter IV).

Anala R benzene (25 ml) was saturated with oxygen and kept in

a flask under oxygen. A pure sample of compound A (1g) was dropped into the benzene while in the closed system. The resulting suspension was shaken under oxygen for several days at room temperature. Changes in the volume of gas were measured manometrically. When gas uptake appeared to be complete, the brown suspension was filtered off. The filtrate was almost colourless. The products were then dried in vacuo. From reactions with an observed Mn : O<sub>2</sub> stoicheiometry of 1 : 1 compound (C) was obtained.

found C53.5%; H4.54%; Mn14.4%; N7.17%.

calculated for  $\left[ \text{Mn}(\text{salpn})(\text{O}_2)(\text{H}_2\text{O}) \right]$   
C53.0%; H4.71%; Mn14.3%; N7.27%.

From reactions with an observed stoicheiometry of 2 : 1 compound (D) was obtained.

found C61.9%; H4.88%; Mn14.2%; N7.17%.

calculated for  $\left[ \text{Mn}(\text{salpn}) \text{O} \cdot \frac{1}{2} \text{C}_6\text{H}_6 \right]$   
C61.6%; H5.01%; Mn14.1%; N7.18%.

#### 9. Oxygen Adducts (E) and (F) derived from (A).

Compound (A) (0.5g) was dissolved in a minimum volume of Anala R. pyridine and refluxed under oxygen for thirty minutes then cooled on ice and allowed to stand for several weeks. The black crystals (E) were filtered off, washed with n-heptane and then dried in a current of air.

found C60.5%; H4.7%; Mn12.8%; N9.3%.

calculated for  $\left[ \text{Mn}(\text{salpn})(\text{O})\text{py} \right]$   
C61.4%; H4.9%; Mn12.8%; N9.8%.

The coordinated pyridine is readily lost, which may explain the slightly low CHN analytical figures for (E). On drying (E) over concentrated sulphuric acid in vacuo rather than allowing to stand, compound (F) is produced.

found C57.9%; H4.82%; Mn15.7%; N7.67%.

calculated for  $[\text{Mn}(\text{salpn}) \text{O}]$   
 C58.1%; H4.59%; Mn15.6%; N7.98%.

10. Oxygen Adducts (G) and (H) derived from (B).

Oxygen gas was passed for several hours over a sample 10.2g of (B) in a heated tube (80°C). The brown product (C) formed cannot be unequivocally described from its analytical data.

found C57.7%; H4.97%; Mn15.0%; N7.84%.

calculated for  $[\text{Mn}(\text{salpn}) \text{O}]$   
 C58.1%; H4.59%; Mn15.6%; N7.98%.

calculated for  $[\text{Mn}(\text{salpn}) \text{O}_2]$   
 C55.6%; H4.39%; Mn15.0%; N7.63%.

The anhydrous compound (B) (0.1g) was transferred to the sealed system under nitrogen. Anala R benzene (5 ml) was then added and oxygen gas introduced. An Mn : O<sub>2</sub> stoichiometry of 2 : 1 was observed. The product was then filtered, washed with benzene and dried.

found C63.3%; H5.41%; Mn12.9%; N7.03%.

calculated for  $[\text{Mn}(\text{salpn}) (\text{O})\text{C}_6\text{H}_6]$   
 C64.4%; H5.17%; Mn12.9%; N6.53%.

11. Bis acetyl acetone - 1, 3 propanediimine (83).

The ligand was prepared by dropwise addition of 1.3 diamino propane (1 mole) to acetyl acetone (2 moles). The mixture was cooled on ice to allow for the reaction's exothermicity. The colourless Schiff base was recrystallised twice from absolute ethyl ether. (Melting point 49°C : literature 51°C).

found C64.0%; H9.28%; N11.6%.

calculated for  $\text{C}_{13} \text{H}_{22} \text{O}_2 \text{N}_2$   
 C65.8%; H9.25%; N11.7%.

12. Attempted Preparation of N, N'-Bis acetyl acetone-1, 3-propanediimine - Manganese (II).

Equimolar aqueous ethanolic solutions of Schiff Base, manganese (II) and hydroxide to deprotonate the ligand, produce white manganous hydroxide (rapidly oxidised to brown  $\text{Mn}(\text{OH})_3$ ) free ketone and amine that is hydrolytic cleavage of the imine group occurs. 1 : 1 neutral aqueous ethanolic solutions of Schiff Base and  $\text{Mn}(\text{NO}_3)_2 \cdot 4\text{H}_2\text{O}$  produce  $\text{Mn}^{\text{II}}(\text{acac})_2$  which rapidly absorbs oxygen in solution. Again the Schiff Base is hydrolysed. Refluxing an acetone solution of the ligand with excess metal acetate (the weakly basic acetate ion deprotonates the ligand) and filtering off unreacted acetate generates the analogous green crystalline copper Schiff base complex on addition of water to the filtrate.

found C51.7%; H7.51%; N9.07%.

calculated for  $\text{Cu C}_{13} \text{H}_{20} \text{O}_2 \text{N}_2$   
C52.1%; H6.73%; N9.35%.

The manganese complex could not be formed by this method. Probably an inert atmosphere is required.

13. Preparation of cis-Dichlorobis-(2, 2'-bipyridyl or 1, 10-phenanthroline) rhodium (III) salts (84).

To 0.26g (1 m mole) of hydrated rhodium trichloride in 5 ml of ethanol, 2.2 m moles of ligand in 5 to 10 ml of hot ethanol were added. The salmon pink precipitate first produced, became yellow. The mixture was stirred and heated under reflux for thirty minutes to ensure completeness of reaction (85). The resultant chloro complexes were filtered in a sinter (porosity 4) washed with ethanol and ice water, finely powdered and redissolved in a large volume (500 ml) of boiling water. Insoluble impurities were removed by filtration, excess sodium nitrate or perchlorate was added as

required and the solution evaporated to about 20 ml. On ice cooling yellow crystals of the chloride, nitrate or perchlorate precipitated. The nitrate salts proved extremely water soluble and occasionally crystallised out with some sodium nitrate. Yields of the chlorides approached 90%; those of the nitrates only 50%.

The rhodium contents of the complexes were estimated spectrophotometrically by destroying the ligand with concentrated sulphuric acid, treating the solution with concentrated hydrochloric acid and 18 % A. R. stannous chloride solution and estimating the 475n.m. peak against a solvent blank (86)(sensitivity 4 - 20ppm Rh). Rhodium trichloride trihydrate containing 42.69% rhodium and pure  $[\text{Rh}^{\text{III}}(\text{bipy})_2\text{Cl}_2]\text{NO}_3 \cdot 2\text{H}_2\text{O}$  were used as calibrants. Sodium contents were estimated by flame spectroscopy using an "E E L" Flame Photometer Mark II with A. R. sodium nitrate as calibrant.

found Rh17.6%; C41.1%; H3.45%; N12.0%; Cl 11.8%.

calculated for  $[\text{Rh}^{\text{III}}(\text{bipy})_2\text{Cl}_2]\text{NO}_3 \cdot 2\text{H}_2\text{O}$

Rh17.6%; C41.8%; H3.00%; N12.1%; Cl 12.1%.

found Rh11.2%; C27.7%; H1.56%; N10.3%; Na 6.42%.

calculated for  $[\text{Rh}^{\text{III}}(4, 4' \text{ Cl bipy})_2\text{Cl}_2]\text{NO}_3 \cdot 2.5\text{Na NO}_3$

Rh11.4%; C26.7%; H1.35%; N10.1%; Na 6.40%.

found Rh16.2%; C44.7%; H4.04%; N11.2%.

calculated for  $[\text{Rh}^{\text{III}}(4, 4' \text{ Me bipy})_2\text{Cl}_2]\text{NO}_3 \cdot 2\text{H}_2\text{O}$

Rh16.1%; C45.0%; H4.41%; N10.9%.

found Rh15.9%; C43.4%; H3.68%; N11.1%.

calculated for  $[\text{Rh}^{\text{III}}(5, 5' \text{ Me bipy})_2\text{Cl}_2]\text{NO}_3 \cdot 2\text{H}_2\text{O}$

Rh16.1%; C45.0%; H4.41%; N10.9%.

found Rh 18.3%; C 41.8%; H 4.53%; N 9.88%.  
 calculated for  $\left[ \text{Rh}^{\text{III}}(\text{bipy})_2 \text{Cl}_2 \right] \text{Cl} \cdot 2\text{H}_2\text{O}$   
 Rh 18.4%; C 43.1%; H 3.61%; N 10.0%.

found Rh 16.5%; C 39.1%; H 2.91%; N 9.36%.  
 calculated for  $\left[ \text{Rh}^{\text{III}}(\text{bipy})_2 \text{Cl}_2 \right] \text{ClO}_4 \cdot 2\text{H}_2\text{O}$   
 Rh 16.6%; C 38.6%; H 3.24%; N 9.01%.

found Rh 14.0%; C 39.3%; H 2.50%; N 12.0%; Na 4.77%.  
 calculated for  $\left[ \text{Rh}(\text{o-phen})_2 \text{Cl}_2 \right] \text{NO}_3 \cdot 1.5 \text{NaNO}_3 \cdot 2\text{H}_2\text{O}$   
 Rh 13.9%; C 38.8%; H 2.45%; N 12.3%; Na 4.65%.

found Rh 9.78%; C 26.5%; H 2.03%; N 13.8%; Na 7.33%.  
 calculated for  $\left[ \text{Rh}(\text{5NO}_2\text{phen})_2 \text{Cl}_2 \right] \text{NO}_3 \cdot 3.5 \text{NaNO}_3 \cdot 4\text{H}_2\text{O}$   
 Rh 9.74%; C 27.3%; H 2.10%; N 13.9%; Na 7.62%.

found Rh 12.9%; C 47.0%; H 4.24%; N 9.69%; Na 1.63%.  
 calculated for  $\left[ \text{Rh}(\text{3,4,7,8Mephen})_2 \text{Cl}_2 \right] \text{NO}_3 \cdot 0.5 \text{NaNO}_3 \cdot 2\text{H}_2\text{O}$   
 Rh 12.9%; C 48.1%; H 4.29%; N 9.65%; Na 1.44%.

#### 14. Preparation of Bis - 2, 2'-bipyridylrhodium (I) Perchlorate Trihydrate.

The vacuum line and apparatus in Figure 10 were used to prepare this air sensitive complex. Vessel (A) contained 20 ml of 0.7 M sodium hydroxide solution and 20 ml of 50% aqueous ethanol with 0.9g of bis-dichloro-bis-bipyridyl rhodium (III) perchlorate in the magnetic cup. The solvent and whole system was repeatedly evacuated and flushed with hydrogen. The rhodium (III) complex was added to the hydrogen saturated solvent and the mixture stirred and heated. The complex dissolved and violet crystals of the reduced rhodium (I) product crystallised out on ice cooling. (The nitrate and chloride rhodium (I) salts were less readily precipitated).

The complex was filtered through a sinter (porosity 4) washed with de-aerated hydrogen saturated water and dried in vacuo overnight. The resultant dry violet solid was extremely air sensitive and became greyish in air. N.B. Hydrogen gas can replace sodium borohydride as reducing agent in alkaline ethanolic solution (87).

found Rh17.5%; C38.8%; H3.78%; N9.31%; Cl15.90%.

calculated for  $[\text{Rh}(\text{bipy})_2]\text{ClO}_4 \cdot 3\text{H}_2\text{O}$

Rh18.1%; C42.3%; H3.90%; N9.86%; Cl16.24%.

15. Preparation of Monohydrogen dichlorobis (dimethylglyoximato) rhodium (III).

This yellow complex was prepared as in reference (88).

Reduced yields were obtained if the solution was strongly acidic.

found Rh24.6%; C23.9%; H3.75%; N13.6%.

calculated for  $\text{H}[\text{Rh}(\text{DMG})_2 \text{Cl}_2]$

Rh25.4%; C23.7%; H3.73%; N13.8%.

16. Preparation of Monohydrogen bis (dimethylglyoximato) rhodium (I) Dihydrate.

A mixture of 0.432g of  $\text{H}[\text{Rh}^{\text{III}}(\text{DMG})_2 \text{Cl}_2]$  in 180 ml 50% aqueous ethanol and 180 ml 0.01192 N sodium hydroxide (that is a two fold excess (89) ) in vessel (A) was de-aerated by evacuation and flushing with white spot nitrogen. The solution was stirred and heated almost to boiling point. Stirring was then discontinued. Immediately red streaks developed in the solution which became completely blue - black in seconds (autocatalytic). The solution was cooled on ice and the fine blue - black precipitate filtered under vacuum through a sinter of porosity 4. The precipitate

was washed with de-aerated nitrogen saturated water and dried in vacuo overnight. Heating to 80°C under vacuum (89) resulted first in charring then in decomposition to metallic rhodium.

found Rh25.1%; C25.7%; H3.43%; N14.2%; Cl 0.24%; Na — .  
 H  $\left[ \text{Rh (DMG)}_2 \right] 2\text{H}_2\text{O}$  requires

Rh26.2%; C24.5%; H4.62%; N14.3%; Cl — ; Na — .

An identical blue - black complex was obtained by adding 0.5g of sodium borohydride to 0.40g of finely ground  $\text{H} \left[ \text{Rh}^{\text{III}} (\text{DMG})_2 \text{Cl}_2 \right]$  in 30 ml of de-aerated ice cooled 9 : 1 methanol water under an argon atmosphere (68). The blue precipitate was washed twice with cold argon or nitrogen saturated water and vacuum dried at 50°C and 1 m.m.Hg. pressure.

found C26.4%; H3.94%; N14.4%; Cl 0.57%.

Both products showed a tendency to form red compounds on exposure to air but not when refluxed in toluene (68). The former when washed with distilled water in air and dried in vacuo formed a red complex of similar composition.

found C26.9%; H4.23%; N15.3%; Cl 0.48%.

#### 17. Preparation of Chlorobis (dimethylglyoximato) triphenyl phosphine rhodium (III).

This yellow complex was prepared by the literature method (90). If rhodium trichloride is dissolved in 10 ml of ethanol instead of water  $\text{H} \left[ \text{Rh} (\text{DMG})_2 \text{Cl}_2 \right]$  is isolated and no triphenyl phosphine substitution occurs.

found Rh16.5%; C49.3%; H4.63%; N8.84%; P5.12%.

calculated for  $\left[ \text{Rh (DMG)}_2 \text{Cl P Ph}_3 \right]$

Rh16.3%; C49.5%; H4.63%; N8.88%; P4.91%.

18. Preparation of Triphenyl Phosphinebis (dimethylglyoximato) rhodium (I) Hydride.

The literature method could not be reproduced (68). Instead two 0.04g portions of sodium borohydride were added to 0.63g of finely divided  $[\text{Rh}^{\text{III}}(\text{DMG})\text{PPh}_3\text{Cl}]$  in suspension in 30 ml de-aerated, hydrogen saturated 9 : 1 methanol water. The mixture was heated. A dark purple solid was deposited as solvent evaporated. The suspension was cooled on ice and filtered. The precipitate was washed with hydrogen saturated water and dried in vacuo. The solid showed a new intense infra-red band at  $1980\text{ cm}^{-1}$  but could be a mixture of  $[\text{Rh}^{\text{I}}(\text{DMG})_2\text{PPh}_3\text{H}]$  and  $[\text{Rh}^{\text{II}}(\text{DMG})_2\text{PPh}_3]_2$  which have almost identical analyses.

found            C52.2%; H4.88%; N9.69%.  
 calculated for     $[\text{Rh}(\text{DMG})_2\text{PPh}_3\text{H}]$   
                     C52.3%; H5.22%; N9.38%.

19. Preparation of Dimeric Triphenylphosphinebis (dimethylglyoximato) rhodium (II).

A red solid showing no infra-red peak at  $1980\text{ cm}^{-1}$  was prepared by using the preceding method but using less reducing agent. The literature methods (55, 68) could not be reproduced.

found            C51.7%; H4.93%; N8.86%.  
 calculated for     $[\text{Rh}(\text{DMG})_2\text{PPh}_3]_2$   
                     C52.4%; H5.06%; N9.39%.

### Chapter III

#### The Uptake of Gaseous Oxygen by Aqueous Solutions Containing Cobalt Ions and Diaminoethane.

There has been much interest recently in the reaction of molecular oxygen with transition metal complexes (36).

In the case of certain cobalt (II) complexes, this reaction acts as a source of binuclear bridged peroxo (91, 92) and superoxo complexes (92, 93). A wide range of these dicobalt complexes have been characterised (32). In general, ammonia, polyamines, amino acids or dipeptides act as non-bridging ligands with, for example  $\text{NH}_2^-$ ,  $\text{OH}^-$ ,  $\text{O}_2\text{H}^-$ ,  $\text{SO}_4^{2-}$ ,  $\text{SeO}_4^{2-}$ ,  $\text{NO}_2^-$ ,  $\text{N}_2\text{O}_2^{2-}$ ,  $\text{HPO}_4^{2-}$  and  $\text{CH}_3\text{CO}_2^-$  as second or, more rarely, third bridges.

These complexes act as simple models for biological oxygen carriers (31, 34) which transport oxygen to the reduced cytochromes of the respiratory system. Their prototype, the biological carrier haemoglobin, (33) consists of four haem units each containing one high spin Fe (II) atom bound to protoporphyrin (IX) and to the imidazole ring of a histidine molecule in the globin protein (five coordinate Fe(II)). When oxygen uptake occurs, the 1 : 1 oxyhaemoglobin complex is formed, in which the oxygen molecule is bound "sideways" to low spin Fe(II).

The reversibility of oxygen uptake is thought to be due to the protective medium of low dielectric strength provided by the globin hydrophobic groups, which prevents irreversible oxidation of the iron atom.

A similar reversible oxygen uptake process occurs in Co(II)

systems with the above mentioned nitrogenous ligands. The substitution labile Co(II) complex rapidly absorbs oxygen forming the  $\text{Co}^{\text{III}} - (\text{O}_2^-)$  species. The latter may be formed in one step or in two steps, via the  $\text{Co}^{\text{II}} - (\text{O}_2)$  species in an intramolecular redox process. When the chelating ligand is bisacetylacetonethylenediimine, the 1 : 1  $\text{Co}^{\text{III}} - (\text{O}_2^-)$  species, analogous to oxyhaemoglobin in stoichiometry is stable and isolable (94, 95). In most other cases, the  $\text{Co}^{\text{III}} (\text{O}_2^-)$  species reacts with a second  $\text{Co}^{\text{II}}$  species to saturate the electron affinity of oxygen forming the  $\text{Co}^{\text{III}} \text{O}_2^{2-} \text{Co}^{\text{III}}$  species. These binuclear complexes are substitution inert but the reversibility of the charge transfer process allows reduction back to Co(II) with the release of oxygen. Thus the cobalt (II) complexes can act as reversible oxygen carriers in a manner similar to haemoglobin.

This chapter reports the results of attempts to study the kinetics of the uptake of oxygen by aqueous solutions of cobaltous ions and diaminoethane and the nature of the initial reaction products, one of which probably contains a bridging diaminoethane group. The effect of added anions, solvent, volume, concentration, ionic strength and temperature on the kinetics of oxygen uptake, stoichiometries, preparations of trans- $[\text{Co}(\text{en})_2 \text{Cl}_2] \text{Cl}$  and  $[\text{Co}_2 (\text{NH}_3)_8 (\text{OH})_2] (\text{ClO}_4)_4$  were performed earlier by Miss S.W. Foong.

The experiments to determine stoichiometric ratios were repeated by the author and reproduced the earlier results. The results of this work were published in a paper by S.W. Foong, J.D. Miller and F.D. Oliver ( J. Chem. Soc. (A), 1969, 2847 ).

Aqueous solutions containing a cobalt (II) salt and diaminoethane, when shaken under an atmosphere of oxygen took up oxygen very rapidly, irrespective of whether the anion present was  $\text{Br}^-$ ,  $\text{Cl}^-$ ,

$\text{ClO}_4^-$ ,  $\text{NO}_2^-$  or  $\text{NO}_3^-$  to give solutions with a characteristic deep brown colour. By varying the ratios of the metal ion to the ligand, the initial reaction was shown to involve  $\text{Co}^{2+} : \text{en} : \text{O}_2$  in the ratio 2 : 5 : 1. Typical results are shown below.

The stoichiometry of the uptake of oxygen by  $\text{Co}^{\text{II}}/\text{en}$   
aqueous solutions at  $25.0^\circ\text{C}$   $\mu = 1.00(\text{NaClO}_4)$   $0.0872 \text{ M Co}(\text{ClO}_4)_2$

Ratio	<u><math>\text{Co}^{\text{II}} : \text{en}</math></u>	<u><math>\text{Co}^{\text{II}} : \text{O}_2</math></u>	<u><math>\text{en} : \text{O}_2</math></u>
	1 : 0.50	1 : 0.10	1 : 0.20
	1 : 1.00	1 : 0.20	1 : 0.20
	1 : 1.25	1 : 0.26	1 : 0.21
	1 : 1.50	1 : 0.29	1 : 0.19
	1 : 2.00	1 : 0.39	1 : 0.20
	1 : 2.50	1 : 0.50	1 : 0.20
	1 : 3.00	1 : 0.50	1 : 0.17

These results were obtained by mixing aqueous solutions of cobalt (II) perchlorate and the ligand (which had been allowed to stand separately under oxygen), under an excess of oxygen at a pressure of one atmosphere; (Apparatus Gallenkamp H.R.160) the temperature of the mixture was kept at  $25^\circ\text{C}$ . When gas uptake was complete, the volume of gas taken up was measured manometrically. The overall stoichiometry is unaffected by the ionic strength of the medium, while pH titration shows that, after oxidation, a solution with a cobalt ligand ratio of 2 : 5 contains less than 3% of the free base.

Experimental conditions under which the uptake of oxygen gas is independent of the conditions of agitation of the reaction vessel could not be found for the anions investigated. That is, the rate of reaction is determined by the rate of solution of the gas.

In an attempt to find such conditions, the solvent, volume, concentration, ionic strength of the solution and temperature were varied. Assuming the reaction scheme shown in Figure 3 is operating, applying the steady state hypothesis for the  $\text{MO}_2$  intermediate, the relationship:-

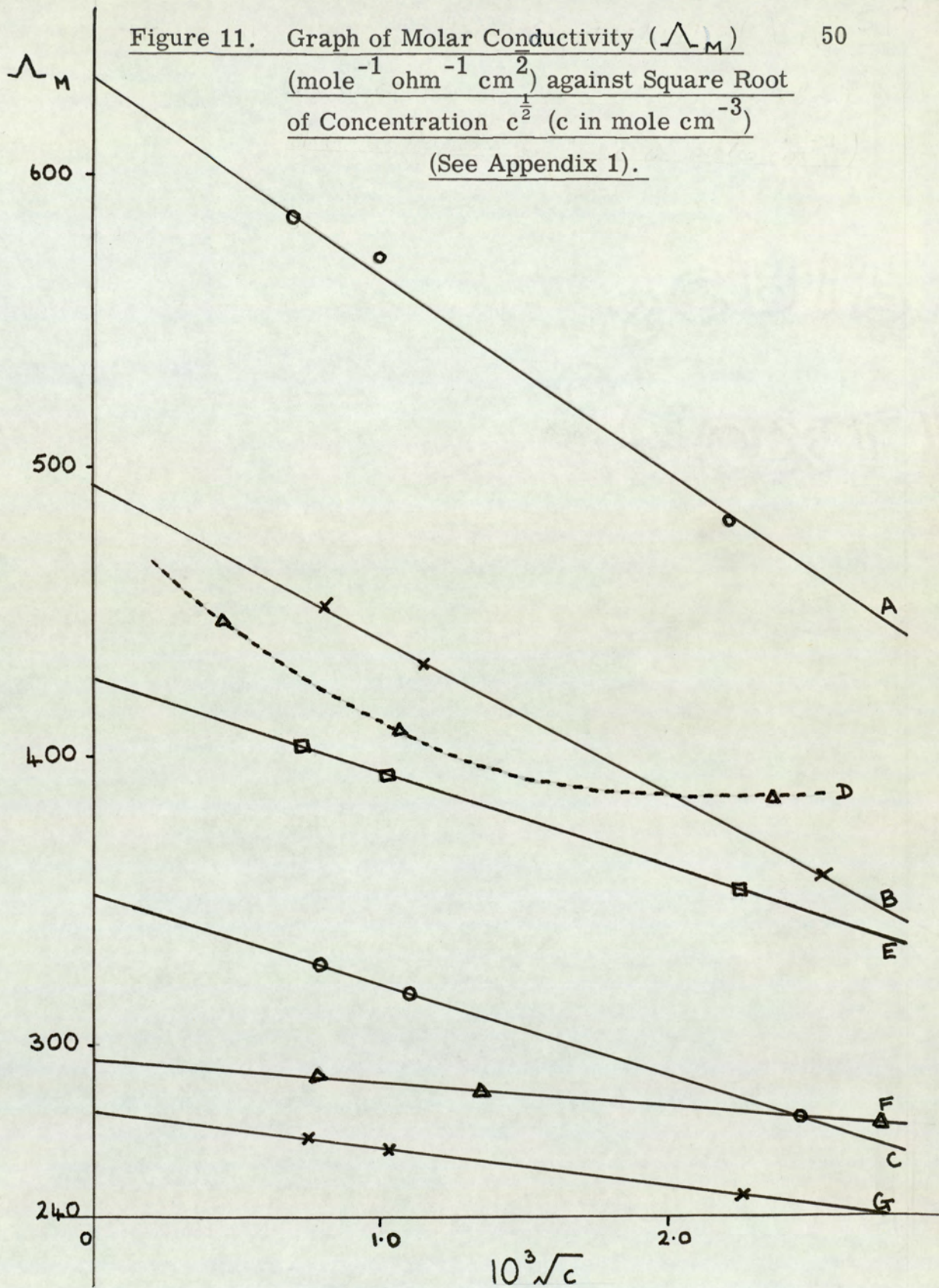
$$\frac{d}{dt} [\text{MO}_2 \text{ M}] = \frac{k_2 k_3 [\text{M}]^2 [\text{O}_2]}{k_2 + k_3 [\text{M}]}$$

is obtained (96, 97). If the overall rate equation for reactions (2) and (3) contains oxygen to a higher power than for reaction (1) then reactions (2) and (3) will become rate determining at lower oxygen partial pressure. In fact, lowering the partial pressure of oxygen ( $\frac{1}{2}$ ,  $\frac{1}{4}$ ,  $\frac{1}{8}$  of an atmosphere) made the rate of oxygen uptake more dependent on the efficiency of agitation. Even when agitation was such that the reaction was complete in less than two minutes, reproducible rate data for differing agitation conditions did not exist. Thus, it appears that the reaction times suggested for the oxidation of diaminoethane cobalt (II) solutions by oxygen are unnecessarily long, (98, 99). A repeat of the literature preparation of trans  $[\text{Co}(\text{en})_2 \text{Cl}_2] \text{Cl}$  in which oxygen was passed for only ten minutes, gave a 67% yield (based on en) of the product.

Subsequent work by Wilkins and co-workers has shown that oxygen uptake by cobaltous complexes with amines (96) and chelating ligands such as L- and D,L- histidine, diethylenetriamine, histamine, 2 - (amino methyl) pyridine, triethylenetetramine and ethylenediamine (97, 100, 101) is complete in the order of seconds or milliseconds. The left hand mechanism of Figure 3 is operating, in several cases, different chelated forms of type  $\text{Co N}_{6-x} \text{O}_x$  (where x is 0 to 2) participate, with differing activities, in oxygen uptake. For example,

$$[\text{Co}^{\text{II}}(\text{dien})_2]^{2+} \quad (k_2 = 1.2 \times 10^3 \text{ mole}^{-1} \text{ sec}^{-1}) \text{ and}$$

$$[\text{Co}^{\text{II}}(\text{dien})(\text{dien} - \text{H})\text{H}_2\text{O}]^{3+},$$



(D)  $[\text{Co}_2(\text{NH}_3)_8(\text{OH})_2](\text{ClO}_4)_4$  (prepared as in reference 103).

(E)  $\text{LaCl}_3$  (from reference 73).

(F)  $[\text{Co}(\text{NH}_3)_5\text{Cl}]\text{Cl}_2$  (from reference 104).

(G)  $\text{BaCl}_2$  (from reference 73).

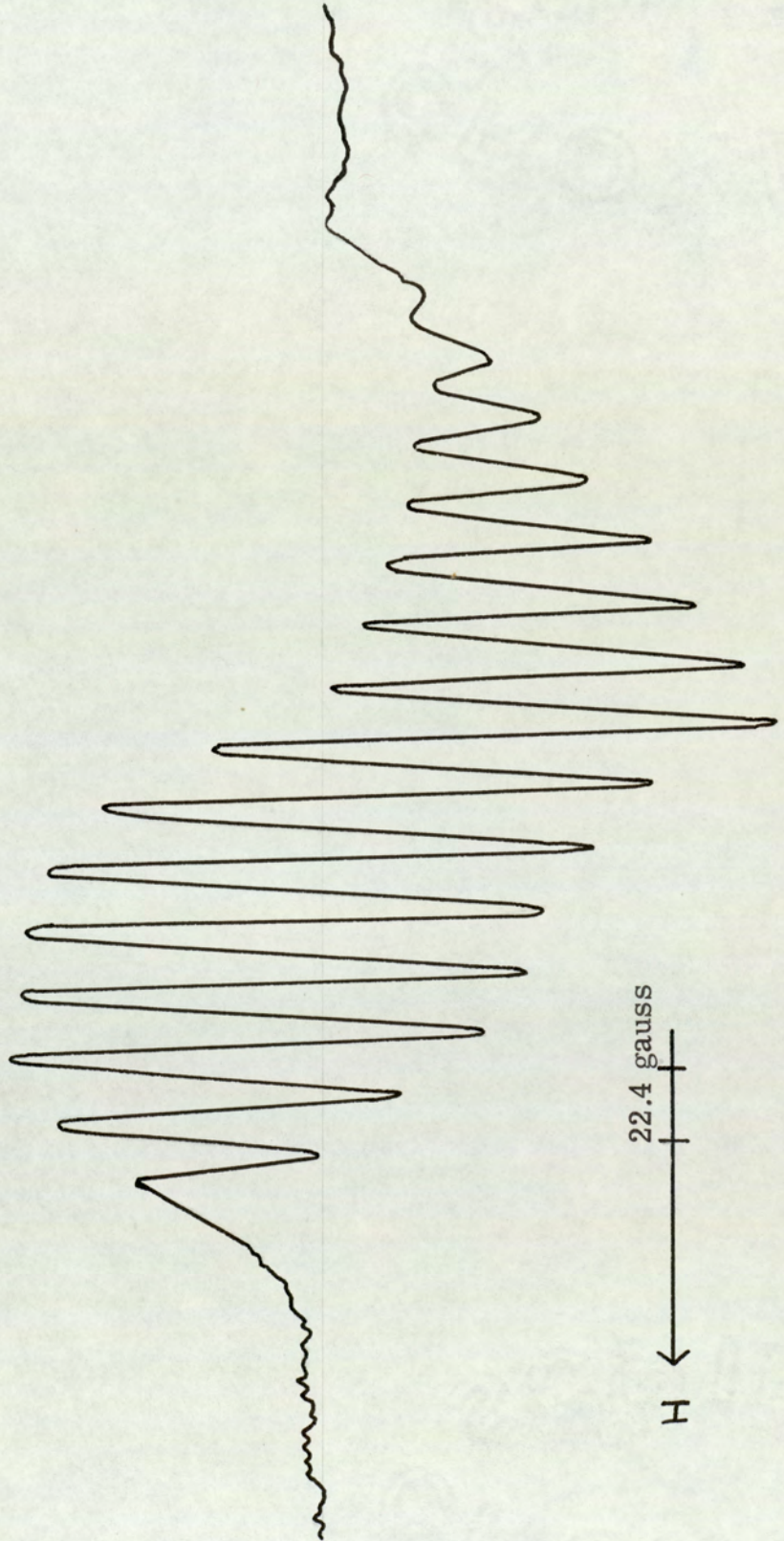
$\left[ \text{Co}^{\text{II}}(\text{trien}) (\text{H}_2\text{O})_2 \right]^{2+}$  ( $k_2 = 2.5 \times 10^4 \text{ mole}^{-1} \text{sec}^{-1}$ ) and  
 $\left[ \text{Co}^{\text{II}}(\text{trien}) (\text{OH}) (\text{H}_2\text{O}) \right]^+$  ( $k_2 = 2.8 \times 10^5 \text{ mole}^{-1} \text{sec}^{-1}$ ),  
 and the  $\text{Co}(\text{L})_3$  and  $\text{Co}(\text{L})_2$  histamine ( $k_2 = 6.8 \times 10^4$ ,  $1.8 \times 10^4$   
 $\text{mole}^{-1} \text{sec}^{-1}$  respectively) and 2- (aminomethyl) pyridine  
 complexes ( $k_2 = 47$ ,  $7.2 \times 10^2 \text{ mole}^{-1} \text{sec}^{-1}$  respectively).

However, in the Co (II) ethylenediamine system, it was found  
 that the rate of oxygen uptake can be explained solely in terms of  
 $\left[ \text{Co}^{\text{II}}(\text{en})_2 (\text{H}_2\text{O})_2 \right]^{2+}$  as the active species (97) ( $k_2 = 4.7 \times$   
 $10^5 \text{ mole}^{-1} \text{sec}^{-1}$ ).

When a quantity of cerium (IV) equivalent to half the initial  
 cobalt (II) was added to a freshly oxidised solution containing a  
 ratio of cobalt (II) : (en) of 2 : 5 an olive green paramagnetic  
 compound (A)  $\left[ \text{Co}_2 \text{en}_5 (\text{O}_2) \right] (\text{NO}_3)_5$  was obtained ( $\mu_{\text{eff.}} =$   
 $1.39 \text{ B.M. per Co}_2 \text{ unit}$ ). This compound showed a sharp infra-  
 red peak at  $820 \text{ cm}^{-1}$  which was ascribed to the  $\mu$ -superoxo  
 group (75). Aqueous solutions of (A) showed absorption maxima  
 at 311 ( $\epsilon$  3.540) 479 ( $\epsilon$  274) and 682 nm. ( $\epsilon$  230) and gave  
 conductivity measurements consistent with a 1 : 5 electrolyte  
 (73, 102, 103, 104) (see Figure 11) and an E. S. R. spectrum  
 containing 15 lines with the binomial distribution of intensities  
 (peak separation =  $19.97 \pm 0.07$  gauss,  $g = 2.055 \pm 0.027$  see  
 Figure 12). The derivative spectrum showed a definite asymmetry,  
 broadening to low field (105). No hyperfine structure due to the  
 coupling of the unpaired electron with the nitrogen atoms of the  
 ethylenediamine bridge was observed. Thus, compound (A) is  
 thought to contain a  $\mu$ -superoxo-dicobalt (III) cation. The E. S. R.  
 spectrum is in agreement with spectra reported for the cations

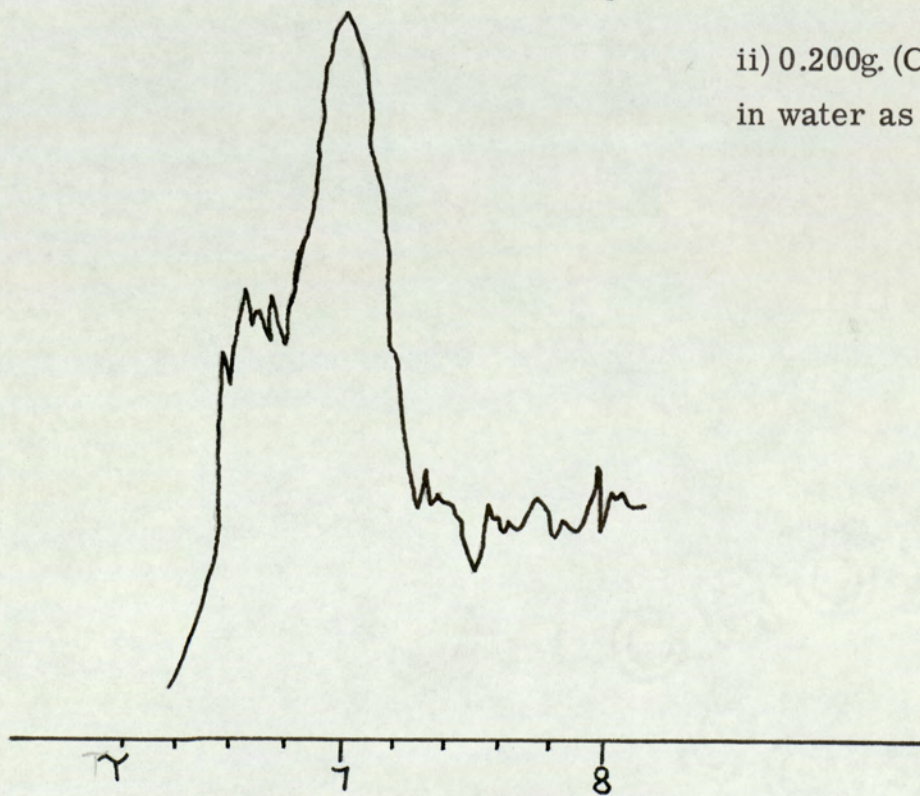
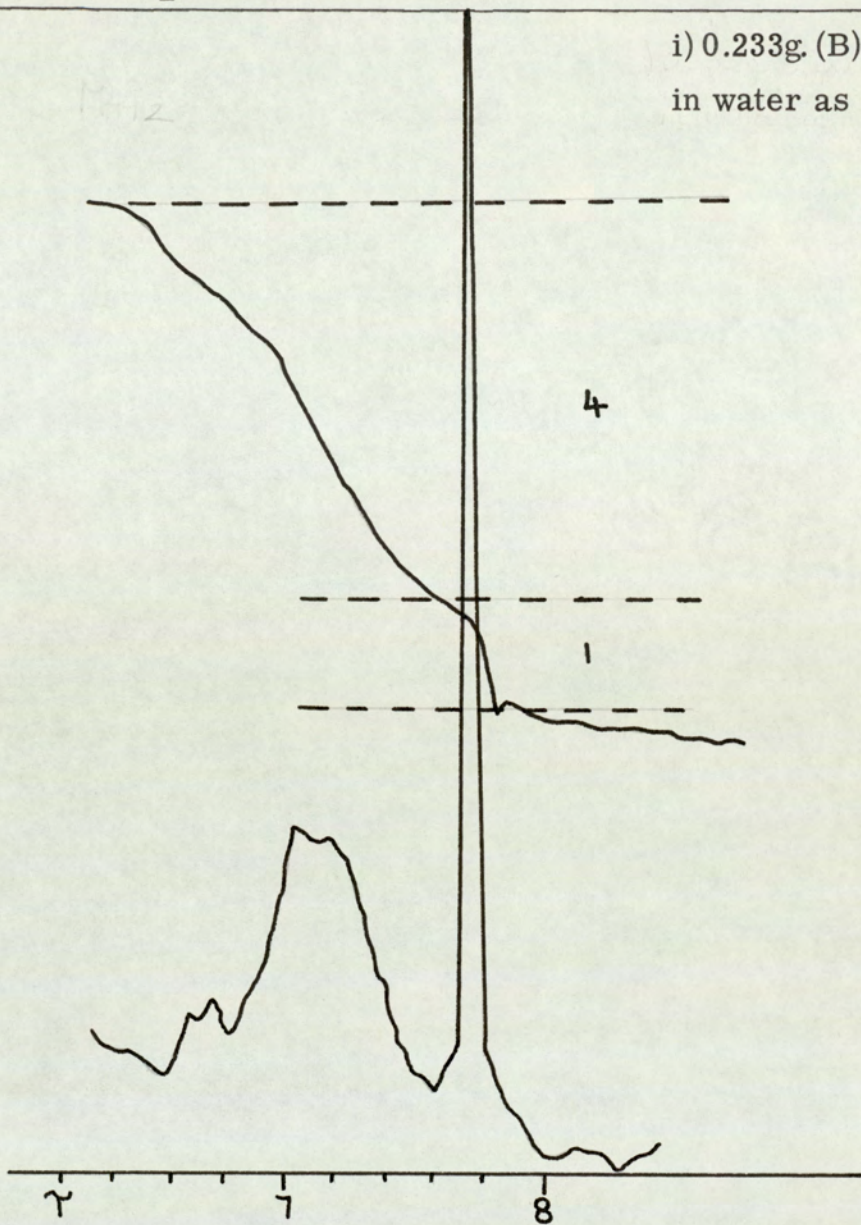
$\left[ (\text{NH}_3)_5 \text{Co} (\text{O}_2) \text{Co} (\text{NH}_3)_5 \right]^{5+}$  and  $\left[ (\text{NH}_3)_4 \text{Co} (\text{O}_2) (\text{NH}_2) \text{Co} (\text{NH}_3)_4 \right]^{4+}$   
 (105, 106) both of which contain the  $\mu$ -superoxo-dicobalt (III) group.

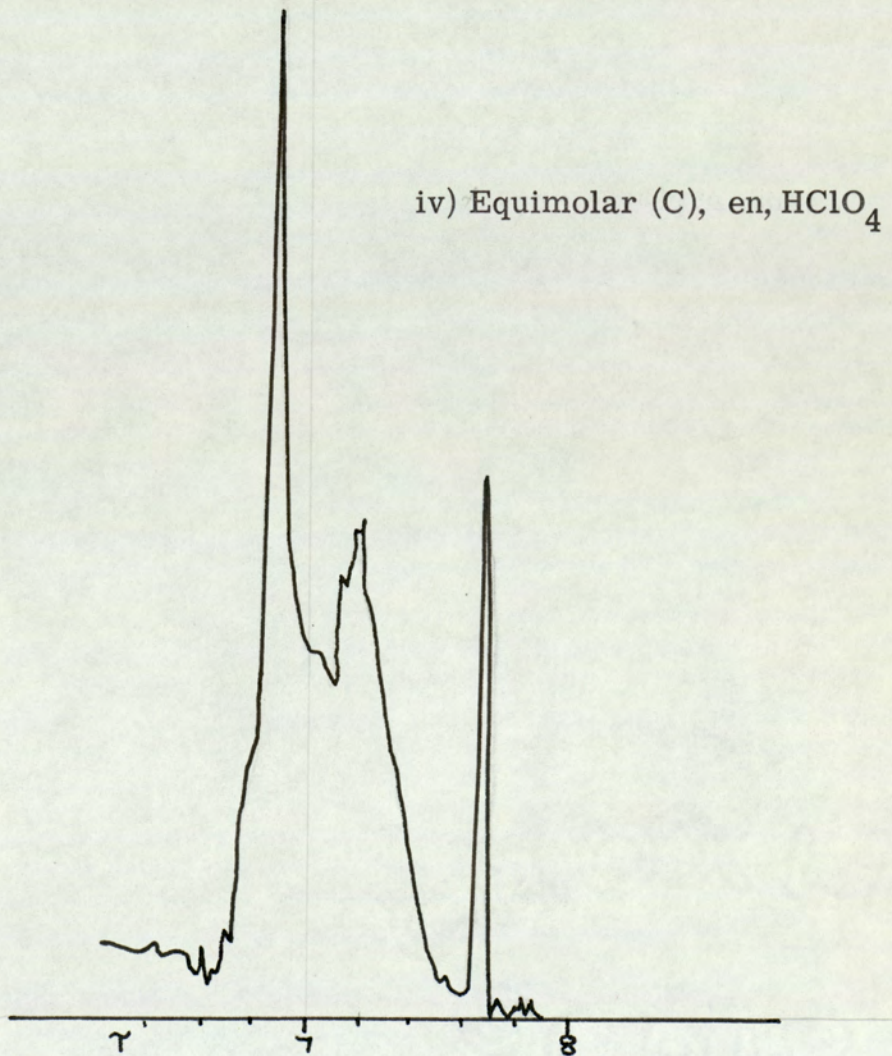
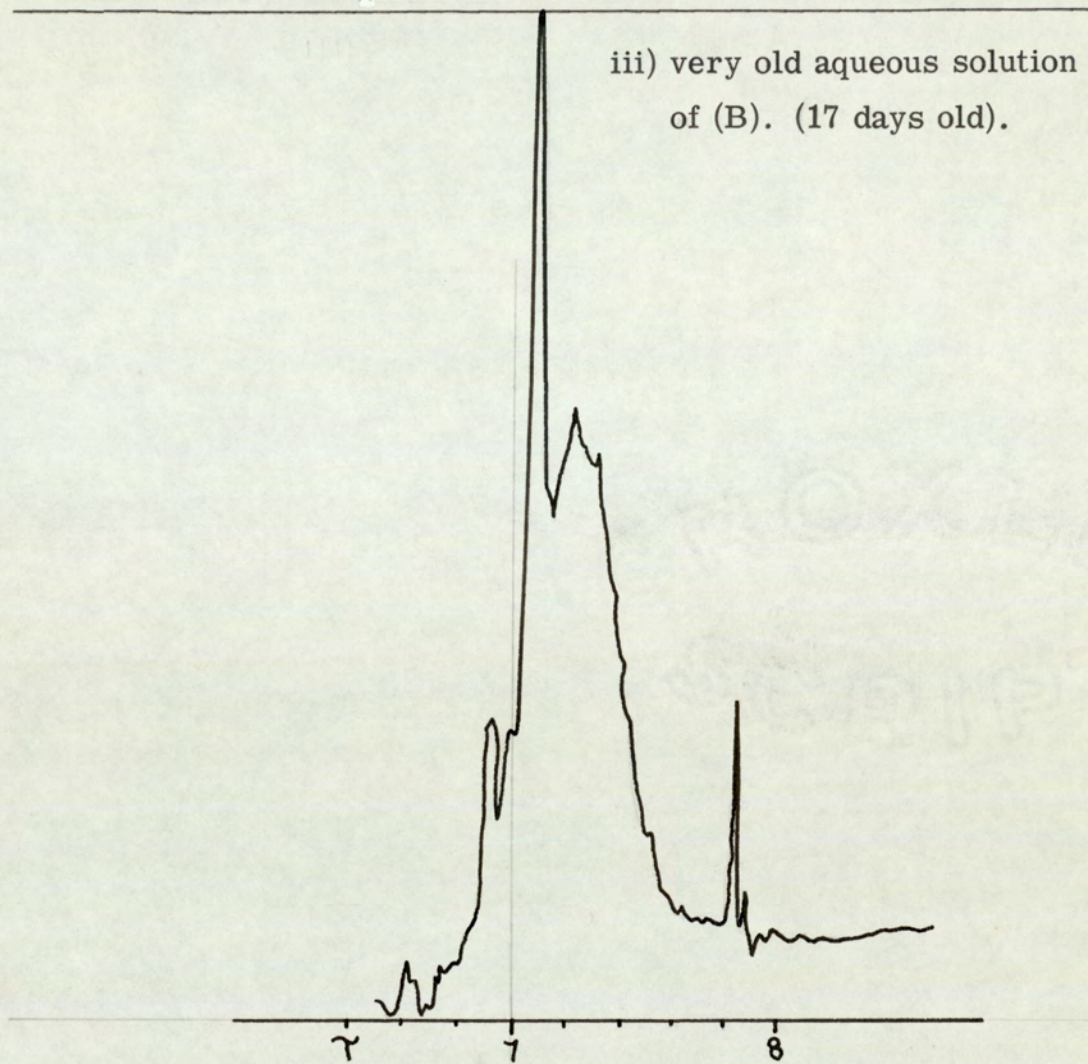
Figure 12. E.S.R. Spectrum of  $[(en)_2Co\mu O_2\mu enCo(en)_2]^{5+}$   
(Scanning Rate 25 gauss per minute).



Evaporation under reduced pressure (at less than 40°C) of the aqueous solution obtained from the reaction of a 2 : 5 cobalt (II) perchlorate / ethylenediamine solution with oxygen gave compound (B) as a dark brown solid. No method of recrystallising or otherwise purifying this compound was found. However, its oxidation to (A) demonstrates the presence of a bridging oxygen group. Analytical results for (B) were consistent with the empirical formula  $[\text{Co}_2(\text{en})_5(\text{O}_2)] 4\text{ClO}_4 \cdot \text{H}_2\text{O}$ . The formation of B is partially reversible as treatment with 2.0 M perchloric acid causes evolution of 84.6% of the oxygen content as oxygen gas. That is decomposition to  $\text{Co}^{\text{II}}$  and oxygen is incomplete, some  $\text{Co}^{\text{III}}$  and  $\text{H}_2\text{O}_2$  probably being formed (32). The absence of a purification technique made it impossible to distinguish between  $\text{Co}^{\text{II}}$  contamination and temperature independent paramagnetism (107) as the cause of the weak paramagnetism ( $\mu_{\text{eff.}} = 1.0 \text{ B M} / \text{Co}_2 \text{ unit.}$ ) For the same reason, the possibility that this product is a mixture cannot be entirely ruled out, although this seems unlikely. However, several different samples gave reproducible magnetic and analytical results. All magnetic measurements were made at ambient temperature. A distinction between  $\text{Co}^{\text{II}}$  contamination and temperature independent paramagnetism should be possible with a variable temperature balance. Aqueous solutions of (B) showed an absorption maximum at 360 nm ( $\epsilon$  2590) with a weak shoulder at 510 nm (340); conductivity results were consistent with it's being a 1 : 4 electrolyte (see Figure 11). Both compounds (B) and (C) show a broad weak infra-red peak at  $800 \text{ cm}^{-1}$ . Therefore (B) is thought to contain a  $\mu$ -peroxo-dicobalt (III) cation.

When 50% aqueous ethanol was used as the solvent for oxygen uptake experiments compound (C)  $[\text{Co}_2(\text{en})_4(\text{O}_2)(\text{OH})] (\text{ClO}_4)_3 \cdot \text{H}_2\text{O}$  was obtained. Again this dark brown compound was weakly paramagnetic ( $\mu_{\text{eff.}} = 0.81 \text{ B M per Co}_2 \text{ unit.}$ ) The aqueous solutions showed absorption maxima at 273 ( $\epsilon$  4,560), 357 (4230)

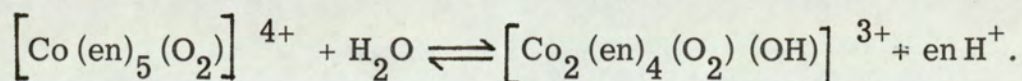




and 649 nm (90); its conductivity results were consistent with a 1 : 3 electrolyte (see Figure 11). The infra-red spectrum showed a sharp peak at  $3570 \text{ cm}^{-1}$  which was ascribed to the  $\mu$ -hydroxo group.

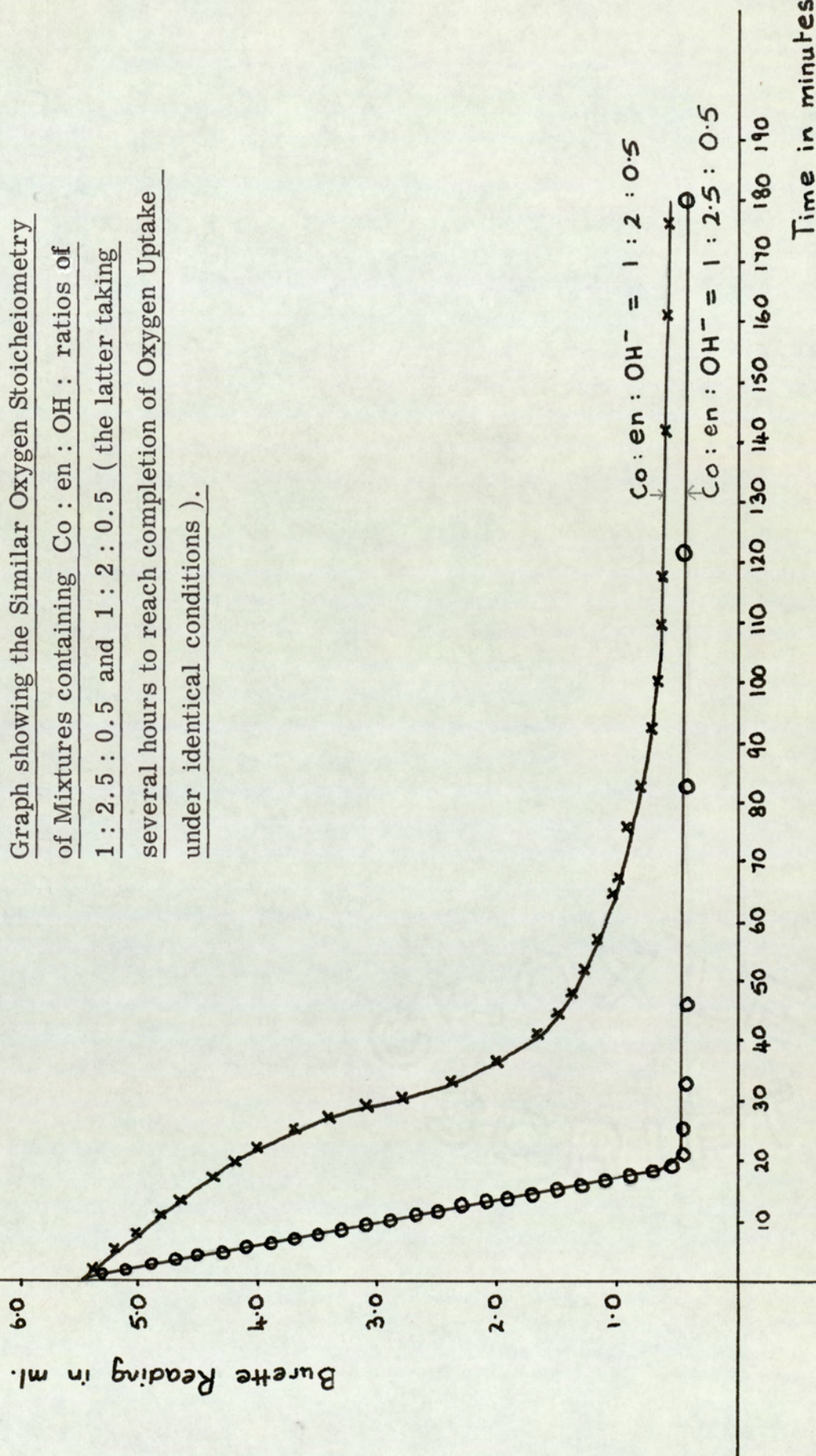
From these observations and the stoichiometry of the reaction, we deduce that the initial product of the reaction is the  $\mu$ -peroxo- $\mu$ -diaminoethano-tetradiamino ethane-dicobalt (III) cation (B). This complex was shown to equilibrate with the equivalent  $\mu$ -peroxo- $\mu$ -hydroxo species (C), mentioned above, by N.M.R., stoichiometric and pH experiments.

The  $^1\text{H}$  N.M.R. spectra of freshly prepared aqueous solutions after oxygen uptake by  $\text{Co}^{\text{II}} : \text{en}$  (2 : 5) (0.27 M) were identical to those of fresh solutions of compound (B) (see Figure 13(a) and (b).) The methylene protons of the ligand gave an incompletely resolved peak system at  $\tau$  7.22 and a singlet at  $\tau$  7.82 (relative intensities 4 : 1) measured against an external  $\text{Si} : \text{Me}_4$  standard. The peak at  $\tau = 7.82$  was absent from solutions of (C). Identical spectra were also obtained from old solutions of (B) or old solutions containing a 1 : 1 : 1 ratio of (C), ethylenediamine and perchloric acid. In these cases, the higher field methylene signal was much reduced in intensity relative to the other peak system. Therefore the peak at  $\tau$  7.82 is thought to be diagnostic for the  $\mu$ -diaminoethane unit; its decay demonstrates the following equilibrium



When a solution containing a 1 : 2 ratio of  $\text{Co}^{\text{II}} : \text{en}$  takes up oxygen, reaction ceases when the supply of free ligand is exhausted to leave 20% of the total cobalt as  $\text{Co}^{\text{II}}$ . If  $\text{OH}^-$  is present a further small quantity of oxygen is taken up during a period of several hours as the establishment of the equilibrium liberates some free diamine. This phenomenon does not occur at  $\text{Co}^{\text{II}} : \text{en}$

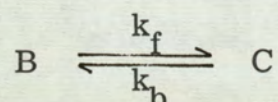
Figure 14.  
 Graph showing the Similar Oxygen Stoichiometry  
 of Mixtures containing Co : en : OH<sup>-</sup> : ratios of  
 1 : 2.5 : 0.5 and 1 : 2 : 0.5 ( the latter taking  
 several hours to reach completion of Oxygen Uptake  
 under identical conditions ).



Time in minutes.

ratios of 2 : 5 or above (see Figure 14).

After an aqueous solution with a metal : ligand ratio of 2 : 5 has taken up oxygen, the pH of the solution is slightly acid. In order to maintain with time, the pH of the solution, acid must gradually be added. By following the rate of this addition at pH 8.2 and 25°C, the equilibrium constant for the reaction



was found to be  $0.43 \pm 0.02$ . The rate of disappearance of B is given by :-

$$\frac{dB}{dt} = k_b (B_0 - B_t) - k_f B_t$$

where  $B_0$  is the initial concentration of B,  $B_t$  the concentration of B at time  $t$  and  $K$  the equilibrium constant. Rearrangement gives

$$\frac{dB}{dt} = -(k_b + k_f) \left( B_t - \frac{B_0}{1+K} \right)$$

On integration the relationship :-

$$\log_e \left\{ \frac{K}{(1+K) \frac{B_t}{B_0} - 1} \right\} = (k_b + k_f) t \text{ is obtained.}$$

Graphs of  $\log_{10} \left\{ \frac{1}{(1+K) \frac{B_t}{B_0} - 1} \right\}$  against time were linear

(see Figure 15). From the gradient, the pseudo first order rate constant for the conversion of (B) to (C) was calculated

$$k_f = (3.62 \pm 0.46) \times 10^{-4} \text{ sec}^{-1}. \text{ The intercept gives the}$$

equilibrium constant. Michailidis and Martin also report that uptake of oxygen by  $\text{Co}^{\text{II}}$  and ethylenediamine solutions to generate complex (C) proceeds with the liberation of one equivalent of acid per mole of (C) (108).

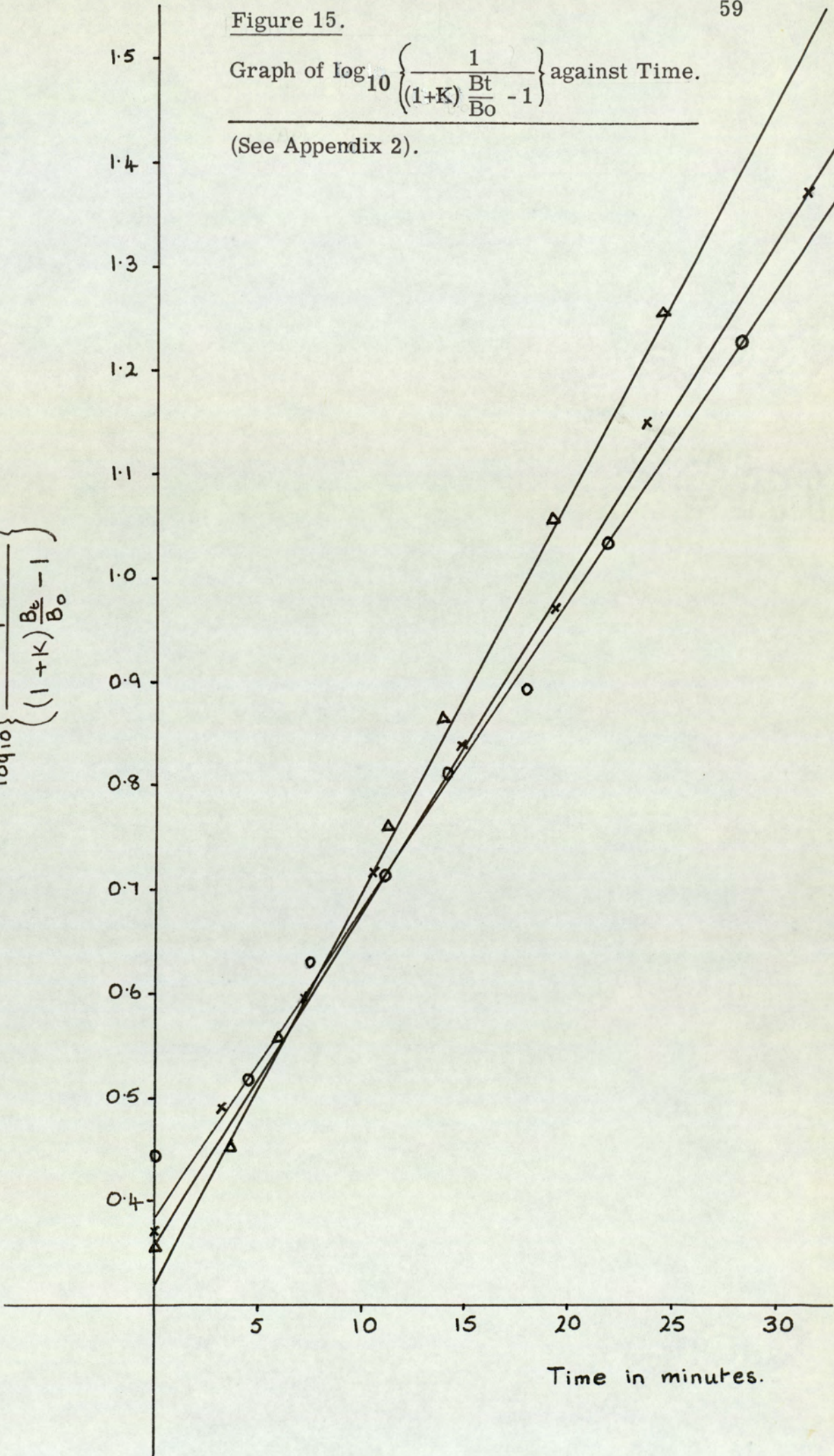
Solutions of (B) and (C) slowly take up carbon dioxide at room temperature from the air or under a pressure of one atmosphere of the gas in a closed system, when uptake is complete in two days.

Figure 15.

Graph of  $\log_{10} \left\{ \frac{1}{(1+K) \frac{Bt}{B_0} - 1} \right\}$  against Time.

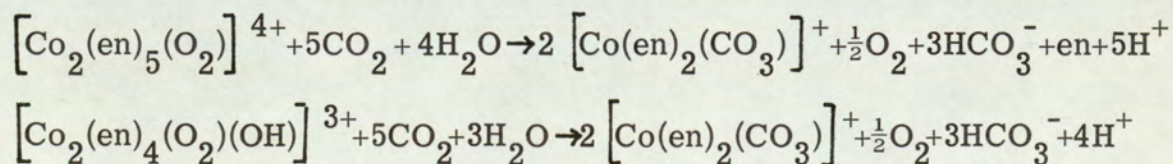
(See Appendix 2).

$$\log_{10} \left\{ \frac{1}{(1+K) \frac{B_t}{B_0} - 1} \right\}$$



The pink  $[\text{Co}(\text{en})_2(\text{CO}_3)]^+$  cation is the end product. Garbett and Gillard (92) were also unable to isolate the solid  $\mu$ -peroxo- $\mu$ -carbonato-dicobalt complex from the analogous  $\mu$ -hydroxo species and carbonate ion. By analogy with the reactions of  $\text{SO}_2$ ,  $\text{SeO}_2$  and  $\text{NO}_2$  with  $\mu$ -peroxo species to form  $\mu$ -sulphato,  $\mu$ -selenato and  $\mu$ -nitrito complexes, reaction probably occurs by carbon dioxide attack at the peroxo bridge. This is followed by oxygen - oxygen bond cleavage to form the acido aquo complex, which then reacts with a second mole of carbon dioxide.

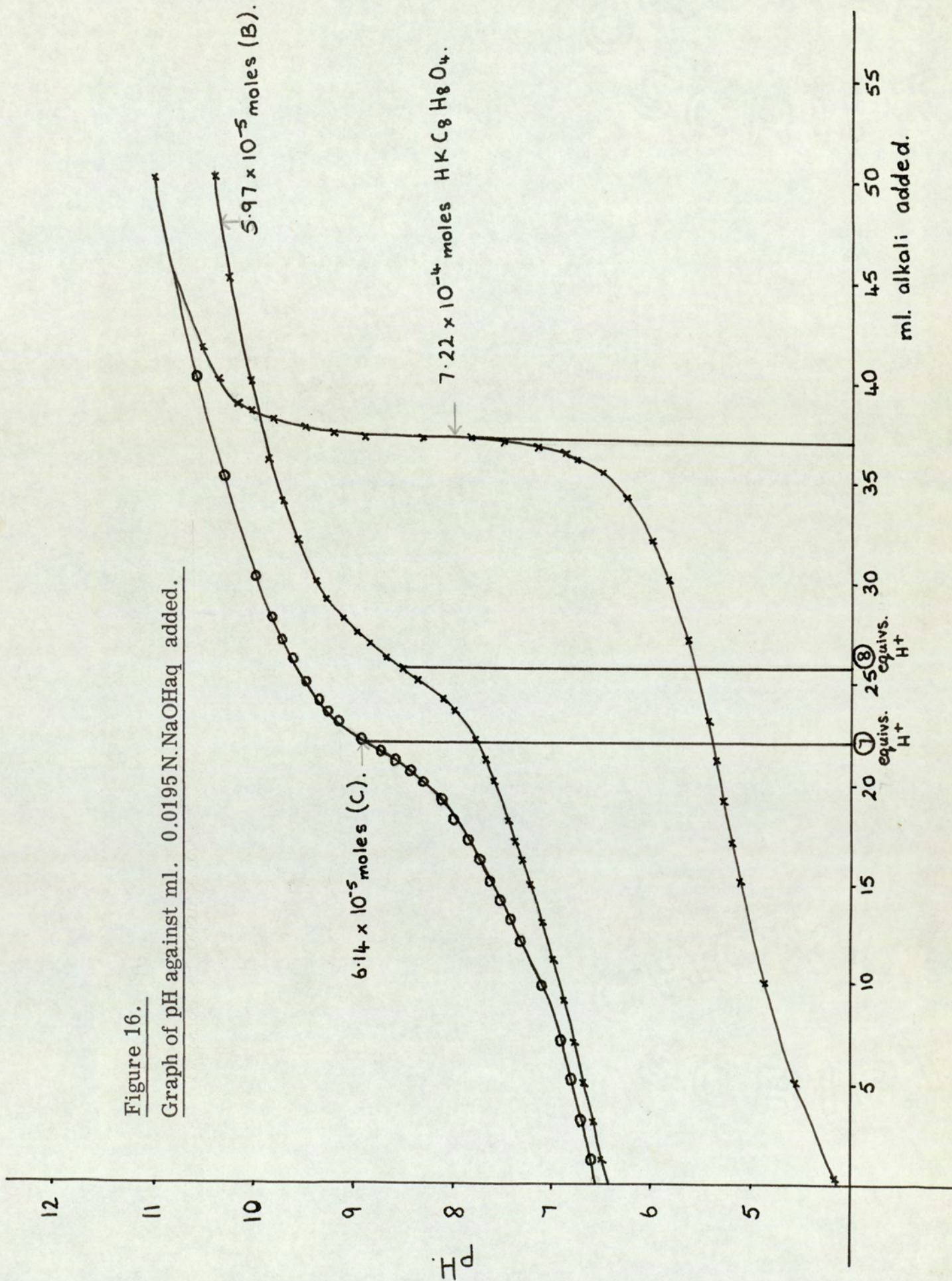
At concentrations of  $5.9$  to  $6.9 \times 10^{-3}$  M both (B) and (C) show a decrease in the volume of gas corresponding to 4.5 moles of gas per mole of the binuclear species. Mass spectroscopic analysis of the final gas showed that oxygen had been liberated. From concentrated aqueous solutions 80% yields of crystalline  $[\text{Co}(\text{en})_2(\text{CO}_3)]\text{ClO}_4 \cdot \frac{1}{2} \text{H}_2\text{O}$  were obtained. The extinction coefficients at 370 ( $\epsilon$  142) and 515 nm (150) were then used to show that for the weaker solutions conversion of 1 mole of the binuclear complex to 2 moles of the carbonato complex was quantitative. pH titrations for the final solutions against standard sodium hydroxide (see Figure 16) show that carbon dioxide uptake by (B) and (C) releases 8 and 7 equivalents of acid respectively. pH titration of a solvent blank showed that no correction was needed for acidity due to dissolved carbon dioxide gas. These results provide additional evidence for the suggested stoichiometry at the low initial concentrations.



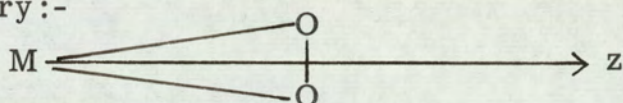
It can be concluded from these studies on the reaction between aqueous solutions containing 1, 2 - diaminoethane and cobalt(II) ions in the presence of a variety of anions that oxygen is taken up

Figure 16.

Graph of pH against ml. 0.0195 N. NaOH aq. added.



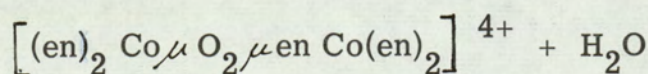
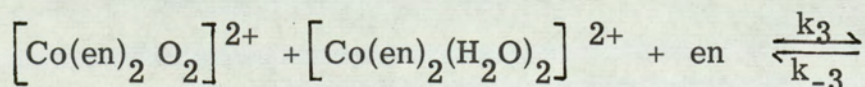
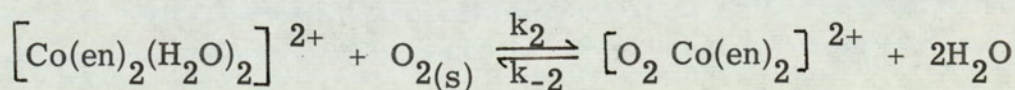
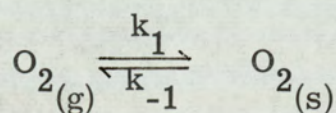
very rapidly by  $[\text{Co(en)}_2(\text{H}_2\text{O})_2]^{2+}$  (97). This is to be expected, since the ease of inner sphere electron transfer from a metal d orbital into oxygen  $\pi$  antibonding orbitals to form a 1 : 1 complex of geometry :-



increases in the order  $d_{x^2-y^2}$ ,  $d_{xy} < d_{z^2} < d_{yz}$ ,  $d_{xz}$  (36)

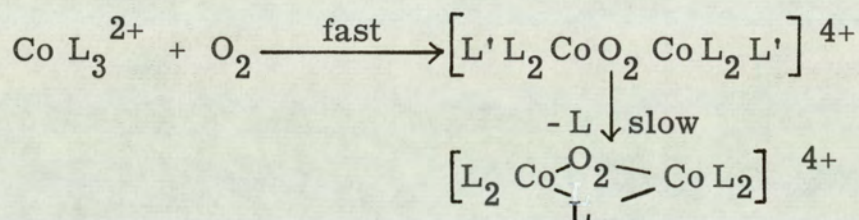
$\text{Co}^{2+}$  (and  $\text{Fe}^{2+}$  as stated by Fallab (36) ) has d-electrons in  $d_{xz}$  and  $d_{yz}$  and therefore rapidly absorbs oxygen, unlike  $\text{VO}^{2+}$  chelates with a single unpaired electron in  $d_{xy}$  (as calculated by Ballhausen (109) ). The original high spin cobalt (II) complex ( $t_{2g}^5 e_g^2$ ) is thought to undergo spin pairing to form low spin cobalt (II) ( $t_{2g}^6 e_g^1$ ) which then donates the  $e_g$  electron to oxygen. This mechanism is preferred to loss of an electron from high spin cobalt (II) to form the unstable cobalt (III) species with two unpaired spins ( $t_{2g}^5 e_g^1$ ) which subsequently undergoes spin pairing, since this latter route has a high energy requirement(110).

It is suggested that a slower reaction follows oxygen uptake yielding the isolated cation (B) ; that is, the following reaction mechanism :-



$\left[ \text{Co(en)}_2(\text{enH})\text{H}_2\text{O} \right]^{2+}$  is an alternative possibility to  $\left[ \text{Co(en)}_2(\text{H}_2\text{O})_2 \right]^{2+} + \text{en}$  (where enH is the unidentate form of the ligand).

An analogous slow reaction apparently independent of metal, ligand and hydroxide concentrations was observed in the reaction of tris-complexes by Miller, Simplicio and Williams (97).



L = (dien), (hist) (en) and (amp) and L' is the unidentate form of the ligand.

Other reports of a bridging polyamine (36) and diamino-ethane group (111) have been made. A similar intermediate  $\left[ \text{Cu}_2(\text{en})_3(\text{OOH}) \right]^{3+}$  has been postulated to account for the decomposition of hydrogen peroxide when catalysed by diamino-ethane and copper (II) salts (112).

In the case of complex (B) no definite evidence is available to distinguish between a  $\mu$ -diaminoethane unit utilising one or both nitrogen atoms as ligand donor atoms. However, it is clear that the bridging diamine has not been deprotonated. The use of both nitrogen atoms is postulated as the  $^1\text{H N.M.R.}$  spectrum favours this structure.

The cation (B) slowly equilibrates with the equivalent  $\mu$ -peroxo- $\mu$ -hydroxo species (C) while it may be oxidised to a  $\mu$ -superoxo- $\mu$ -diaminoethane complex (A). This oxidation strongly suggests the existence of a peroxo bridge

in (B) and confirms the stoichiometry maximum of 2 Co to 5 en.

The peroxo bridges of both (B) and (C) are attacked by carbon dioxide to give the carbonato-bis-diaminoethane-cobalt (III) salt.

## Chapter IV .

### A Study of the Reaction between Oxygen and Manganese (II) Complexes of N, N' - Disalicylaldehyde - 1, 3 - Propanediimine.

This study was undertaken in view of the reported reversible 1 : 1 coordination of oxygen, carbon monoxide and nitrogen with this manganese (II) chelate. (78). Therefore, the complex was thought to be potentially useful as a model for reversible biological oxygen carriers. Analogous Co(II) tetradentate Schiff base complexes, by virtue of the  $E^0$  values and vacant coordination positions, act as reversible 1 : 1 or 1 : 2 oxygen carriers (33, 113, 114). Also, manganese is known to be essential in the oxygen evolving systems of photosynthesis, although oxygen uptake by the manganese (II) phthalocyanine model complex results in irreversible formation of phthalocyanine - oxo - pyridine - manganese (IV) and phthalocyanine ring oxidation (115).

As mentioned in the introduction, comparison of the properties of salicylaldoximes with cobaloximes as models for vitamin B<sub>12</sub> coenzyme has brought to light many factors governing the physico-chemical properties and analogies between the systems. Study of the structure of this manganese salicylaldoxime complex is of relevance in this field.

The reported reaction between this manganese (II) chelate and nitrogen is also of interest in view of the current trend in the field of nitrogen fixation towards the use of left hand side transition metals, which form less stable and potentially more easily hydrogenated nitrogen complexes.

There has been considerable academic interest in the structures of transition metal / Schiff base complexes. The stereochemistry

of the ligand, (116, 117, 118), the molecular complexity (118, 119) and magnetochemistry of the complexes (120) have been studied. It has been found that the coordination number of the metal can be increased by dimerisation, (121, 122) combination with monodentate basic ligands, (113, 123), and reactions with small gaseous molecules for example oxygen (113) and nitric oxide (124). The stoichiometry of the reaction of oxygen with such complexes in coordinating and non-coordinating solvents has also been studied (113, 125, 126).

In particular, in the range of tetradentate Schiff base ligands formed by the condensation of two moles of salicylaldehyde and one mole of an  $\alpha, \omega$  - diamine  $H_2N(CH_2)_xNH_2$ , the stereochemistry of the transition metal complex is found to vary from planar monomeric to tetrahedral monomeric to polymeric as  $x$  increases. The great length of the methylene chain prevents both ends of the same ligand from coordinating to a single metal atom (127). When  $x = 2$ , the resulting cobalt (II) complex is square planar and monomeric; while a pseudo-tetrahedral, polymeric structure occurs, in both the solid state and in solution, when  $x = 5$  or  $6$  (117, 118). The intermediate case, when  $x = 3$ , Co(II) - N, N' - disalicylaldehyde - 1, 3 - propanediimine differs in structure from both of these. Geometrical isomerism and a flattened tetrahedral structure have been postulated (117). Structural investigations on this manganese (II) complex are of considerable interest in this context.

Two distinct manganese (II) complexes of the Schiff base 'salpn' were prepared (78, 82). These compounds have empirical formulae  $[Mn(salpn)H_2O]$  and  $[Mn(salpn)]$  referred to here as (A) and (B) respectively. Both (A) and (B) are yellow but (A) is an amorphous powder whilst (B) is prepared as a crystalline material. (B) is extremely air sensitive whilst (A) is much less so. When handled under an atmosphere of nitrogen,

Figure 17.Ultra violet and visible spectra in solution.

Absorption maxima quoted in  $\text{cm}^{-1}$  with extinction coefficient.

(per monomeric formula) in brackets.

Solute	Solvent	Absorption Maxima
Salpn.	$\text{CHCl}_3$	38,500(19,500);31,500(7,500);24,300sh(2,100)
<u>A</u>	$\text{CCl}_4$	34,150(8,100);25,700(8,900)
<u>C</u>	$\text{CHCl}_3$	32,800(10,500);30,800(9,700);21,000sh(3,400)
<u>D</u>	$\text{CHCl}_3$	33,800(13,500);30,800(11,600);21,000sh(3,500)
<u>G</u>	$\text{CHCl}_3$	32,300(10,300);30,300(9,000);21,000sh(3,000)
<u>H</u>	$\text{CHCl}_3$	32,500(10,000);31,200(9,400);21,000sh(3,000)

Figure 18.

Diffuse Reflectance spectra of solids\* between 45,000 and 10,000cm<sup>-1</sup>

Complex	Absorption Maxima (cm <sup>-1</sup> ) .
<u>A</u>	36,700; 26,300; 21,500(sh); 17,200(sh); 10,100(sh)
<u>C</u>	44,200(sh); 42,000(sh); 37,000; (29,200 and 20,000); 17,100(sh); 15,900(sh); 13,000(sh); 11,000(sh).
<u>D</u>	44,200; 37,000; (29,200 and 20,000); 17,100(sh); 15,900(sh); 13,000(sh); 11,000(sh).
<u>F</u>	42,000; 38,000; (29,200 and 20,000); 17,100(sh); 15,900(sh); 13,000(sh); 11,000(sh).
<u>G</u>	37,000; (29,200 and 20,000); 17,100(sh); 15,900(sh); 13,000(sh); 11,000(sh).
<u>H</u>	43,200; 40,000; (29,200 and 20,000); 17,100(sh); 15,900(sh); 13,000(sh); 11,000(sh).

\*For all samples other than A, a very broad peak, with slight maxima at 29,200 and 20,000 cm<sup>-1</sup>, was observed. This is shown by (29,200 and 20,000).

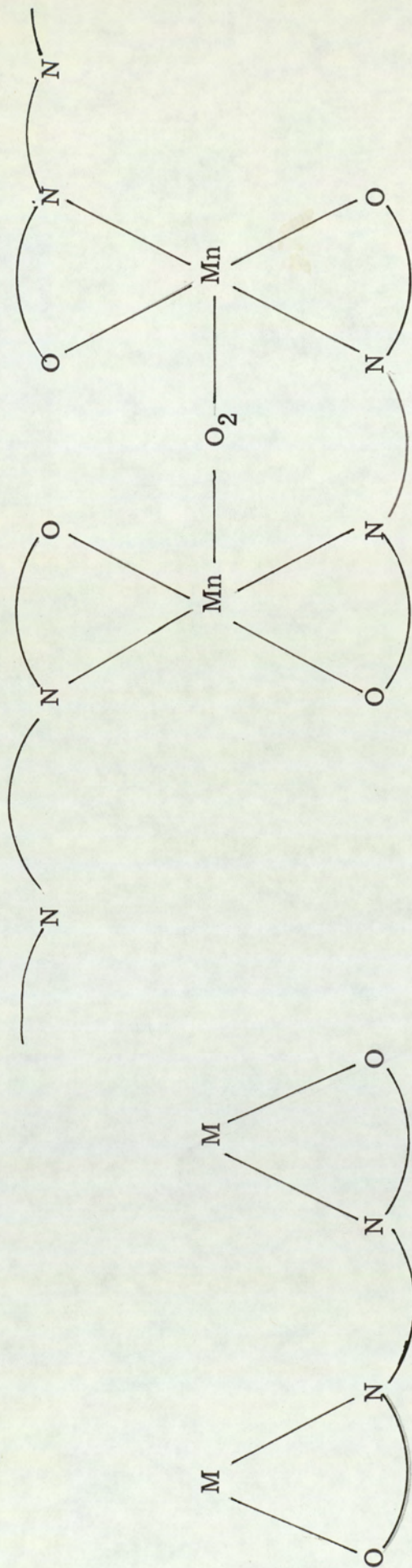
(A) was found to have a magnetic moment at 23.6°C of 5.93 B.M. per gram atom of manganese, a value consistent with high spin manganese (II). The diamagnetic correction for disalicylaldehyde-1, 3-propanediimine is  $\chi_M = 2.63 \times 10^{-4}$  cgs. at 22.9°C. The magnetic moment is therefore not reduced by superexchange via oxygens in associated molecular aggregates (128), by antiferromagnetism (129), by spin orbit coupling (130) nor by contamination by the oxidised form. When (A) was handled in air a lower value for the magnetic moment was obtained.

The expected d to d transitions in the visible and ultra-violet spectrum of (A) (131) in the 15,000 to 30,000  $\text{cm}^{-1}$  range were masked by charge-transfer and ligand bands. The observed spectrum in solution is summarised in Figure 17 and the diffuse reflectance spectrum in Figure 18. Judging from their similarity (A) appears to have the same structure in the solid state and carbon tetrachloride solution (116).

The mass spectrum of (A) at 70 electron volts showed a small parent peak at  $670 \pm 5$  atomic mass units, corresponding to  $[\text{Mn}_2(\text{salpn})_2]^+$ . No peaks were observed between this value and the large monomer peak at 335 a.m.u. A peak at 18 a.m.u. larger than the background peak or that seen for non-hydrated complexes was also observed. Hariharen and Urbach also observed that the parent peak of the analogous cobalt complex agreed with the molecular weight of the monomeric unit (117).

The molecular weight of (A) could not be determined by vapour pressure osmometer owing to its high oxygen sensitivity and low solubility. Determination by freezing point depression in carbon tetrachloride might be feasible. However, the determined molecular weight of (D) (see below) implies a non-monomeric structure for this oxygenated derivative of (A). It is therefore

Figure 19.



(a)

Arrangement of ligand when one ligand molecule bridges two metal ions.

(b)

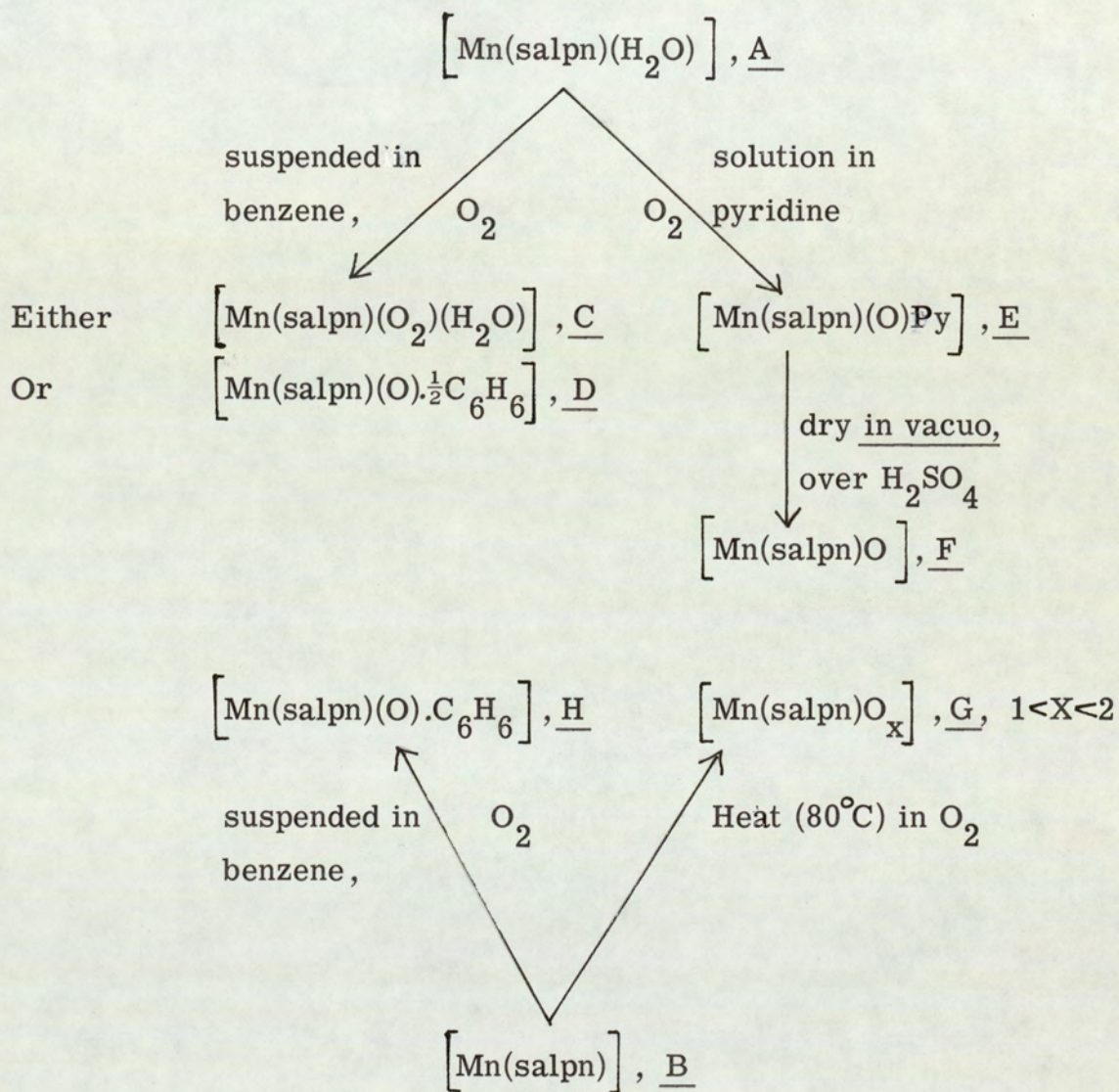
Possible structure of a polymeric oxygenated product.

likely that (A) is oligomeric or polymeric with all the salen ligands bridging neighbouring manganese ions. A dimeric structure or a polymeric structure with the ligands staggered along the chain is then possible (see Figure 19(a) and (b)). This situation occurs in the  $x = 2$  case when the coordinated metal is cobalt; monomeric structures (132) and dimeric units are known (133). In the dimer  $\text{Co}_2^{\text{III}}(\text{salen})_3$ , (133) one ligand behaves as a bidentate ligand relative to each of two cobalt III ions (see Figure 19(a)). The magnetic moment of 5.93 B.M. for (A) shows that molecular aggregates are not formed by the sharing of ligand oxygen atoms (121) as this phenomenon causes lowering of the spin only value of  $\mu$  by superexchange.

The role of the water molecules in compound (A) could not be determined from the above observations. The relative sensitivity to oxygen of (A) and (B) as solids or as suspensions in benzene suggests that the water molecules in (A) rendered attack of molecular oxygen at a manganese ion more difficult. The rate of reaction of (A) and oxygen became much more rapid when a solution in chloroform or pyridine was used. Various products derived from the reaction between oxygen and (A) or (B) were prepared. These preparations are summarised schematically in Figure 20.

Suspensions of (A) in benzene reacted slowly with oxygen at 25°C and one atmosphere pressure. Several days were required to achieve complete uptake. The quantity of oxygen consumed in apparently identical experiments was found to vary. Thus suspensions equivalent to a  $10^{-2}$  M concentration of manganese(II) gave  $\text{O}_2 : \text{Mn}$  ratios varying from 1 : 1 to 0.25 : 1. In half the experiments, the measured ratio was approximately 0.8 : 1. The variation in oxygen uptake is thought to be caused by some variation in the nature of (A) or in the ratio of products formed

Figure 20. Relationship, Empirical Formulae and Symbols used for Products discussed in Chapter IV.



not by partial oxygen uptake by the reagent before the experiment was started.

When a ratio of 1 : 1 was observed, the brown product (C) of empirical formula  $[\text{Mn}(\text{salpn})(\text{O}_2)\text{H}_2\text{O}]$  was isolated. Complex (D)  $[\text{Mn}(\text{salpn})(\text{O})\frac{1}{2}\text{C}_6\text{H}_6]$  was isolated when an  $\text{O}_2$  to Mn ratio of 0.5 : 1 was observed. Intermediate ratios produced solids which seem to be mixtures of (C) and (D) as judged by their analytical data.

Although (A) has been reported (78) to take up both carbon monoxide and nitrogen, the results obtained did not confirm this observation. When suspensions of (A) in deoxygenated benzene were kept under these gases, only the formation of (C) was observed. This product was slowly formed only after several weeks as air gradually leaked into the apparatus. Calderazzo and his co-workers (82) similarly reached the conclusion that no reaction occurred between nitrogen and compound (B).

Neither (C) nor (D) released oxygen on refluxing in benzene or chloroform (cf 78, 113). However, the action of 2 M perchloric acid on both products resulted in the slow release of approximately 0.2 moles of gas per gram atom of manganese. Orange - yellow solids were slowly produced from these reaction mixtures. These solids proved to be too air sensitive to study. The uptake of oxygen by  $[\text{Mn}(\text{salpn})(\text{H}_2\text{O})]$  (A) is therefore not readily reversible.

The infra-red spectra of the oxidised products (C) to (H) in the range  $4000 - 400 \text{ cm}^{-1}$  (see Figure 21(a) and (b) ) provide little information. Water, benzene or pyridine peaks are shown by those products containing these molecules. The only distinctive feature for all products (C) to (H) is the presence of a strong, broad band

	$\nu \text{ cm}^{-1}$			
	A	C	D & H	E
Salpn	$[\text{Mn}(\text{salpn})\text{H}_2\text{O}]$	$[\text{Mn}(\text{salpn})\text{O}_2\text{H}_2\text{O}]$	$[\text{Mn}(\text{salpn})\text{O}_x\text{C}_6\text{H}_6]$	$[\text{Mn}(\text{salpn})\text{OPy}]$
			$x = \frac{1}{2} \text{ or } 1$	
2700(br)		3470(br)		
1630(s)	1628(s)	1626(s)	1630(s)	
1607(w)	1618(s)			
	1595(w)	1593(s)	1593(s)	1595(s)
1580(m)		1540(s)	1540(s)	1540(s)
1490(m)	1538(s)	1450(s)		
1420(w)	1445(s)	1450(s)	1445(s)	1445(s)
	1395(w)	1380(s)		
	1343(m)		1370(s)	1375(m)
		1340(m)	1338(m)	
1335(m)	1315(m)			1335(s)
1310(w)		1307(s)		1307(s)
1280(s)	1270(w)		1305(s)	
		1220(w)	1217(w)	1213(w)
1205(m)		1200(w)	1200(w)	1200(m)
	1190(m)	1150(m)	1150(m)	1150(s)
1148(m)	1150(m)	1120(w)	1125(w)	1125(m)
1120(w)	1120(m)	1083(w)	1083(w)	1084(m)
1080(w)	1050(w)			
1048(m)	1033(w)	1033(w)	1034(w)	
1020(w)				1030(w)
970(m)	970(w)	990(w)		
		960(w)	965(w)	963(w)
		940(w)	940(w)	940(w)
930(w)	900(m)	900(m)	900(w)	900(m)
875(s)		852(w)		860(w)
850(s)			850(w)	
			840(w)	
			800(w)	800(m)
778(m)	795(w)	796(m)		
		770(m)	770(m)	
750(s)	750(m)	754(s)	760(s)	750(s)
730(s)		740(m)	740(m)	
			720(w)	
		690(s)	690(s)	
660(m)				
640(m)		620(s)	600-650(s)	600-650(s)
	570(w)	560(w)	560(w)	560(m)
		540(w)	545(w)	540(w)
540(m)	508(w)			
460(s)	460(w)			
		450(m)	452(m)	450(s)
			420(w)	415(w)
		383(m)	385(m)	382(w)
325(m)				

Figure 21(b). Infra-Red Spectra of Benzene, Pyridine and  $\text{MnPy}_2\text{Cl}_2$

(182) for comparison with Figure 21(a).

$\nu \text{ cm}^{-1}$				
F	G(KBr disc)			
[Mn(salpn)O]	[Mn(salpn)O <sub>x</sub> ] 1 < x < 2	Py (from ref. 182)	MnPy <sub>2</sub> Cl <sub>2</sub> (from ref 182)	C <sub>6</sub> H <sub>6</sub>
	2920(w)			
	2850(w)			
		1627	1632	
	1595(s)	1592	1597	
1590		1575		
	1540(m)		1573	
1530(m)		1478		
	1465(m)		1471	1473
	1440(s)		1442	
	1390(w)	1436	1390	
1370(m)		1372	1362	
	1335(w)	1350		
1330(w)	1300(s)			
1295(s)			1237	
			1223	
1213(w)	1210(w)	1212		
1200(w)	1200(w)			
1150(w)	1150(m)		1152	
1125(w)	1125(w)	1142		
1080(w)				
		1064	1076	
1030(vw)	1030(vw)	1030		
		989	1005	1030
950(w)	900(m)	942		
893(w)	850(w)			
847(w)	800(w)			
793(w)	757(s)			
750(s)		747	750	
		702		
600-650(s)			691	670
	620(s)		625	
560(w)	560(w)	597		
540(w)	540(vw)			
445(s)	445(w)			
415(w)	415(vw)		417	
380(m)		403		
320(m)				

in the region  $600 - 650 \text{ cm}^{-1}$ . This absorption is absent from the spectrum of the free ligand and of (A). The absorption could not be assigned with any certainty. An Mn-O-Mn grouping would probably show absorption in the region around  $820 \text{ cm}^{-1}$  by analogy with the Fe-O-Fe vibration in  $[\text{Fe}(\text{salen})]_2\text{O}$  (129). The M-O-M grouping usually shows a stretching vibration in the region  $650$  to  $920 \text{ cm}^{-1}$  (119). A bridged peroxide might also show weak absorption in the region around  $890 \text{ cm}^{-1}$  (134). When the reversible carrier  $[\text{Co}^{\text{II}}(\text{salen})]$  takes up oxygen, a weak band appears at  $565 \text{ cm}^{-1}$  (135). This is ascribed to the stretching vibration of the Co-O-O-Co linkages in the oxygenated crystals. The vanadyl group when complexed with salen in a five coordinate planar monomer shows an intense band at  $1298 \text{ cm}^{-1}$  (135). In most other cases the V = O stretch occurs in the range  $910$  to  $1010 \text{ cm}^{-1}$  (119). However, where salpn is the ligand, the vanadyl frequency is found at  $854 \text{ cm}^{-1}$  (119). This low V = O stretch is thought to be diagnostic for vanadyl bridged polymeric species. Thus, there appears to be no obvious agreement with any previously assigned absorption for related complexes in this region.

The differences between the ultra-violet and visible spectra (see Figure 17) of the oxygenated products were also slight but could indicate a difference in structure between the solid state and chloroform solution (116).

The highest mass spectral peak observable for both (C) and (D) occurs at 335 atomic mass units, corresponding to  $[\text{Mn}(\text{salpn})]^+$  (cf 117, 130). The presence of water in (C) and benzene in (D) is confirmed. A slight amount of benzene is also present in (C). Small peaks, slightly above the background values, and absent for (A) are observed at 16 a.m.u., but no peaks are present at 32 a.m.u. Both compounds are soluble to a limited extent in

potentially coordinating solvents. This solubility decreases in the order pyridine > dimethylformamide > tetrahydrofuran or dimethylsulphoxide. A molecular weight determination for a solution of (D) in anhydrous A.R. pyridine in the concentration range  $1 \times 10^{-4}$  to  $5 \times 10^{-4}$  M gave a value of  $820 \mp 40$ . Since the benzene incorporated in (D) is likely to be replaced by pyridine on solution, this observation is taken to demonstrate that (D) is oligomeric or polymeric. (D) is insufficiently soluble in purified chloroform for the molecular weight to be determined by vapour pressure osmometer in this solvent.

The magnetic moments (per manganese atom) of (C) and (D) are 2.88 B.M. at 22.6°C and 2.15 B.M. at 22.8°C. These determined values differ slightly from sample to sample. Large reductions in the magnetic moment relative to the starting material in such systems have been ascribed to antiferromagnetic behaviour (130). However, low spin  $\text{Mn}^{\text{III}}$  is an alternative interpretation of these values (79). The magnetic moment of (D) is close to that quoted for  $\left[ \text{Mn}^{\text{IV}} (\text{salen}) \text{O} \right]_n$ ,  $\mu = 1.97$  B M (79) and an analogous structure cannot be entirely ruled out on the basis of the molecular weight determination.

Thermogravimetric analysis shows that (C) undergoes a weight loss between 170° and 200°C equivalent to a decrease in molecular weight of approximately 30g per gram of manganese. This value is consistent with the loss of  $\text{O}_2$ . The corresponding experiment for (D) shows a weight loss of approximately 14 mass units per manganese between 165° and 200°C. This is ascribed to loss of one oxygen atom. This weight loss is followed by a further loss in weight, complete by 250°C equivalent to approximately 34 mass units per manganese.

The available evidence strongly suggests that these oxygenated

products are not monomeric. The use of molecular models suggests that a possible structure is one in which  $O_2$  units bridge neighbouring manganese atoms, as shown in Figure 19(b). Complexes with an Mn :  $O_2$  ratio of 1 : 1 would have polymeric structures, containing  $\mu$ -peroxo groups and Mn (IV). Those with a 2 : 1 Mn :  $O_2$  ratio would be dimeric  $\mu$ -peroxo complexes of manganese (III). However, the absence of a mass spectral peak at 32 a.m.u. is surprising if (C) and (D) have such a structure. An alternative explanation is that the O - O bond of molecular oxygen is broken. 2 : 1 Mn :  $O_2$  adducts (D) would then be polymeric  $\mu$ -oxo complexes of manganese (IV). However, a polymeric  $\mu$ -oxo structure seems unlikely for 1 : 1 Mn :  $O_2$  adducts (C) since these would contain two  $O^{2-}$  groups per manganese. Manganese formally in oxidation state (VI) is unlikely to be achieved with Schiff base ligands.

When the hydrated manganese (II) complex (A) is in solution, it takes up oxygen more rapidly than do suspensions. Solutions in anhydrous pyridine or a benzene pyridine mixture (1 : 1 by volume) or chloroform show completed oxygen uptake in less than half an hour. The observed Mn :  $O_2$  stoichiometry is 2 : 1. Attempts to prove dimer formation were made by following the kinetics of oxygen uptake at atmospheric pressure, using different concentrations of manganese (II) chelate (A) in homogeneous chloroform solution. If reaction (3) in Figure 3 is rate determining a dependence :-

$$-\frac{d[O_2]}{dt} = \frac{d[M_2 O_2]}{dt} = k_3 (M)^2$$

(where  $-\frac{d[O_2]}{dt}$  is the rate of consumption of oxygen) would prove dimer formation (see 33 page 345) like the 3-fluoro salen  $Co^{II}$  case. However, if (2) is rate determining or (2) and (3) comparable in rate the results would be inconclusive. In fact, it was found impossible to obtain reproducible kinetic data owing to the slow rate of dissolution of the complex and the volatility of chloroform, making it difficult to maintain a constant partial pressure of oxygen.

Kinetic runs in anhydrous pyridine were also irreproducible owing to oxygen uptake by the solid complex in the presence of pyridine vapour. When (A) is dissolved in dimethylformamide, oxygen uptake continues after an Mn : O<sub>2</sub> ratio of 1 : 1 has been passed. This is presumably due to a catalysed oxidation of the solvent (95).

After oxygen uptake by (A) in pyridine, complex (E) crystallised out of solution. Analysis showed the empirical formula to be  $[\text{Mn}(\text{salpn})(\text{O})\text{Py}]$ . When this oxidation product is allowed to stand in vacuo over concentrated sulphuric acid, a compound (F) which does not contain pyridine is obtained. The empirical formula of (F) is  $[\text{Mn}(\text{salpn})(\text{O})]$ . Unlike other oxygenated products (F) is insoluble in chloroform. On heating, (F) shows a weight loss at approximately 200°C, equivalent to the loss of one atom of oxygen per atom of manganese. Spectroscopically the material differs little from the products discussed earlier.

The anhydrous material (B) is extremely air sensitive (82). On heating (B) in a stream of oxygen, in an attempt to achieve complete oxygenation of the solid, (G) was produced. Both analytical and thermogravimetric analysis show an Mn : O ratio between 1 : 1 and 1 : 2. Thus, apart from the analytical data no distinction could be found between (G) and (F).

A suspension of (B) in benzene takes up oxygen rapidly giving an Mn : O<sub>2</sub> ratio of 2 : 1. The brown product (H) has empirical formula  $[\text{Mn}(\text{salpn})(\text{O})(\text{C}_6\text{H}_6)]$ . This product is indistinguishable from D, in its infra-red spectrum, while the electronic spectrum differs only slightly. (H) shows a weight loss between 120° and 150°C equivalent to the loss of one oxygen atom per atom of manganese. Although there is a gradual weight loss with increasing temperature, the incorporated benzene molecule

does not appear to be lost at any definite temperature in the experimental range (up to 500°C).

Without crystallographic information, it is not possible to provide conclusive evidence of the nature of the compounds produced. However, all the evidence is consistent with the postulate of polymeric species. Thus, the manganese (II) product  $[\text{Mn}(\text{salpn})\text{H}_2\text{O}]$  is probably a mixture of polymeric units. The water molecules in this compound render the solid less susceptible than is the anhydrous complex to reaction with oxygen. This difference disappears when the compounds are dissolved in coordinating organic solvents. Oxygen uptake by (A) and (B) yields a variety of products although (F) and (G) and (D) and (H) are almost identical. The variable stoichiometry of oxygen uptake by (A) in benzene could be explained by the differing activity of the various solid samples used. This difference in crystal lattice structure could be maintained in benzene suspension (33 page 341). Alternatively, stoichiometries of 0.5 to 1.0 are explained by retention of the  $\text{O}_2$  grouping as bridging peroxide. Thus on oxygen uptake a dimer would have an  $\text{Mn} : \text{O}_2$  ratio of 2 : 1 while higher polymers with the  $\dots\text{O}_2\text{MnO}_2\text{MnO}_2\dots$  grouping would yield ratios down to 1 : 1. This type of variable stoichiometry is attributable to the existence of a series of equilibria (113). Stoichiometries below 0.5 can only be explained by postulating the existence of  $[\text{Mn}^{\text{IV}}(\text{salpn})\text{O}]_n$  units. The formation of both  $\mu$ -oxo- $\text{Mn}^{\text{IV}}$  and  $\mu$ -peroxo- $\text{Mn}^{\text{III}}$  complexes could be occurring by parallel competing processes.

Coordinating solvents, for example pyridine and chloroform may be capable of breaking down the polymeric structure of (A) by coordination and when used as solvents result in the formation of dimeric  $\mu$ -peroxo- $\text{Mn}^{\text{III}}$  species.

The polymeric nature of all these complexes is believed to arise as a result of the behaviour of the ligand salpn which coordinates each of two manganese ions in a bidentate fashion. Molecules of water, benzene or pyridine may be incorporated in these products.

From this study, it is evident that the N, N'-disalicylaldehyde-1, 3-propanediimine is of no use as a model for reversible biological oxygen carriers. Neither does the complex fix nitrogen. The ligand salpn should be avoided in the preparation of salicylaldoxime complexes to act as models for vitamin B<sub>12</sub> coenzyme, in view of its tendency to form polymeric species.

Chapter V.

Kinetics of the Autocatalytic Reduction of cis-Dichlorobis-(2, 2' bipyridyl) Rhodium(III) Nitrate Dihydrate in Alkaline Ethanolic Solution under a Hydrogen Atmosphere.

The reduction of cis  $\left[ \text{Rh}^{\text{III}} (\text{L})_2 \text{Cl}_2 \right]^+$  salts, where L is 2, 2'-bipyridyl or 1, 10-phenanthroline, was found to occur in an autocatalytic reaction.

This study of the kinetics of the reduction was undertaken in view of the previously reported, kinetically interesting, homogeneous reductions of rhodium (III) to rhodium (I) complexes by carbon monoxide (136, 137) hydrogen (138) and ethylene (139). Carbon monoxide reduces aqueous hydrochloric acid solutions of  $\text{RhCl}_3 \cdot 3\text{H}_2\text{O}$  to  $\left[ \text{Rh}^{\text{I}} (\text{CO})_2 \text{Cl}_2 \right]^-$  in an autocatalytic reaction involving a mixed valence  $\text{Rh}^{\text{III}} - \text{Rh}^{\text{I}}$  bridged intermediate analogous to the Pt IV ... Cl ... PtII case (140).

Similar catalytic intermediate species have been postulated in nucleophilic substitutions of octahedral rhodium (III) centres ( $d^6$ ). Such substitution reactions are generally slow (31, page 179), however, in the case of cis -  $\left[ \text{Co}^{\text{III}} (\text{L})_2 \text{Cl}_2 \right]^+$  complexes (L = bipy or phen) (141) where the conjugate base mechanism of chloride hydrolyses (142, 143) cannot operate, catalysis by Co(II), reducing agents and base has been observed. Two electron reducing agents, such as ethanol, have been found to catalyse nucleophilic substitutions in the formation (144, 145) of trans -  $\left[ \text{Rh}^{\text{III}} (\text{py})_4 \text{Cl}_2 \right]^+$ , reactions (146) of trans -  $\left[ \text{Rh}^{\text{III}} (\text{en})_2 \text{Cl}_2 \right]^+$ , and halogen interchange in both complexes (147). In the catalytic formation of trans  $\left[ \text{Rh}^{\text{III}} (\text{py})_4 \text{Cl}_2 \right]^+$ ,  $\text{Rh}^{\text{II}} - \text{H}$  (84) or  $\text{Rh}^{\text{I}}$  (145) have been postulated as the catalytic intermediate species. Catalysis by an  $\text{Rh}^{\text{III}} - \text{H}$  species would occur because of the high trans -

effect of the ligand and would proceed without change in the oxidation state of the metal, whereas catalysis by Rh (I) which was assumed to be formed by a direct two electron reduction of Rh(III) would be analogous to catalysis by Pt(II) in Pt(IV) substitutions (140).

A kinetic study on the reduction of the cis-dichlorobis-bipyridyl-rhodium(III) cation in alkaline ethanolic solution under hydrogen could be of importance in understanding the mechanism of similar catalysed rhodium (III) nucleophilic substitutions.

The end product of the reduction of cis-dichlorobis-(bipyridyl)-rhodium(III) cationic complexes is also of interest in view of the potential catalytic activity of four or five coordinate  $d^8$  Rh(I) species. Unlike the phosphine ligands, 2, 2'-bipyridyl and 1, 10-phenanthroline are not susceptible to aerial oxidation and subsequent loss of catalytic activity of their complexes. Many reactions between various Rh(I) complexes and oxygen, (148) nitric oxide, (149) hydrogen and carbon monoxide (150) ethylene, (151) butadiene, (152) electronegative olefins (153) and nitriles (154) have been characterised. Oxidative addition reactions of methyl iodide to a rhodium (I) carbonyl (155) or of ethylene or acetylene to a hydrido-rhodium (III) complex (151) generates a  $\sigma$  alkyl or vinyl complex which can undergo reversible carbon monoxide insertion reactions. Similar complexes are generated by addition of acyl or aroyl halides to rhodium (I) complexes. The homogeneous hydrogenation of alkenes, (138, 156) alkynes, (157, 158) quinones and aromatic nitro compounds in the presence of borohydride, (26, 159) the isomerisation of olefins (16) and the polymerisation of acrylonitrile (160) are catalysed by a variety of rhodium (I) complexes.

Cis-dichlorobis-(bipyridyl)-rhodium(III) cations in alkaline ethanolic solution of concentration  $2$  to  $9 \times 10^{-3}$  M absorbed hydrogen at atmospheric pressure and  $60^\circ\text{C}$ . The total measured gas uptake

Figure 22(a). Ultra Violet Spectra of  $[\text{Rh}^{\text{III}}(\text{bipy})_2\text{Cl}_2]^+$  salts.

(Compare Reference 84).

Rhodium(III)Complex	$\lambda$ max(nm)	$\epsilon$ litre <sup>-1</sup> mole <sup>-1</sup> cm <sup>-1</sup>
$[\text{Rh}^{\text{III}}(\text{bipy})_2\text{Cl}_2]\text{NO}_3 \cdot 2\text{H}_2\text{O}$	303	28,000
	313	31,800
	375	121
$[\text{Rh}^{\text{III}}(\text{bipy})_2\text{Cl}_2]\text{Cl} \cdot 2\text{H}_2\text{O}$	305	23,400
	313	26,900
	385	1,390
$[\text{Rh}^{\text{III}}(\text{bipy})_2\text{Cl}_2]\text{ClO}_4 \cdot 2\text{H}_2\text{O}$	303	30,400
	313	34,700
	384	241

Figure 22(b). Absorption Maxima in the Visible of Various Rhodium(I) Complexes and the Corresponding Extinction Coefficients.

Rhodium (III) Complex	$\lambda$ max(nm) of corresponding Rhodium(I) complex	$\epsilon$ litre <sup>-1</sup> mole <sup>-1</sup> cm <sup>-1</sup>
$[\text{Rh}^{\text{III}}(\text{bipy})_2\text{Cl}_2]\text{NO}_3 \cdot 2\text{H}_2\text{O}$	557	3,550
$[\text{Rh}^{\text{III}}(\text{bipy})_2\text{Cl}_2]\text{Cl} \cdot 2\text{H}_2\text{O}$	530	4,260
$[\text{Rh}^{\text{III}}(\text{bipy})_2\text{Cl}_2]\text{ClO}_4 \cdot 2\text{H}_2\text{O}$	530	3,940
$[\text{Rh}^{\text{III}}(4,4'\text{Cl bipy})_2\text{Cl}_2]\text{NO}_3 \cdot 2.5\text{NaNO}_3$	510	5,940
$[\text{Rh}^{\text{III}}(4,4'\text{Me bipy})_2\text{Cl}_2]\text{NO}_3 \cdot 2\text{H}_2\text{O}$	511	4,910
$[\text{Rh}^{\text{III}}(5,5'\text{Me bipy})_2\text{Cl}_2]\text{NO}_3 \cdot 2\text{H}_2\text{O}$	513	4,690
$[\text{Rh}^{\text{III}}(\text{phen})_2\text{Cl}_2]\text{NO}_3 \cdot 1.5\text{NaNO}_3 \cdot 2\text{H}_2\text{O}$	530	13,300
$[\text{Rh}^{\text{III}}(5\text{NO}_2\text{ phen})\text{Cl}_2]\text{NO}_3 \cdot 3.5\text{NaNO}_3 \cdot 4\text{H}_2\text{O}$	530	15,500
$[\text{Rh}^{\text{III}}(3,4,7,8\text{Me phen})_2\text{Cl}_2]\text{NO}_3 \cdot 0.5\text{NaNO}_3 \cdot 2\text{H}_2\text{O}$	530	11,700

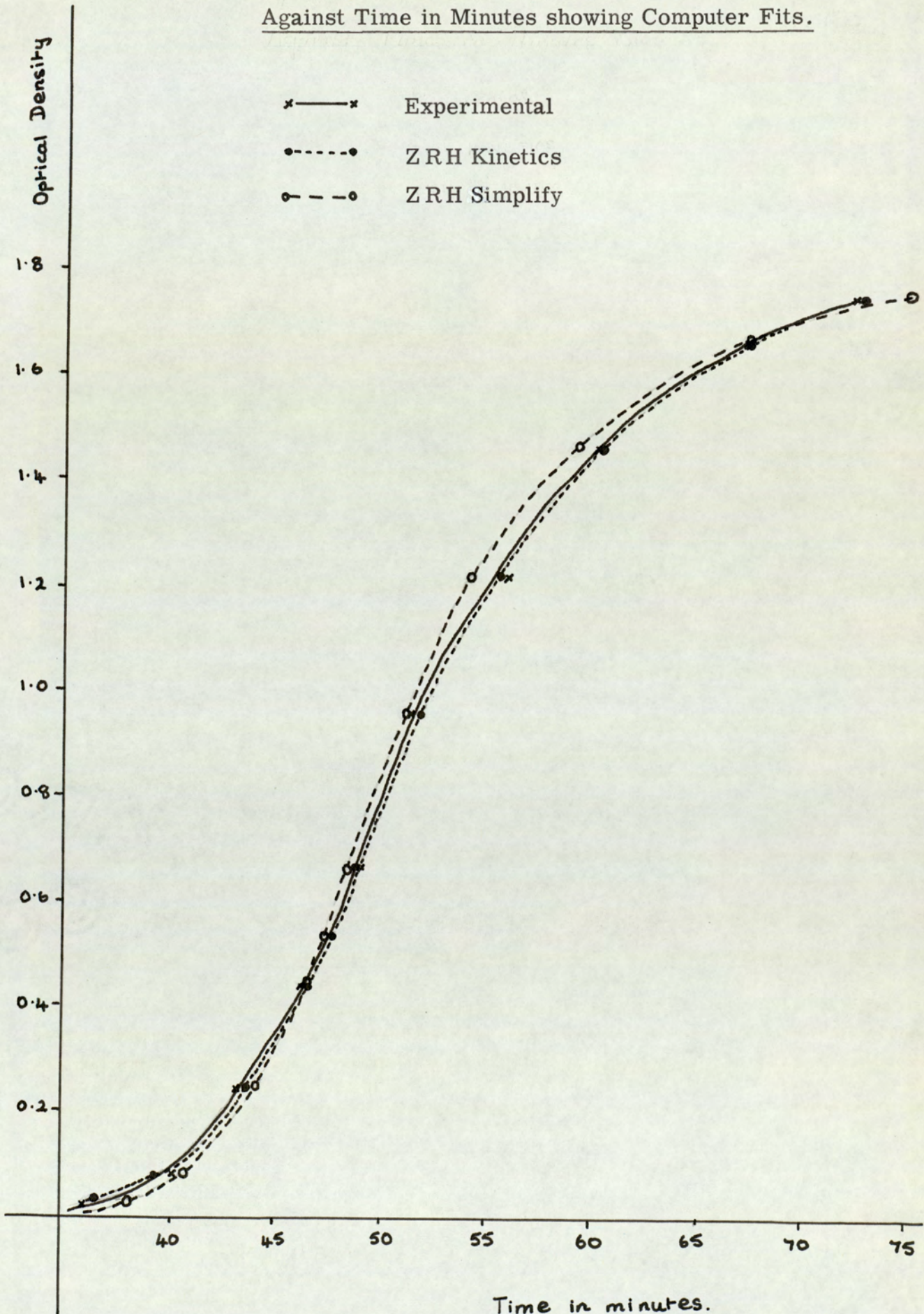
corresponded to a 1 : 1 mole ratio of hydrogen to rhodium. The original yellow rhodium (III) solutions (see Figure 22(a) and (b) for ultra-violet and visible absorption maxima and corresponding molar extinction coefficients) became violet due to the rhodium (I) species. Analytical data on the corresponding less soluble perchlorate salt support the formula  $[\text{Rh}^{\text{I}}(\text{bipy})_2] \text{NO}_3 \cdot 3\text{H}_2\text{O}$  as the rhodium(I) end product. The isolation and identification of this complex has been previously described (87). On exposure to air the violet suspensions returned to their original yellow colour.

The kinetics of the reaction were studied by observing the increase in absorbance at 557 nm ( $\epsilon$ , 3550) which obeys Beer's Law. Observations at other wavelengths were less favourable owing to the overlapping of the ultra-violet absorption spectra of rhodium(I) and rhodium(III) bipyridyl complexes (87) and the low intensity of the visible absorption maxima of  $[\text{Rh}^{\text{III}}(\text{bipy})_2 \text{Cl}_2]^+$  cations.

An induction period of variable length always preceded the reaction (147). Addition of the rhodium (I) end product or rhodium (I) contamination in the reaction vessel or starting material (for example that prepared by the method of Gillard, Osborn and Wilkinson (84) using the reducing agent hydrazinium chloride as catalyst) decreased the length of the induction period, whereas presence of dissolved oxygen gas increased it. These facts, together with the rate plots of optical density at 557 nm against time (see Figure 23) suggest that a slow oxygen sensitive initial reaction generates some of the rhodium (I) species, which then participates in an autocatalytic reaction.

The autocatalytic plots yield a maximum slope at a point representing approximately one third part of the total rhodium (I) produced, regardless of the initial concentration of the rhodium (III) used. Graphical differentiation of the concentration of rhodium (I) versus

Figure 23. Specimen Graph of Optical Density at 557 nm  
Against Time in Minutes showing Computer Fits.



time curves gave rise to curves of type shown in Figure 24, which are nearly symmetrical about the 33.3% reaction point. It is easily shown that a rate proportional to the product  $[\text{Rh}^{\text{III}}]^2 [\text{Rh}^{\text{I}}]$  becomes a maximum when  $\frac{1}{2} [\text{Rh}^{\text{III}}] = [\text{Rh}^{\text{I}}] = 33.3\%$  of the total rhodium. Thus the rate equation probably has a rhodium dependence given by :-

$$\frac{d}{dt} [\text{Rh}^{\text{I}}] = k_{\text{obs}} [\text{Rh}^{\text{III}}]^2 [\text{Rh}^{\text{I}}] \quad (1)$$

where  $k_{\text{obs}}$  is the pseudo third order rate constant containing all other chemical and physical variables except the dependence on rhodium. The integrated form of this rate equation is :-

$$k_{\text{obs}} t = \frac{1}{T^2} \left[ \left( \frac{T}{T-x} \right) + \ln \left( \frac{x}{T-x} \right) \right] + \text{constant} \quad (2)$$

where T is the total concentration of rhodium and x is the concentration of rhodium (I).

In terms of the observed optical densities this equation becomes :-

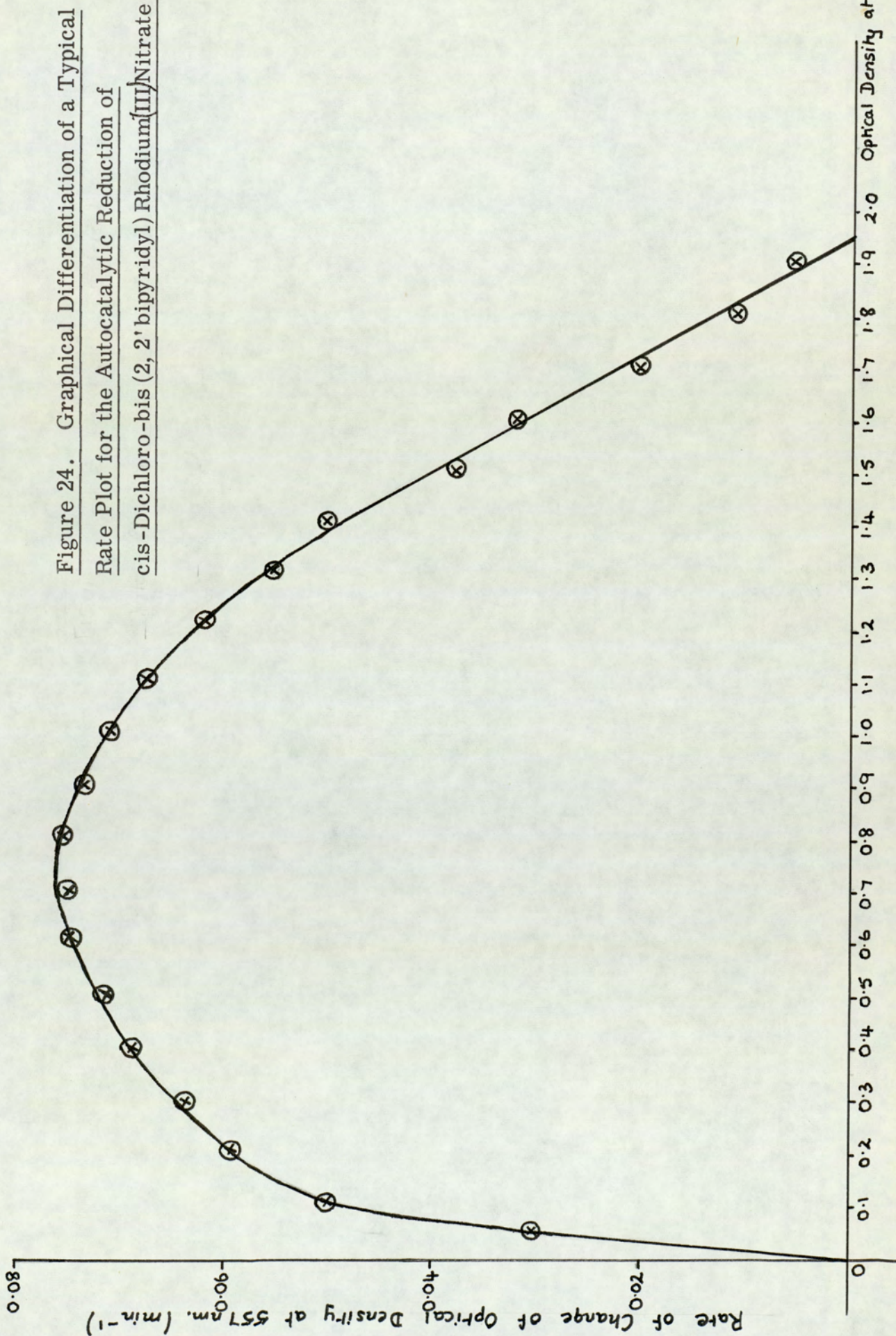
$$kt = \frac{1}{(\text{OD}_\infty)^2} \left[ \left( \frac{\text{OD}_\infty}{\text{OD}_\infty - \text{OD}_t} \right) + \ln \left( \frac{\text{OD}_t}{\text{OD}_\infty - \text{OD}_t} \right) \right] + \text{constant} \quad (3)$$

where  $\text{OD}_t$  is the observed optical density at 557 nm at time t,  $\text{OD}_\infty$  is the optical density at infinity and

$$k_{\text{obs}} = k \frac{(\text{OD}_\infty)^2}{[\text{Rh}_0^{\text{III}}]^2}$$

$[\text{Rh}_0^{\text{III}}]$  is the concentration of rhodium (III) at zero time.

Good linear plots of the right hand side function of equation (3) versus time were obtained up to 90% reaction. A least squares computer program (ZRH SIMPLIFY see Appendix 9) was used to find the best values of the rate constant and integration constant using the experimentally determined infinity value and feeding in pairs of optical density and time readings. A more complicated least squares program (ZRH KINETICS see Appendix 10) was written to allow the experimentally determined  $\text{OD}_\infty$



to be varied slightly to allow for change in initial rhodium (III) concentration caused by solvent evaporation and to improve the fit (see Figure 23). This program found the best values of the rate constant, infinity reading and constant (time of induction period in minutes) to fit the experimental data.

The rhodium dependence of the rate equation was checked by varying the initial rhodium (III) concentration from  $2.77 \times 10^{-4}$  to  $1.14 \times 10^{-3}$  M at hydroxide concentration of 0.1865 M. All runs gave values of  $k_{\text{obs}}$  which were constant within the limits of experimental error ( $k_{\text{obs}} = 1.47 \mp 0.17 \times 10^6$  litre<sup>2</sup> mole<sup>-2</sup> minutes<sup>-1</sup>) see below.

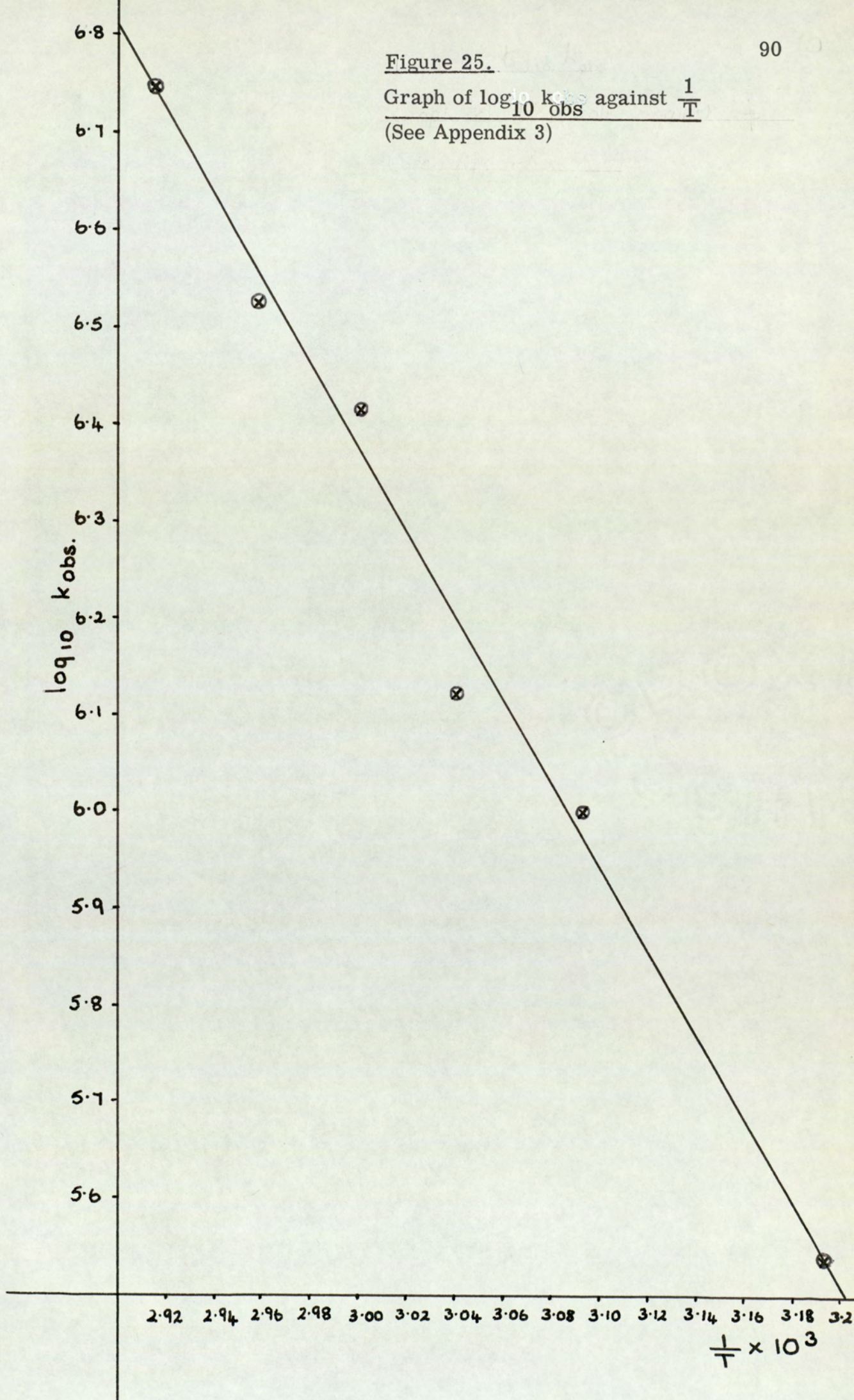
Effect of  $[\text{Rh}_{\text{O}}^{\text{III}}]$  on the Reaction Rate at 60°C, 1 Atmosphere of  
 Hydrogen Pressure,  $[\text{OH}^-] = 0.186$  M in 25% Ethanol / Water.

$[\text{Rh}_{\text{O}}^{\text{III}}] \times 10^4$ (M)	$k_{\text{obs}} \times 10^{-6}$ (litre <sup>2</sup> mole <sup>-2</sup> minutes <sup>-1</sup> )
2.77	1.61
4.25	1.70
5.65	1.83
7.02	1.69
8.40	0.92
10.1	1.65
11.4	0.87

Measurements at 5°C intervals over the temperature range 40° to 70°C yielded a good Arrhenius plot (see Figure 25). A value of  $20.1 \mp 1.6$  k.cals / mole was obtained for that parameter for the observed overall rate constant equivalent to an activation energy.

Figure 25.

Graph of  $\log_{10} k_{\text{obs}}$  against  $\frac{1}{T}$   
(See Appendix 3)



Investigation of the hydroxide dependence of the reaction showed that as the concentration of hydroxide is increased in the range 0.02 to 1.00 M, the reaction rate increases.  $k_{\text{obs}}$  varied with the hydroxide concentration according to :-

$$k_{\text{obs}} = \frac{k' [\text{OH}^-]}{(k'' + [\text{OH}^-])}$$

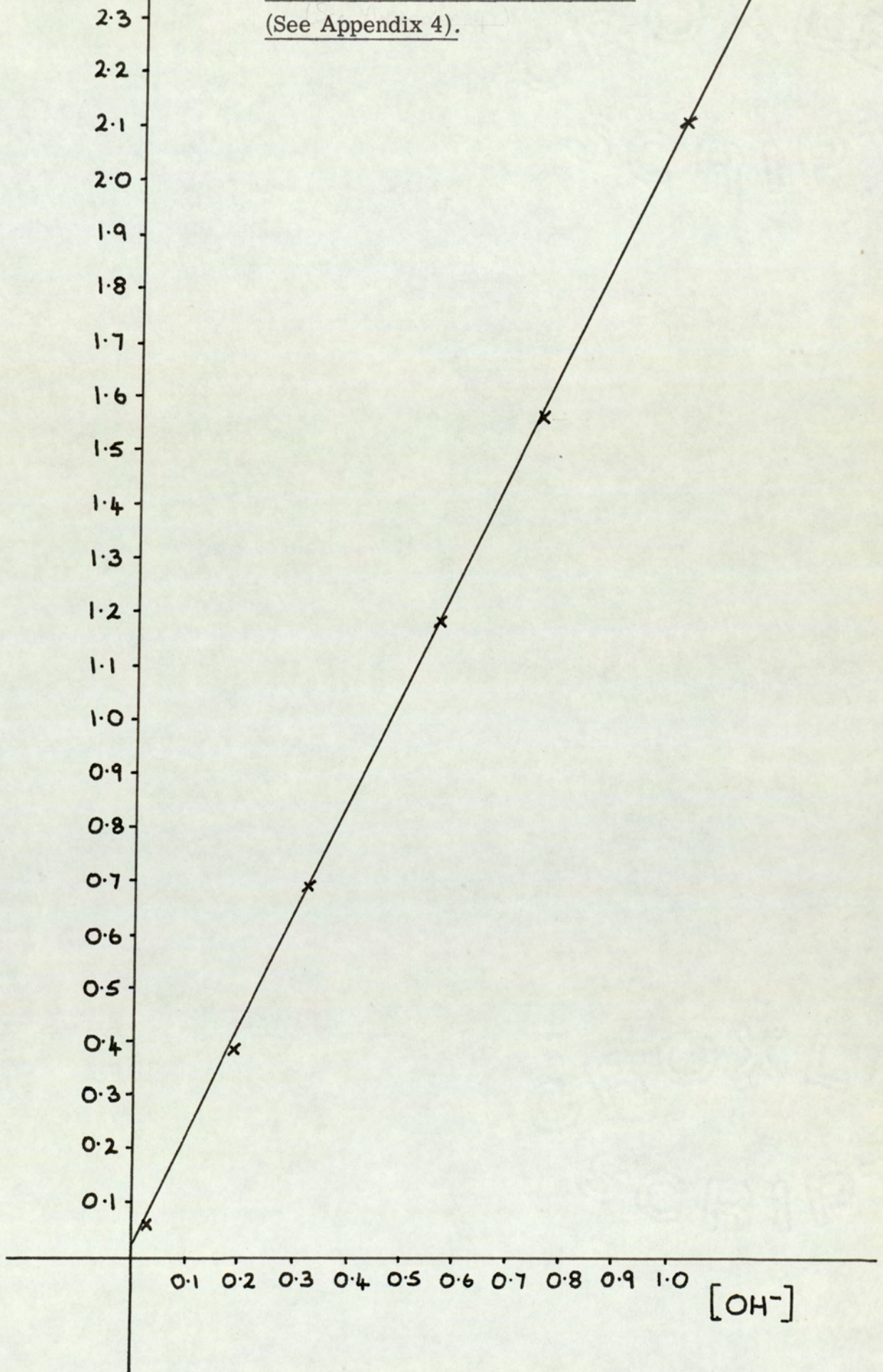
as shown by the linearity of the graph of  $\frac{[\text{OH}^-]}{k_{\text{obs}}}$  against  $[\text{OH}^-]$

(see Figure 26). These runs were done in duplicate and the average value of  $k_{\text{obs}}$  calculated (experimental error  $< 9\%$ ).

The ionic strength of the reaction mixture was varied from 0.341 to 0.557 (values corrected for the density of the solvent at 60°C by using 0.02 to 0.2 A.R. sodium nitrate solutions at constant hydroxide concentration of 0.315 M. At ionic strengths in excess of 0.557, purple-black precipitates thought to be  $[\text{Rh}^{\text{I}}(\text{bipy})_2] \text{NO}_3 \cdot 3\text{H}_2\text{O}$  appeared at 25 - 33% reaction. The reaction could not be followed to completion spectrophotometrically as the precipitation resulted in low, inaccurate optical density readings and correspondingly low calculated values for the rate constants. In the ionic strength range 0.341 to 0.557 the solutions appeared visually homogeneous and the reaction rate showed a systematic decrease as ionic strength increased. However, an analogous, apparent ionic strength dependence was observed at much higher chloride concentration (see below, 1.00 M  $\text{NaCl}_{\text{aq}}$  compared to 0.20 M  $\text{NaNO}_3_{\text{aq}}$ ) and the low solubility of the rhodium (I) nitrate (and, to a lesser extent, chloride) may account for the apparent decrease in rate as the concentration of nitrate (or chloride) is increased. Nevertheless, a graph of  $\log_{10}(k_{\text{obs}})$  against the square root of the ionic strength gave a straight line of gradient -3 (see Figure 27).

$10^7 \times \frac{[\text{OH}^-]}{k_{\text{obs}}}$ Figure 26.  
Graph of  $\frac{[\text{OH}^-]}{k_{\text{obs}}}$  against  $[\text{OH}^-]$ 

(See Appendix 4).



The addition of chloride ion as a solution of A.R. sodium chloride in the range 0.06 to 1.00 M at constant hydroxide concentration 0.315 M had no apparent effect on reaction rate nor induction period. At concentrations of chloride in excess of 1.00 M, purple - black precipitates, thought to be  $\text{Rh}^{\text{I}}(\text{bipy})_2\text{Cl}$ , separated out and the reactions could not be followed to completion.

Effect of  $[\text{Cl}^-]$  on the Reaction Rate at  $60^\circ\text{C}$ , 1 Atmosphere of Hydrogen Pressure  $[\text{OH}^-] = 0.315 \text{ M}$ ,  $[\text{Rh}_o^{\text{III}}] = 5.63 \times 10^{-4} \text{ M}$  in 25% Ethanol / Water.

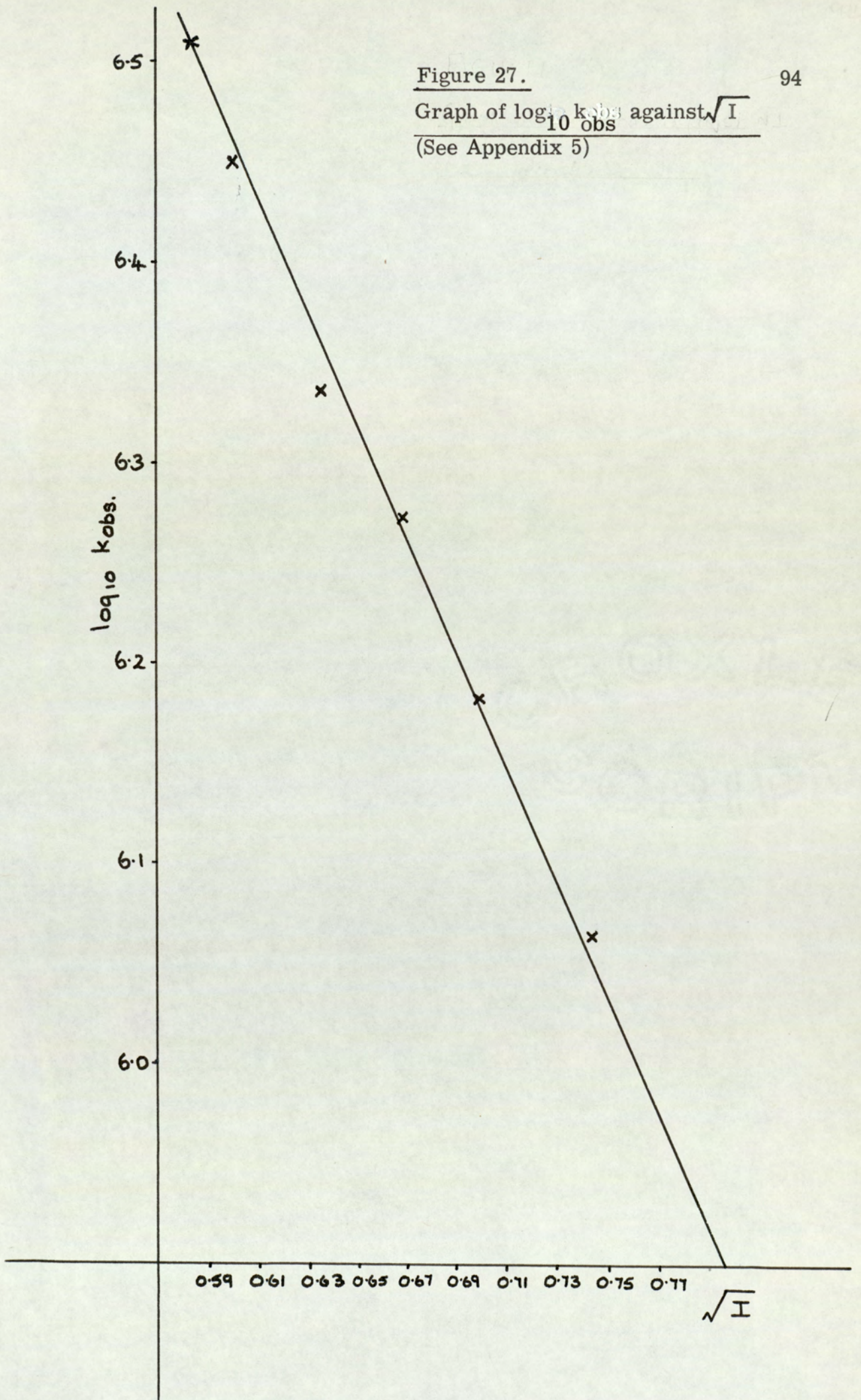
$[\text{Cl}^-] (\text{M})$	$k_{\text{obs}} \times 10^{-6} (\text{litre}^2 \text{ mole}^{-2} \text{ minutes}^{-1})$
0	3.27
0.06	3.42
0.10	2.63
0.20	2.94
0.40	3.16
0.60	2.93
1.00	2.34

Ethanol is well known as a catalyst for reduction of rhodium (III) to rhodium (I) (84, 144, 145, 146). In this reaction, the kinetic results suggest that there is an optimum concentration of ethanol for reduction. No reaction occurs in pure water, even if rhodium (I) is added, nor when ethanol is replaced by n-butanol but the reaction rate decreases considerably in the concentration range 1.43 to 7.63M ethanol (8 - 45%). At ethanol concentration 11.2 M (66%) the initial solution is a much more intense yellow green than is observed for other runs and a more oxygen sensitive orange - brown solution is produced. The induction period was approximately constant in the 8 - 45% ethanol range but showed a tendency to increase in the

Figure 27.

Graph of  $\log_{10} k_{obs}$  against  $\sqrt{I}$

(See Appendix 5)



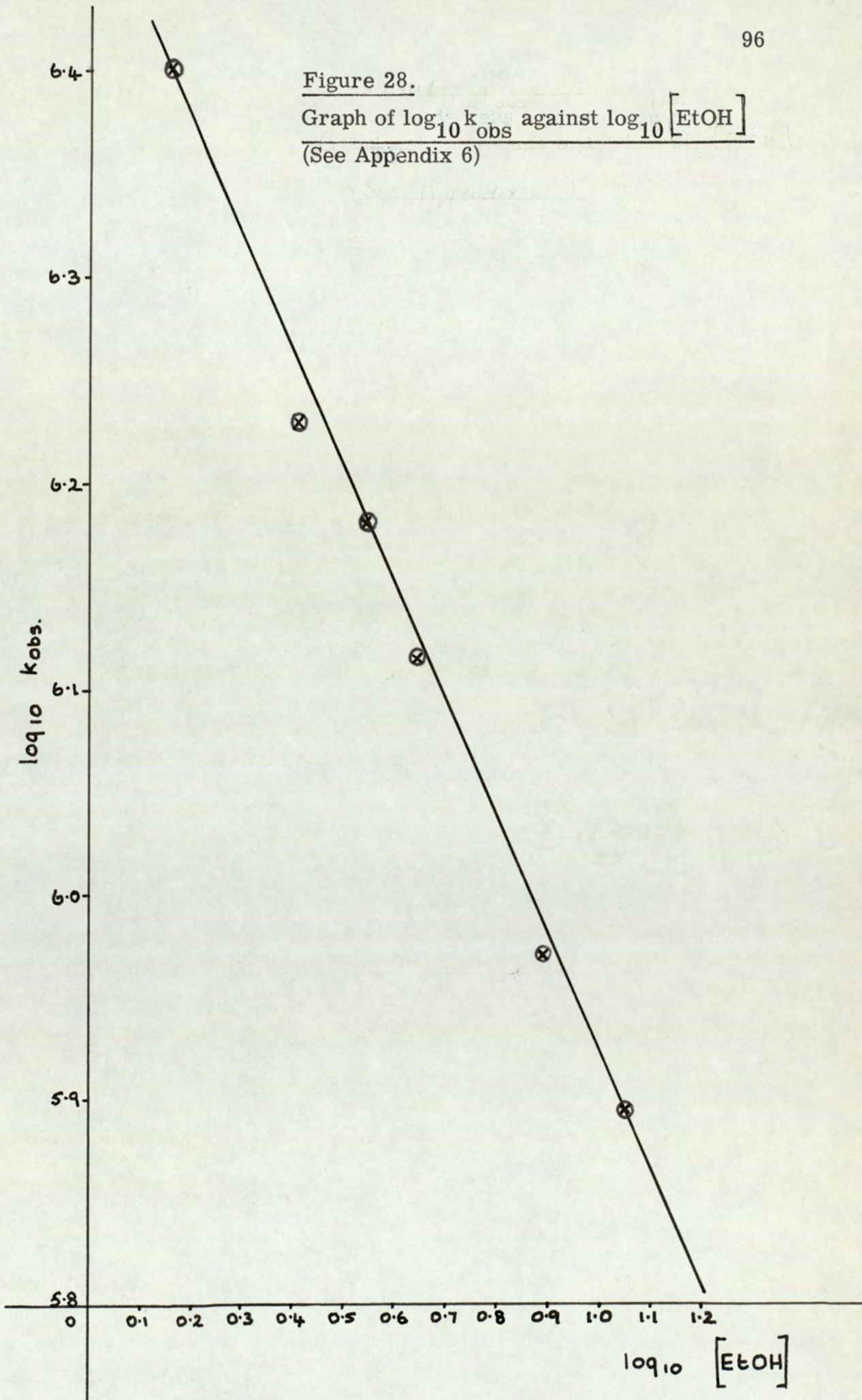
45 - 66% range.

Two factors make it difficult to compare the kinetics of the reactions at different ethanol concentrations. Firstly as the ethanol concentration is increased, the nature of the solvent is altered and it is difficult to predict the effect of this on the kinetics, although the Pt (II) catalysed rate of chloride substitution by bromide in  $\left[ \text{Pt} (\text{dien}) \text{NH}_3 (\text{Cl})_2 \right]^{2+}$  is known to be decreased as the polarity of the solvent is increased (161). Secondly, other parameters for example the solubility of hydrogen in the medium, and the hydrogen ion activity in solution, will also be altered by a change in medium composition. If reaction is assumed to occur when the equilibrium concentration of dissolved contaminant oxygen, an inhibitor, has been reduced to a specific low level by reaction with rhodium (I) in the induction period, the monotonic decrease in the solubility of oxygen inhibitor as the ethanol concentration is decreased, will have little effect on reaction rate (162). Although the ethanol dependence cannot be too precisely interpreted, the results suggest that the reaction rate is inversely proportional to the square root of the ethanol concentration (see Figure 28).

The addition of bipyridyl dissolved in the 25 ml of absolute alcohol in the reaction mixture exerted a marked inhibitory effect on the reaction. Solutions containing greater than a twenty-fold excess of bipyridyl with a concentration of hydroxide of 0.315 M and rhodium (III) of  $5.63 \times 10^{-4}$  M at 60°C took six hours to reach 50% reaction. Such reactions could not be followed to completion as equilibria were established between the rhodium (I) product and small quantities of oxygen which slowly leaked into the apparatus whilst samples were removed for examination. Thus, using the same reaction conditions as previous runs, it was not possible to investigate reactions containing a sufficient excess of bipyridyl to

Figure 28.

Graph of  $\log_{10} k_{\text{obs}}$  against  $\log_{10} [\text{EtOH}]$   
(See Appendix 6)



assume that the concentration of bipyridyl remained constant throughout reaction. The following results were obtained at lesser excesses. A graph of  $k_{\text{obs}}^{-1}$  against bipyridyl concentration was linear in the range 0 to  $1.03 \times 10^{-3}$  M bipyridyl.

Effect of Bipyridyl on the Reaction Rate at 60°C, 1 Atmosphere of Hydrogen Pressure  $[\text{OH}^-] = 0.315\text{M}$ ,  $[\text{Rh}_0^{\text{III}}] = 5.63 \times 10^{-4}\text{M}$  in 25% Ethanol / Water.

$[\text{BIPY}] \times 10^4 \text{M}$	$k_{\text{obs}} \times 10^{-6} (\text{litre}^2 \text{mole}^{-2} \text{minutes}^{-1})$
0	0.694
5.01	0.143
10.3	0.0764
103	0.0492

The rate of hydrogen uptake by cis- $[\text{Rh}^{\text{III}}(\text{bipy})_2\text{Cl}_2]^+$  cations in 25% ethanol / water at 60°C and hydroxide concentration 0.186M under an atmosphere of the gas was investigated. It was found that if the reaction mixture was stirred, using a magnetic bead, the rate of hydrogen dissolving into the reaction medium became rate determining. Plots of volume of gas absorbed against time were linear and had the same gradient regardless of the initial rhodium (III) concentration. When the partial pressure of hydrogen was varied, the rates of gas uptake were inversely proportional to the partial pressure of hydrogen (Henry's Law) again showing that diffusion control was operating. It was therefore necessary to shake the reaction vessels in the hydrogen atmosphere to ensure adequate gas / solution contact. Although difficulty was experienced in recording volume changes as the system was agitated, sigmoid shaped gas uptake plots were obtained. Hydrogen uptake was found to obey the same rate equation as that observed spectrophoto-

metrically, that is :-

$$-\frac{d}{dt} [\text{H}_2] = k_{\text{obs}} [\text{Rh}^{\text{III}}]_0^2 [\text{Rh}^{\text{I}}]$$

where  $-\frac{d}{dt} [\text{H}_2]$  is the rate of consumption of hydrogen.

Rate constants ( $k_{\text{obs}}$ ) of the same magnitude as those observed in the rhodium (III) dependence runs were observed as the initial rhodium III concentration was varied from  $4.28 \times 10^{-3}$  to  $1.29 \times 10^{-3}$  M (see below).

Effect of  $[\text{Rh}_0^{\text{III}}]$  on the Reaction Rate at  $60^\circ\text{C}$  (as measured by the rate of hydrogen uptake) 1 Atmosphere of Hydrogen Pressure  
 $[\text{OH}^-] = 0.186$  M in 25% Ethanol / Water.

$[\text{Rh}_0^{\text{III}}] \times 10^3$ (M)	$k_{\text{obs}} \times 10^{-6}$ (litre <sup>2</sup> mole <sup>-2</sup> minutes <sup>-1</sup> )
4.28	1.05
3.00	0.566
1.71	0.452
1.29	0.864

These results show that the amount of hydrogen consumed is equivalent to the amount of rhodium (I) produced; if any rhodium hydrides are produced they are in very low concentration. Hydrogen is not involved in a slow post - rhodium (I) - producing reaction.

Induction periods were also observed in these runs. No hydrogen uptake occurred during the induction period, unlike the significant initial rate of carbon monoxide uptake by rhodium (III) at zero rhodium (I) concentration reported in reference 136.

A  $4.25 \times 10^{-3}$  M  $[\text{Rh}^{\text{III}}(\text{bipy})_2\text{Cl}_2]^+$  solution in 25% ethanol/

water, 0.309 M in hydroxide at 60°C underwent reaction even under an atmosphere of white spot nitrogen. The reduced rhodium (I) species was formed very slowly; six hours (approximately) being required for 50% completion of the reaction. Hence, there is a route by which some rhodium (I) can be produced which does not involve hydrogen. This route presumably involves ethanol as reducing agent. Since the latter is so slow, the route studied is thought to use hydrogen gas as reductant.

The counter ion has little effect on the rate of reduction of  $\left[ \text{Rh}^{\text{III}}(\text{bipy})_2 \text{Cl}_2 \right]^+$  cations as shown by the similar values of  $k_{\text{obs}}$  obtained for the nitrate, chloride and perchlorate salts (see below).

Effect of Counter Ion on the Reaction Rate at 60°C, 1 Atmosphere of Hydrogen Pressure  $[\text{OH}^-] = 0.315 \text{ M}$   $[\text{Rh}_0^{\text{III}}] = 5.58$  to  $5.63 \times 10^{-4} \text{ M}$  in 25% Ethanol / Water.

COUNTER ION	$k_{\text{obs}} \times 10^{-6}$ (litre <sup>2</sup> mole <sup>-2</sup> minutes <sup>-1</sup> )
$\text{Cl}^-$	4.60
$\text{ClO}_4^-$	4.31
$\text{NO}_3^-$	4.34

In the series of substituted bipyridyl complexes used cis -  $\left[ \text{Rh}^{\text{III}}(\text{L})_2 \text{Cl}_2 \right] \text{NO}_3$ , the order of increasing reaction rate was L = 4,4'-dichloro - bipyridyl < 4,4'-dimethyl - bipyridyl < 5,5'-dimethyl bipyridyl < bipyridyl. All substituents lowered the rate of reaction (see below). The reductions were done in duplicate and the average value of  $k_{\text{obs}}$  calculated (experimental error < 9%).

Effect of Bipyridyl Substituents on the Reaction Rate. 1 Atmosphere of Hydrogen Pressure.  $[\text{OH}^-] = 0.194$  to  $0.198$  M.  $[\text{Rh}_o^{\text{III}}] = 4.38$  to  $5.63 \times 10^{-4}$  M in 25% Ethanol / Water.

BIPYRIDYL SUBSTITUENT	Temperature	$k_{\text{obs}} \times 10^{-6}$ (litre <sup>2</sup> mole <sup>-2</sup> minutes <sup>-1</sup> )
5,5'-Me	60°C	0.616
4,4'-Me	60°C	0.416
4,4'-Cl	70°C	0.100
None	60°C	3.98

The phenanthroline complex cis -  $[\text{Rh}^{\text{III}}(\text{phen})_2\text{Cl}_2]^+$  reacted approximately three times more slowly than the bipyridyl one. The order of increasing reaction rate in substituted phenanthroline complexes was L = 3, 4, 7, 8 - tetramethyl phenanthroline < 5 nitro phenanthroline < phenanthroline as can be seen from the table below.

Effect of Phenanthroline Substituents on the Reaction Rate. 1 Atmosphere of Hydrogen Pressure,  $[\text{OH}^-] = 0.315$  M.  $[\text{Rh}_o^{\text{III}}] = 1.94$  to  $5.12 \times 10^{-4}$  M in 25% Ethanol / Water.

PHENANTHROLINE SUBSTITUENT	Temperature	$k_{\text{obs}} \times 10^{-6}$ (litre <sup>2</sup> mole <sup>-2</sup> minutes <sup>-1</sup> )
None	60°C	1.37
None	70°C	1.50
5NO <sub>2</sub>	70°C	0.430
3, 4, 7, 8 Me	70°C	0.0390

In an attempt to identify the reaction intermediates a variety of physical techniques were employed. Intermediate hydride species are likely to be diamagnetic, not paramagnetic.

Therefore proton exchange with the solvent, which occurs in paramagnetic hydride species, causing signal broadening and making it difficult to observe, should be avoided. The presence of spin - spin coupling of one proton (doublet) or two protons (triplet) with  $^{103}\text{Rh}$  ( $I = \frac{1}{2}$ ) would provide conclusive evidence for the presence of Rh - H bonds (163, 164). Consequently an N.M.R. spectrum was run on a 50% reduced  $\sim 0.3 \text{ M } [\text{Rh}^{\text{III}}(\text{bipy})_2\text{Cl}_2]^+$  solution in 25% ethanol / water, 0.35 M in hydroxide. No high field signal was observed. However, greater than 1% solutions of hydride species (containing one M - H bond) are needed to ensure detection by N.M.R.. The absence of a signal may be due to the low concentration of the solution, ( $\sim 0.2\%$ ) enforced by the low solubility of the rhodium (I) species in the reaction medium, or to the low concentration of any hydride intermediate formed .

Similarly, infra-red spectra of the half - reduced rhodium (III) complex on silver chloride plates did not show any stretching frequency which could be assigned to  $\nu$  Rh - H.

The rhodium (III) reagent and rhodium (I) product are expected to be diamagnetic, but any intermediate paramagnetic rhodium (II) monomer would give an E.S.R. signal. However, an E.S.R. spectrum of the above 50% reduced solution showed no signal.

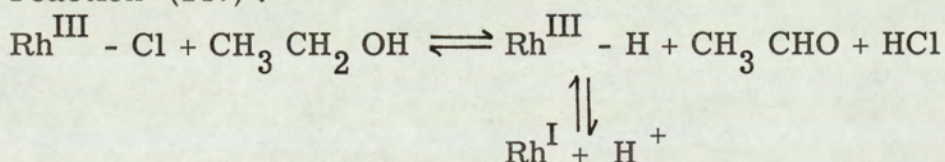
Thus physical techniques give only negative information about the possible reaction intermediates. Analytical figures show that the end product is the  $[\text{Rh}^{\text{I}}(\text{bipy})_2]^+$  cation (87).

The following deductions can be made from the above experimental observations.

Firstly, the reaction mechanism involves build up of an autocatalytic rhodium (I) species by some slow initiation process

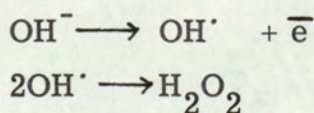
in the induction period. This is supported by the reduction of the induction period in the presence of rhodium (I) end product. Since oxygen reacts readily with such rhodium (I) species (148) some of the induction period is probably due to partial removal of oxygen from the system. In view of the observations that no hydrogen uptake occurs in the induction period, that a very much slower rhodium (III) reduction occurs under a nitrogen atmosphere and that no reaction occurs in the absence of ethanol or hydroxide ion, ethanol and / or hydroxide is thought to be acting as the reducing agent in the initiation sequence.

Ethanol could act as a two electron reducing agent by the slow reaction (147) :-



That is, nucleophilic displacement of chloride by ethanol followed by disproportionation to give acetaldehyde and  $\text{Rh}^{\text{III}} - \text{H}$ , which is in equilibrium with  $\text{Rh}^{\text{I}}$  in neutral and basic solution. However, the fact that neither decreasing ethanol concentration nor addition of chloride appear to increase the induction period is surprising if this mechanism operates (147). No reaction occurs if rhodium (I) is added in the absence of ethanol or if ethanol is replaced by n-butanol which also contains C-H groups. Hence ethanol may only be required to provide a suitable reaction medium in which the rhodium (I) (and / or II) species is soluble. This is supported by the accumulation of a brown species probably containing  $\text{Rh}_2^{2+}$  at high ethanol concentration.

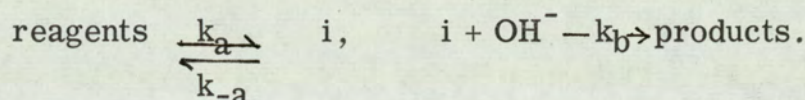
Hydroxide ion could act as the reducing agent in the induction period by the reaction :-



providing that only traces of hydrogen peroxide are produced. Otherwise, decomposition of this molecule would prevent rhodium(III) reduction going to completion and the 1 : 1 hydrogen : rhodium (III) ratio would not be observed.

The induction period is followed by a fast autocatalytic reaction. The rhodium dependence of  $k_{\text{obs}}$  indicates that two moles of a rhodium (III) complex and one of a rhodium(I) complex are involved in the rate-determining step.

The hydroxide dependence fits most readily a scheme involving an intermediate " i " to which the steady-state hypothesis can be applied.



$$\text{Thus } \frac{d}{dt} [\text{Products}] = \frac{k_a k_b [\text{reagents}] [\text{OH}^-]}{(k_{-a} + k_b [\text{OH}^-])}$$

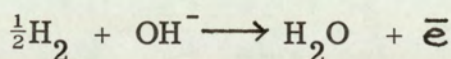
In view of the substitution inertness of rhodium (III) and the displacement of both coordinated chloride ions during the formation of the rhodium (I) end product, attack by hydroxide is most likely to occur in a fast reaction with a rhodium (I) or (II) species after the rate-determining step.

Subject to consideration of the above mentioned solubility problems and the composite nature of  $k_{\text{obs}}$  the -3 gradient of  $\log_{10} (k_{\text{obs}})$  versus  $I^{\frac{1}{2}}$  graphs could indicate reaction between oppositely charged reactants in a rate determining step. The negative species is probably  $\text{OH}^-$ .

The absence of a chloride dependence of the reaction indicates that rhodium chloride bonds are either broken after the slow step or in irreversible reactions. Mechanisms involving nucleophilic

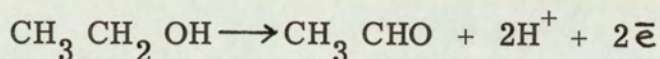
displacement of chloride from  $[\text{Rh}^{\text{III}}(\text{bipy})_2 \text{Cl}_2]^+$  by hydroxide in a pre-equilibrium step, can be excluded.

In view of the slowness of the reaction under white spot nitrogen, during which reduction occurs by the induction period reaction, the real reducing agent in the autocatalytic reaction is presumably hydrogen gas picked up by rhodium (I). The other alternatives are firstly :-



This reaction would have the wrong hydroxide dependence.

Secondly :-

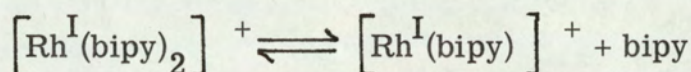


The hydrogen gas, known to be needed for the autocatalytic reaction, would have to be involved in a fast rhodium (I) catalysed reduction of acetaldehyde. The fact that the reaction rate decreases as the ethanol concentration increases and that acetaldehyde forms polymeric resins in hydroxide media suggests that ethanol does not act as the reducing agent in the autocatalytic reaction although it may produce some initial rhodium (I) in the induction period. However, if hydrogen is not required as the true reducing agent, one could argue that it should not be needed at all since the autocatalytic reduction of  $[\text{Rh}^{\text{III}}(\text{DMG})_2 \text{Cl}_2]$  in alkaline ethanolic solution occurs under white spot nitrogen (see Chapter VI).

The observed decrease in the autocatalytic reduction rate as the concentration of ethanol is increased may be due to changing the solvent nature. The behaviour of ethanol or water as a ligand could also account for the observed rate change in varying the ethanol to water ratio.

In view of the substitution inertness of rhodium(III) complexes, the inhibitory effect of bipyridyl is thought to be caused by one of

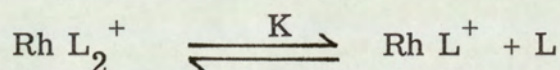
two alternatives, firstly the added bipyridyl suppressing an equilibrium to generate the active rhodium (I) species  $[\text{Rh}^{\text{I}}(\text{bipy})]^+$



(although solvent molecules might be involved in such a process, their presence is not shown here).

or secondly the excess bipyridyl coordinating to the active rhodium(I) species and blocking off an active site. The latter is thought to be unlikely since rhodium centres with more than six coordinated ligand donor atoms would have to be postulated in the reaction mechanism.

An attempt was made to interpret the kinetic data obtained at less than a twenty - fold excess of bipyridyl by considering two extreme situations. If an equilibrium :-



is set up and the rhodium (I) exists as essentially 100% bis complex, then with no added bipyridyl :-

$$[\text{L}] = [\text{Rh L}^+]$$

$$\text{and :- } [\text{Rh L}^+] = K^{\frac{1}{2}} [\text{Rh}^{\text{I}}]^{\frac{1}{2}}$$

It is found experimentally that the total rate of reduction is proportional to  $[\text{Rh}^{\text{I}}]_{\text{total}}$ . If the postulated dissociation equilibrium occurs and satisfies the assumptions, then this means that the reaction rate is proportional to  $[\text{Rh L}^+]^2$ . Thus, when bipyridyl is added :-

$$[\text{Rh L}^+] = K [\text{Rh}^{\text{I}}]_{\text{total}} / [\text{L}]$$

and the observed rate equation would alter from :-

$$\frac{d}{dt} [\text{Rh}^{\text{I}}] = k_{\text{obs}} [\text{Rh}^{\text{III}}]^2 [\text{Rh}^{\text{I}}]_{\text{total}}$$

$$\text{to } \frac{d}{dt} [\text{Rh}^{\text{I}}] = k_1 [\text{Rh}^{\text{III}}]^2 \frac{[\text{Rh}^{\text{I}}]_{\text{total}}^2}{[\text{L}]^2}$$

$k^{-\frac{1}{2}}$  would be proportional to the concentration of extra bipyridyl

added.

The integrated form of this equation is :-

$$\left(\frac{k T}{2}\right) t = \frac{1}{T^2} \left[ \left(\frac{T}{T-x}\right) - \frac{T}{x} + \ln\left(\frac{x}{T-x}\right) \right] + \text{constant} \quad (5)$$

using the previous notation.

Secondly, if all the species produced from the dissociation of bipyridyl are in the steady state, the concentration of bipyridyl ligand will be constant for the reaction and :-

$$\frac{d}{dt} [\text{Rh}^{\text{I}}] = k_{\text{obs}} [\text{Rh}^{\text{I}}] [\text{Rh}^{\text{III}}]^2$$

$k_{\text{obs}}^{-1}$  is then proportional to the concentration of bipyridyl added.

The integrated form of this equation is given by equation (2) as before.

All the bipyridyl dependence runs gave almost exact fits to equation (2) and the change of rate equation, expected from the first assumption was not observed. This shows that the second assumption of steady state conditions for the concentration of  $\text{Rh L}^+$  and dissociated bipyridyl is in agreement with the results obtained. A graph of  $k_{\text{obs}}^{-1}$  against bipyridyl concentration is linear in the range 0 to  $1.03 \times 10^{-3}$  M bipyridyl again suggesting that the bipyridyl inhibition resulted from suppression of an equilibrium involving bipyridyl dissociation to generate the active rhodium(I) species  $[\text{Rh}^{\text{I}}(\text{bipy})]^+$ .

The observed bipyridyl and phenanthroline substituent effects are difficult to interpret. The major reason for this difficulty is probably that several different steps are involved in the overall rate equation and each may be affected differently by substitution in the reagents. The observed trends cannot be correlated with ease of loss of a bipyridyl or phenanthroline ligand to generate the active rhodium (I) species. If electronic factors determine the reduction rate, the increasing electron-withdrawing effect of the ligand in the series  $\text{L} = 4, 4'\text{-Me bipyridyl} < 5, 5'\text{-Me}$

bipyridyl  $<$  bipyridyl  $<$  4, 4'-Cl bipyridyl should make the  $E^{\circ}$  value for reduction successively more positive, by analogy with  $M(\text{bipy})_3^{3+} / M(\text{bipy})_2^+$  (where  $M = \text{Fe}, \text{Ru}, \text{Os}$ ) (165, 166) thereby favouring reduction. However, the observed order of increasing reaction rate shows that this is not the case and suggests the importance of steric factors. When L is 4, 4'-dichloro-bipyridyl, the bulky chloride substituent exerts more steric hindrance than the methyl groups in 4, 4' and 5, 5'-dimethyl bipyridyl (as judged from the covalent radii). The reaction is at its slowest in this case. The 4, 4'-dimethyl bipyridyl ligand is similar to 5, 5'-dimethyl bipyridyl in the extent of steric hindrance at the rhodium (III) centre. It is assumed to react more slowly than its isomer on electronic grounds.

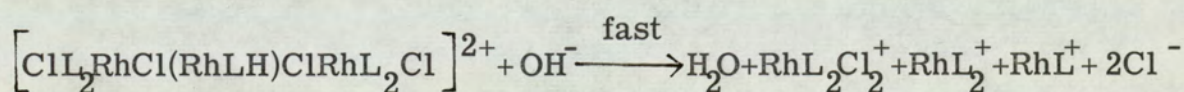
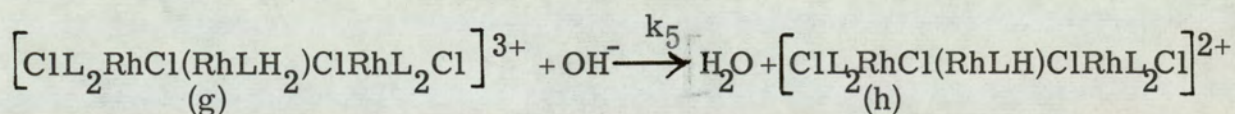
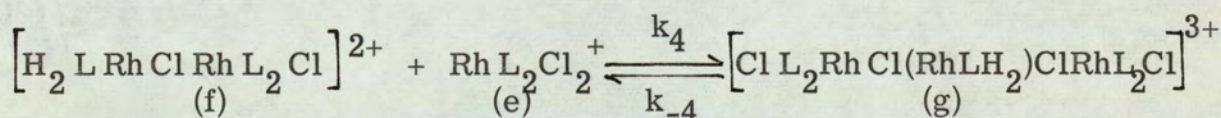
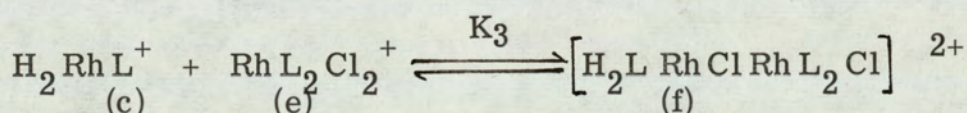
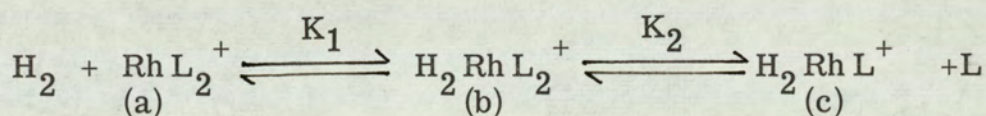
When L is phenanthroline, the  $E^{\circ}$  value for reduction is slightly more favourable than for the bipyridyl complex. The slower rate of reaction may be caused by the rigidity of phenanthroline relative to the more flexible bipyridyl. The most satisfactory configuration may be more easily attained by bipyridyl complexes. Alternatively, increased steric hindrance in phenanthroline relative to bipyridyl complexes may be responsible for the slower rate of reaction.

Again, on electronic grounds the reaction rate in substituted phenanthroline complexes is expected to decrease in the order  $L = 5 \text{NO}_2$  phenanthroline  $<$  phenanthroline  $<$  3, 4, 7, 8-tetramethyl phenanthroline. The observed reaction rate increases in the order of decreased steric hindrance.

Thus the observed substituent effects suggest steric reaction control (with electronic factors possibly having a small mitigating effect) and support a mechanism involving dimer and trimer formation. Further support for a dimeric intermediate is provided by the characterisation of the perchlorate and nitrate of the dihydrate of

a chloro-bis-2, 2'-bipyridyl rhodium (II) cation by Martin, McWhinnie and Waind (161). The solids are thought to have a chloride-bridged dimeric structure and are diamagnetic. On solution an equimolar mixture of  $[\text{Rh(I) (bipy)}_2]^+$  and  $[\text{Rh}^{\text{III}}(\text{bipy})_2 \text{Cl}_2]^+$  is obtained.

On the basis of the experimental observations, the following mechanism is postulated for the autocatalytic reaction. Solvent molecules are not shown but are assumed to be present where a species appears to be written as five coordinate. The steady state hypothesis is assumed to apply to (b), (c), (e), (f), (g) and (h). This will render the bipyridyl concentration also constant.



This last step could go via  $2\text{Rh}^{\text{II}} + \text{Rh}^{\text{I}}$  then a fast disproportionation.

$$[f] = K_1 K_2 K_3 [\text{H}_2] [a] [e] / [L]$$

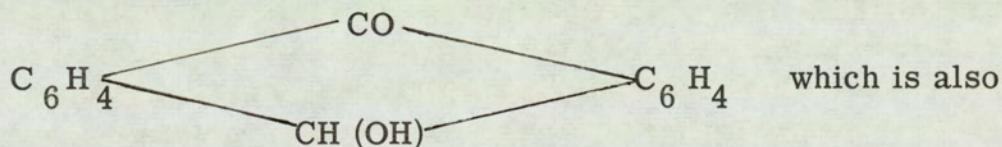
Applying the steady state hypothesis for (g) then gives

$$k_4 [e] [f] = k_{-4} + k_5 [\text{OH}^-] [g]$$

Thus

$$\frac{d[\text{Rh}^{\text{I}}]}{dt} = k_5 [\text{OH}^-] [g] = \frac{K_1 K_2 K_3 k_4 k_5 [\text{H}_2] [\text{OH}] [a] [e]^2}{[L] \{ k_{-4} + k_5 [\text{OH}^-] \}}$$

The  $[\text{Rh}^{\text{I}}(\text{bipy})_2]\text{Cl}$  end product was qualitatively tested as a hydrogenation catalyst. The species was generated in homogeneous alkaline ethanolic solution under a hydrogen atmosphere which was then replaced by nitrogen and the reagent to be hydrogenated was added under nitrogen. When maleic acid was added, effervescence but no immediate purple to yellow colour change occurred. One day later, a violet-black solid, presumably  $[\text{Rh}^{\text{I}}(\text{bipy})_2\text{olefin}]^+$  had precipitated and the clear upper solution gave the fluorescein test for succinic acid suggesting that slow hydrogenation by a rhodium hydride species had occurred (136, 137, 138, 167). When anthroquinone was added to the heated reduced solution under nitrogen, an immediate violet to red colour change occurred. The red coloration was thought to be oxanthranol



produced by reduction of anthroquinone by zinc and alkali. On replacing the nitrogen atmosphere by oxygen the solution decolorised and anthroquinone was reformed as a flocculent yellow precipitate. Therefore, the rhodium (I) complex is probably acting as a hydrogen transfer agent (163). Reactions of the rhodium (I) complex with benzonitrile (154) and 1 decene (157) slowly yielded oily violet droplets in suspension, probably indicating complex formation.

Chapter VI.

The Kinetics of the Autocatalytic Reduction of Monohydrogen-Dichloro-bis-dimethylglyoxime-Rhodium(III) in Alkaline Ethanolic Solution under a Nitrogen Atmosphere.

Recently bis-dimethylglyoximato-rhodium analogues of (III), (II) and (I) cobaloximes have been characterised (68, 69, 168). These rhodoxime complexes show great similarity to the cobaloximes although rhodoxime (I) complexes are less nucleophilic than their cobalt (I) analogues and undergo slower  $S_N2$  alkylation (52). The greater stability of the rhodium-carbon bond causes methyl rhodoximes to act as competitive inhibitors in vitamin  $B_{12}$  dependent methyl transfer enzymic reactions.

Kinetic studies have been carried out on the alkylation of cobaloximes (I) (59) and (II) (58). The mechanisms of methyl cobaloxime photolysis (61, 62, 169) and enzymatic demethylation (170) have been studied. However, no analogous mechanistic studies have been done on rhodoximes, nor have the kinetics of the reduction of cobaloximes or rhodoximes been investigated.

The complexes  $\left[ \text{Rh} (\text{DMG})_2 (\text{P Ph}_3) \text{Cl} \right]$  and  $\text{H} \left[ \text{Rh} (\text{DMG})_2 \text{Cl}_2 \right]$  (in the solid state, the isolated proton is considered to be bonded to one  $\text{O}^-$  of a dimethylglyoxime ligand) are reported to be reduced to rhodoxime (I) nucleophiles by the addition of an equimolar amount of sodium borohydride in 0.1 M sodium hydroxide (52). In view of the previously studied homogeneous reduction of cis  $\left[ \text{Rh} (\text{bipy})_2 \text{Cl}_2 \right]^+$  cations, in which hydrogen in alkaline ethanolic solution can be used instead of borohydride as reducing agent, it was decided to investigate the kinetics of the reduction of the two rhodoxime complexes using the former reducing medium.

The structures of the two rhodoxime complexes were investigated by physical techniques and their reduction products were characterised.

Aqueous solutions of the monobasic acid  $\text{H} \left[ \text{Rh}^{\text{III}}(\text{DMG})_2\text{Cl}_2 \right]$  (171) showed ultra-violet absorptions at  $\lambda_{\text{max}}$ . 205 nm. ( $\epsilon$  48,400) 272 nm. (7,960) and 353 nm. (1,380). In ethanolic solutions the absorptions occurred at 215 nm. ( $\epsilon$  40,800), 281 nm. (7,570) and 365 nm. (1,310). The infra-red spectrum showed peaks at  $3,300 \text{ cm}^{-1}$ , the OH stretching mode and  $1597 \text{ cm}^{-1}$ , the OH deformation. An extremely broad band centred at  $2440 \text{ cm}^{-1}$  appeared due to the O — H---O stretch of the dimethylglyoxime ligand (84). The corresponding O — H---O bond for the analogous cobalt complex is at  $1800 \text{ cm}^{-1}$ , indicating the longer, weaker hydrogen bond in this rhodium complex. In the solid state the structure of the complex is considered to be like that of the analogous cobalt complex (172).

The  $\text{H} \left[ \text{Rh}^{\text{III}}(\text{DMG})_2\text{Cl}_2 \right]$  complex, being acidic is only soluble in basic solvents such as formamide, dimethyl-formamide and dimethylsulphoxide. A saturated formamide solution shows a peak at  $\gamma = 7.95$  relative to  $\text{Si}(\text{Me})_4$  in its  $^1\text{H}$  N.M.R. spectrum. The absence of a proton resonance due to the intramolecular hydrogen bond suggests that a rapid proton transfer to formamide is occurring, that is  $\text{HCO NH}_3^+$  formation (84). A base weaker than the dimethylglyoxime complex is needed as a suitable solvent for this proton to be examined by N.M.R. but even then there would probably still be rapid exchange.  $\text{CH}_3 \text{CO N}(\text{Me})_2$  could be tried.

When  $\text{H} \left[ \text{Rh}^{\text{III}}(\text{DMG})_2\text{Cl}_2 \right]$  is reduced by an equimolar amount of sodium borohydride using the literature method (68) a dark blue - black, oxygen sensitive, product thought to contain  $\text{H} \left[ \text{Rh}^{\text{I}}(\text{DMG})_2 \right]$  is produced. This product also shows broad infra-red absorptions at  $3,400 \text{ cm}^{-1}$ ,  $2,400 \text{ cm}^{-1}$  and  $1,650 \text{ cm}^{-1}$ . No information could

be obtained by N.M.R. spectroscopy as the complex was readily oxidised in the basic solutions required. The ultra-violet spectrum of  $\text{H} \left[ \text{Rh}^{\text{I}}(\text{DMG})_2 \right]$  in alkaline ethanolic solution under an inert atmosphere showed two peaks in the visible at 458 nm ( $\epsilon$  7,060) and 575 nm (670) which obey Beer's Law. An apparently identical sample was isolated by reduction of  $\text{H} \left[ \text{Rh}^{\text{III}}(\text{DMG})_2\text{Cl}_2 \right]$  in hot 25% ethanolic solution under a nitrogen atmosphere using a two-fold excess of hydroxide. Attempts to prepare a red rhodium (II) dimeric complex from  $\text{H} \left[ \text{Rh}^{\text{III}}(\text{DMG})_2\text{Cl}_2 \right]$  (168) or  $\text{H} \left[ \text{Rh}^{\text{I}}(\text{DMG})_2 \right]$  (68) were unsuccessful.

The yellow complex  $\left[ \text{Rh}^{\text{III}}(\text{DMG})_2(\text{PPh}_3)\text{Cl} \right]$  in ethanolic solution gave ultra-violet absorptions at 213 nm ( $\epsilon$  50,700) and 270 nm (28,100). The infra-red spectrum showed a broad absorption at  $2,400 \text{ cm}^{-1}$  less pronounced than that of  $\text{H} \left[ \text{Rh}^{\text{III}}(\text{DMG})_2\text{Cl}_2 \right]$  due to the two intramolecular  $\text{O}-\text{H}\cdots\text{O}$  bonds of the ligand but no absorptions due to OH stretch or deformation. The complex is non-acidic. The N.M.R. spectrum in methylene chloride showed peaks at  $\gamma = 2.48, 8.05$  and  $-0.73$  of relative intensities 15 : 12 : 2 due to the triphenylphosphine, dimethylglyoxime and hydrogen bonded protons respectively. The expected doublet splitting of the  $\gamma = 8.05$  signal due to coupling of the methyl group protons with  $^{31}\text{P}$  by long range interaction (173) or due to two different methyl group environments imposed by the triphenylphosphine stereochemistry, was not observed. The peak at  $\gamma = -0.73$  indicates that longer, weaker  $\text{O}-\text{H}\cdots\text{O}$  bonds exist in the rhodium complex relative to cobalt and nickel dimethylglyoxime complexes which give peaks at approximate tau values of  $-8.5$  and  $-8$  respectively.

Borohydride reduction of  $\left[ \text{Rh}^{\text{III}}(\text{DMG})_2\text{PPh}_3\text{Cl} \right]$  (168) generated the red dimer  $\left[ \text{Rh}(\text{DMG})_2(\text{PPh}_3) \right]_2$  (55) which, in ethanolic solution, showed a peak in the visible at 458 nm ( $\epsilon$  9,600). The infra-red spectrum showed the  $\text{O}-\text{H}\cdots\text{O}$  peak centred at  $2400 \text{ cm}^{-1}$

N.M.R. peaks at  $\gamma = 8.10, 2.53$  and  $-2.5$  of relative intensities  $15 : 12 : 2$  were obtained from methylenechloride solutions.

More prolonged reduction of  $[\text{Rh}^{\text{III}}(\text{DMG})_2(\text{P Ph}_3)\text{Cl}]$  generated a purple product which showed a sharp infra-red peak at  $1985 \text{ cm}^{-1}$  assigned to a rhodium-hydride stretch. No N.M.R. high field resonance could be detected when deuteriochloroform was used as solvent. The purple product was thought to contain a mixture of the blue monomer  $[\text{Rh}(\text{DMG})_2(\text{P Ph}_3)\text{H}]$  and the red dimer. The preparation of pure  $[\text{Rh}(\text{DMG})_2(\text{P Ph}_3)\text{H}]$  by borohydride reduction of ice cold methanolic solutions of  $[\text{Rh}(\text{DMG})_2\text{P Ph}_3\text{Cl}]$  under an argon atmosphere could not be reproduced (68).

Thus physical studies indicate that the kinetics of the homogeneous reductions of  $\text{H} [\text{Rh}^{\text{III}}(\text{DMG})_2\text{Cl}_2]$  to give  $\text{H} [\text{Rh}^{\text{I}}(\text{DMG})_2]^+$  and  $[\text{Rh}^{\text{III}}(\text{DMG})_2\text{P Ph}_3\text{Cl}]$  to  $[\text{Rh}^{\text{II}}(\text{DMG})_2\text{P Ph}_3]_2$  and  $[\text{Rh}^{\text{I}}(\text{DMG})_2\text{P Ph}_3\text{H}]$  could be followed spectrophotometrically by observing the increase in optical density at  $458 \text{ nm.}$  and / or  $575 \text{ nm.}$  Infra-red and N. M.R. studies show that  $[\text{Rh}^{\text{III}}(\text{DMG})_2\text{P Ph}_3\text{Cl}]$  has two acidic protons in the intramolecular  $\text{O}-\text{H}\cdots\text{O}$  bonds of the dimethylglyoxime ligands. Similarly,  $\text{H} [\text{Rh}^{\text{III}}(\text{DMG})_2\text{Cl}_2]$ , in the solid state, contains one  $\text{O}-\text{H}\cdots\text{O}$  bond per mole and two  $\text{O H}$  groups. The complex acts as a monobasic acid by loss of one of the  $\text{O H}$  protons forming the conjugate base, which has two  $\text{O}-\text{H}\cdots\text{O}$  intramolecular bonds and therefore two further acidic protons.

Preliminary experiments on the reduction of  $0.01 \text{ M}$  solutions of  $[\text{Rh}^{\text{III}}(\text{DMG})_2\text{Cl}_2]$  and  $[\text{Rh}^{\text{III}}(\text{DMG})_2\text{P Ph}_3\text{Cl}]$  in  $25\%$  ethanolic solution,  $0.5 \text{ M}$  in sodium hydroxide at  $60^\circ\text{C}$  under a hydrogen atmosphere showed that both complexes developed peaks in the visible at  $458 \text{ nm.}$  and  $575 \text{ nm.}$  Whereas reactions of  $\text{H} [\text{Rh}^{\text{III}}(\text{DMG})_2\text{Cl}_2]$  solutions were complete in approximately ten minutes,  $[\text{Rh}^{\text{III}}(\text{DMG})_2\text{ClPPh}_3]$

reacted much more slowly, taking many hours to reach completion. Therefore  $\text{H} \left[ \text{Rh}^{\text{III}}(\text{DMG})_2\text{Cl}_2 \right]$  was selected as the starting material for the first kinetic study.

Both hydroxide and ethanol were found to be essential for reaction. However, hydrogen could be replaced by nitrogen without the rate of reaction being altered, showing that hydrogen is not the reducing agent in this system. Although the reaction is not strictly within the scope of the title of this thesis, it was decided to continue the kinetic study because of the interesting reaction and its difference from that occurring for the  $\text{Rh}^{\text{III}}$  bipyridyl complex. The reduction is of relevance to previous work and is performed by a simple reducing medium.

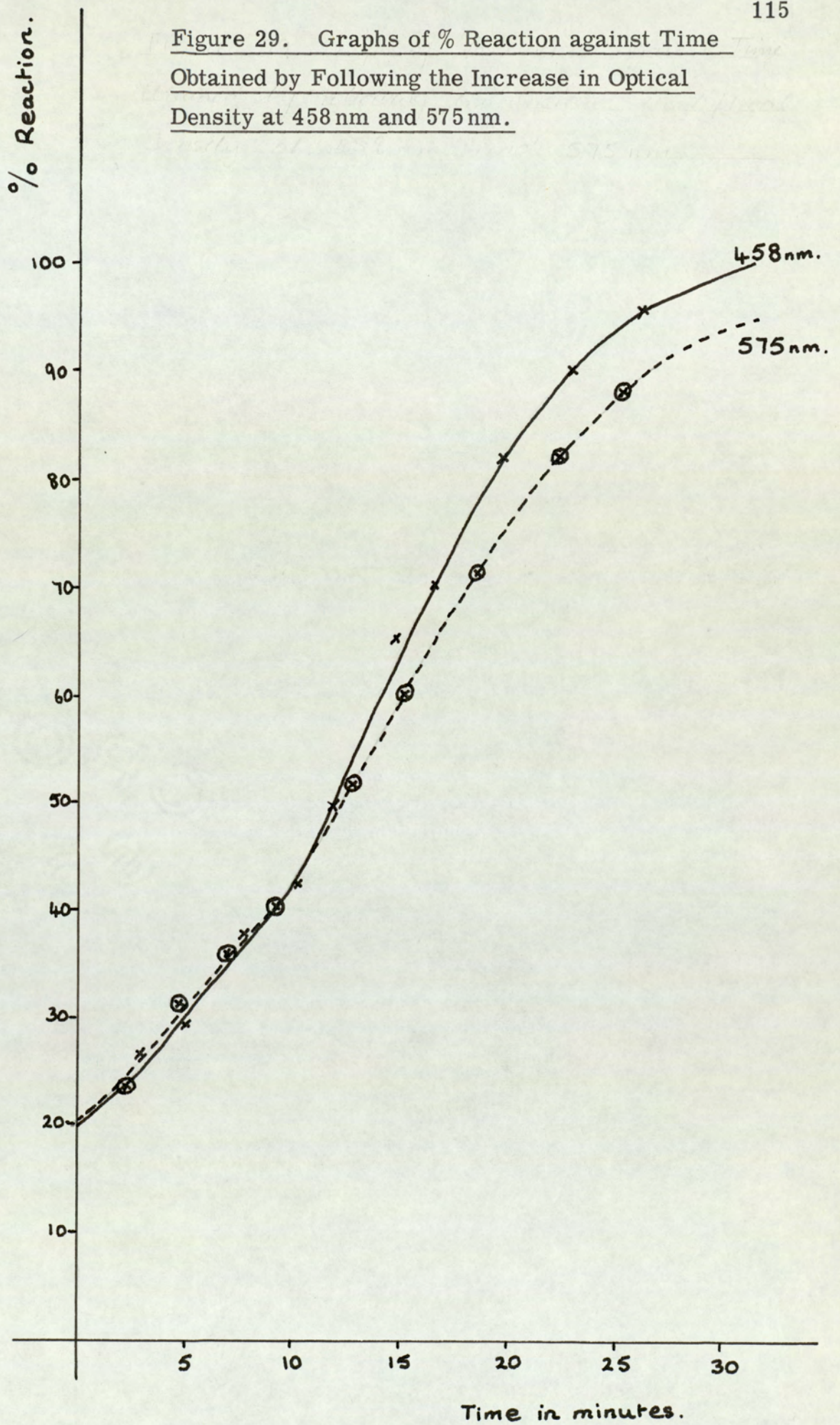
The absorptions of the complex at 458 nm and 575 nm, which obey Beer's Law, were always found to occur in the ratio 10.5 to 1 as the initial concentration of rhodium(III) complex was altered (see below).

Effect of the Initial Concentration of  $\text{H} \left[ \text{Rh}^{\text{III}}(\text{DMG})_2\text{Cl}_2 \right]$  on the Ratio of Absorptions at 458 nm. and 575 nm.  $[\text{OH}^-] = 0.309 \text{ M}$  in 25% Ethanol / Water under a Hydrogen Atmosphere at 60°C.

$\left[ \text{Rh}^{\text{III}} \right]_0 \times 10^3 \text{ M}$	ratio of optical densities at 458 nm. : 575 nm.
1.125	10.7
0.900	10.5
0.675	11.8
0.450	10.4

This shows that a dimer / monomer equilibrium is not responsible for the two absorptions. Although the visual colour of the solutions

Figure 29. Graphs of % Reaction against Time  
Obtained by Following the Increase in Optical  
Density at 458 nm and 575 nm.



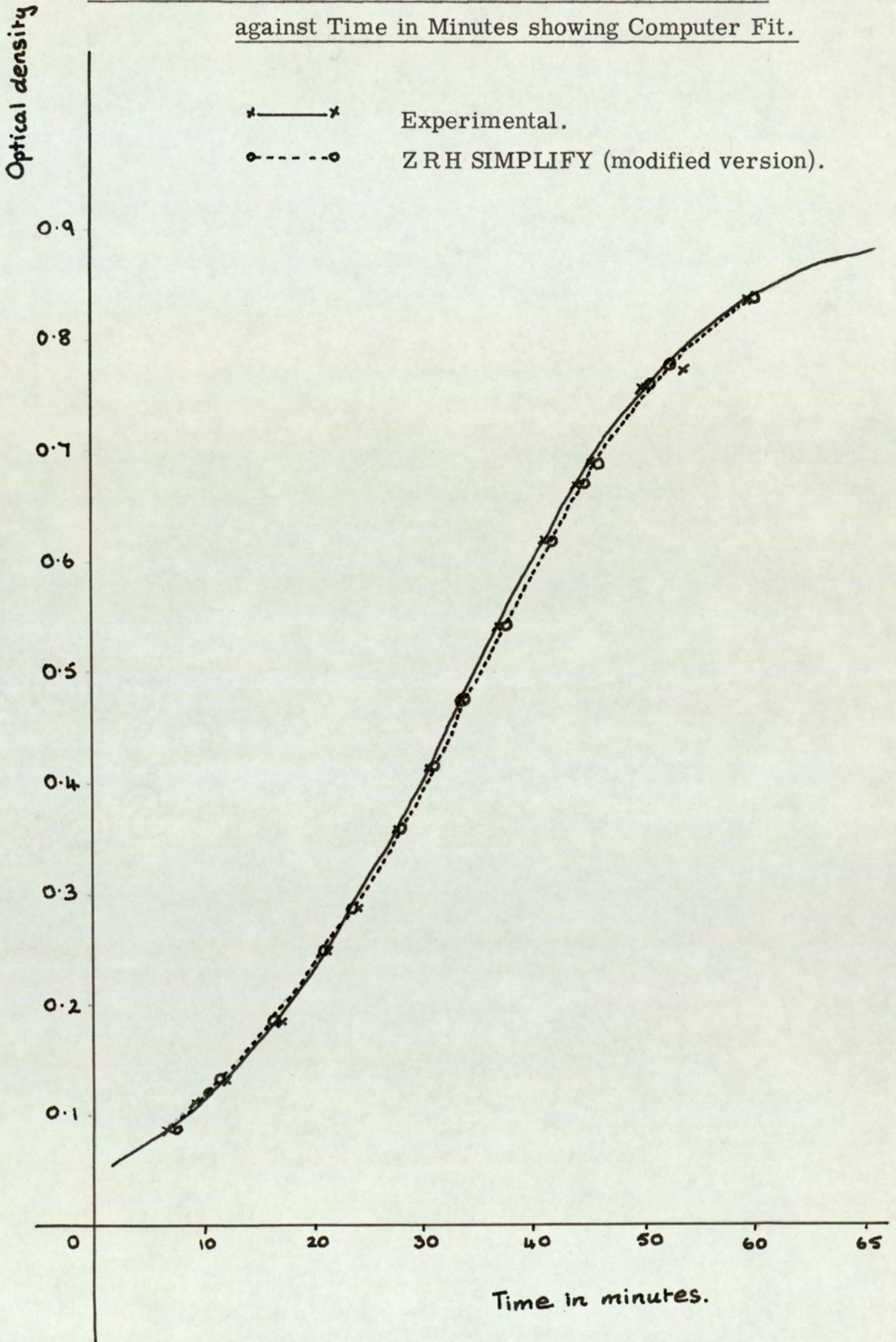
changed slightly from green to red - brown as the concentration of hydroxide was increased in the range 0.012 M to 1.05 M, the peak ratio stayed approximately constant (see below).

Effect of the Hydroxide Concentration on the Ratio of Absorptions  
at 458 nm. and 575 nm. Concentration of H  $[\text{Rh}^{\text{III}}(\text{DMG})_2\text{Cl}_2]$   $2.98 \times 10^{-3}$  M  
in 25% Ethanol / Water under a Nitrogen Atmosphere at 60°C.  $\mu = 1.5$   
 (maintained by A. R. sodium nitrate).

$[\text{OH}^-]$ (M)	ratio of optical densities at 458 nm. : 575 nm.
0.0562	10.4
0.179	10.5
0.317	10.5
0.393	9.8
0.526	10.4
0.787	9.1
0.972	9.4

Therefore, a hydroxide dependent equilibrium between two complexes is unlikely to be the cause of the colour change. A change in absorption maxima of the peaks as concentration of hydroxide is altered is thought to be responsible for the apparent colour change of the solutions. Finally, when the reaction rate was followed at the two wavelengths individually, kinetic plots of the same rate profile were obtained (see Figure 29). Rate constants of the same magnitude were obtained when the extinction coefficients at 458 nm. and 575 nm. were calculated on the assumption that they were absorptions of the same rhodium (I) complex ( $\text{H} [\text{Rh}^{\text{I}}(\text{DMG})_2]$ ) present at a concentration equal to that of the initial rhodium (III) complex used. It is therefore reasonable to suppose that only one product is formed, this product causing both absorptions.

Figure 30. Specimen Graph of Optical Density at 575 nm  
against Time in Minutes showing Computer Fit.



When the reduction was followed by increase in optical density at 575 nm, at constant ionic strength maintained by A.R. sodium nitrate solutions, plots of the concentration of the rhodium (I) complex produced versus time were obtained which again show an autocatalytic process to be operating (see Figure 30). These plots yielded a maximum slope at a point representing 50% of the total rhodium (I) produced regardless of the initial rhodium (III) concentration used. Graphical differentiation of the plots gave rise to curves which were nearly symmetrical about the 50% reaction point (see Figure 31). A rate proportional to the product  $[\text{Rh}^{\text{III}}][\text{Rh}^{\text{I}}]$  becomes a maximum when  $[\text{Rh}^{\text{III}}] = [\text{Rh}^{\text{I}}] = \text{half the total rhodium}$ . Therefore the dominant term in the rate expression probably has a rhodium dependence given by:-

$$\frac{d[\text{Rh}^{\text{I}}]}{dt} = k_{\text{obs}} [\text{Rh}^{\text{III}}][\text{Rh}^{\text{I}}]$$

where  $k_{\text{obs}}$  is a pseudo second order rate constant containing all chemical and physical variables except the dependence on rhodium.

The integrated form of this rate equation is :-

$$k_{\text{obs}} t = \frac{1}{T} \log \left( \frac{x}{T-x} \right) + \text{constant.}$$

where T is the total concentration of rhodium and x is the concentration of rhodium (I).

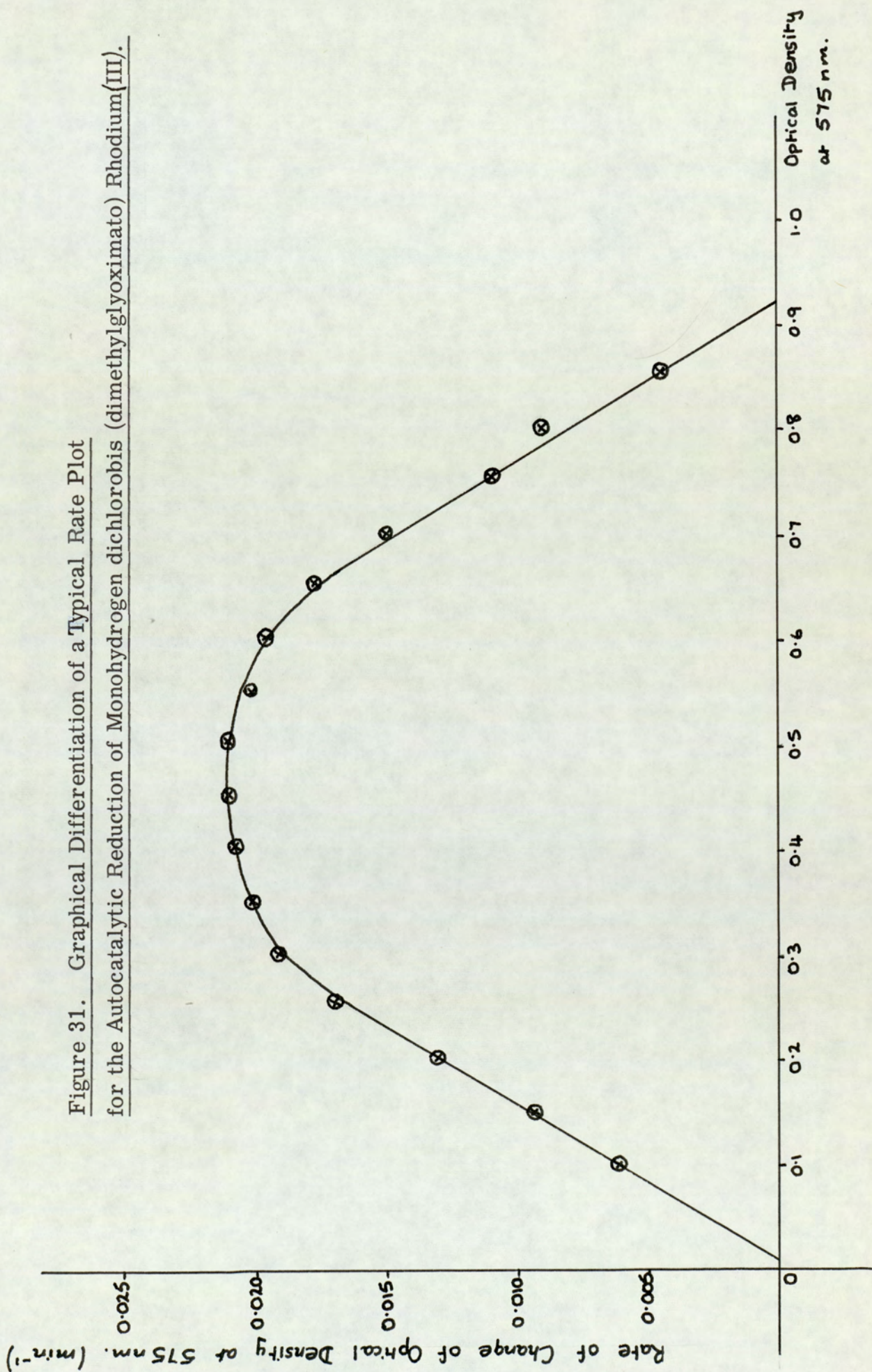
In terms of the observed optical densities this equation becomes :-

$$k t = \frac{1}{O D \infty} \ln \left( \frac{O D t}{O D \infty - O D t} \right) + \text{constant.}$$

where O D t is the observed optical density at 458 nm or 575 nm at time t, and O D  $\infty$  is the optical density at infinity.

$$k_{\text{obs}} = \frac{k (O D \infty)}{[\text{Rh}^{\text{III}}]_0}$$

$[\text{Rh}^{\text{III}}]_0$  is the concentration of rhodium (III) at zero time. Plots of the right hand side of this equation against time gave good straight lines up to 90% reaction. A least squares computer program, which was a modification of ZRH SIMPLIFY was used to find the best values for the rate constant and integration constant using the experimentally



determined infinity value and feeding in pairs of optical density and time readings.

In this autocatalytic reaction, induction periods were only observed when the reduction rate was very slow. This observation may demonstrate slight contamination within the reagent sample. Frequently inefficient mixing caused the build up of local concentrations of rhodium (I) causing an erroneous rapid initial rise in the optical density at 575 nm. After this, the reaction proceeded smoothly.

The rhodium dependence of the rate equation was checked by measuring  $k_{\text{obs}}$  by using different initial rhodium (III) concentrations at constant temperature and hydroxide concentration.  $k_{\text{obs}}$  was found to be constant at  $67.6 \mp 3.7$  litre mole<sup>-1</sup> minutes<sup>-1</sup> within the limits of experimental error (see below).

Effect of  $[\text{Rh}_{\text{O}}^{\text{III}}]$  on the Reaction Rate at 50°C 1 Atmosphere Nitrogen Pressure,  $[\text{OH}^-] = 0.623$  M in 25% Ethanol/Water  $\mu = 1.5$  (maintained by A. R. sodium nitrate.)

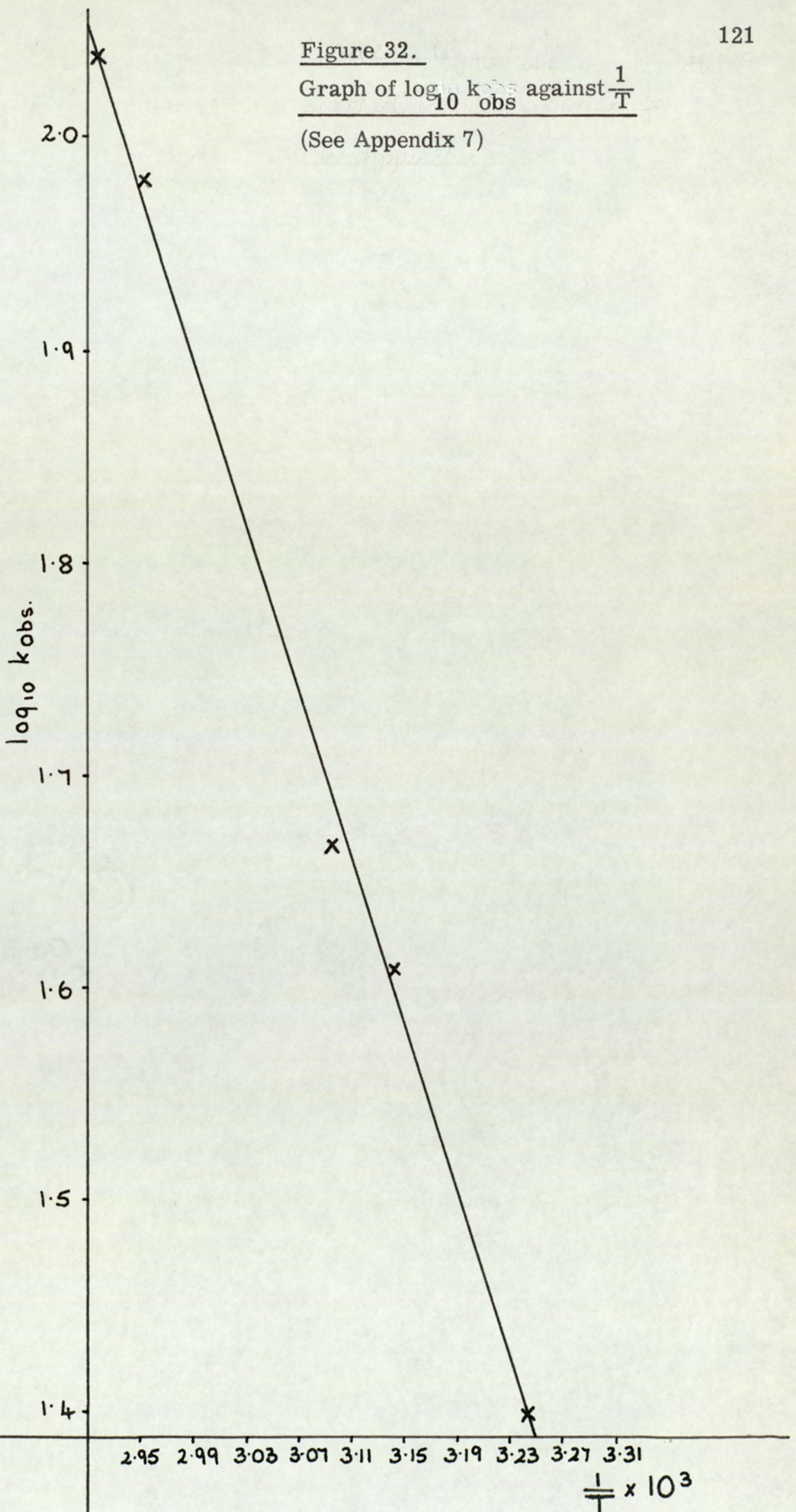
$[\text{Rh}_{\text{O}}^{\text{III}}] \times 10^3$ (M)	$k_{\text{obs}}$ (litre mole <sup>-1</sup> minutes <sup>-1</sup> )
0.994	88.2
1.99	58.8
2.98	62.5
3.95	66.4
4.89	67.1
6.01	63.8

Measurements over the temperature range 35°C to 70°C yielded a good Arrhenius plot (see Figure 32). A value of  $8.8 \mp 0.3$  k./cal./mole was obtained for that parameter of the observed overall rate constant equivalent to an activation energy.

Figure 32.

Graph of  $\log_{10} k_{\text{obs}}$  against  $\frac{1}{T}$ 

(See Appendix 7)

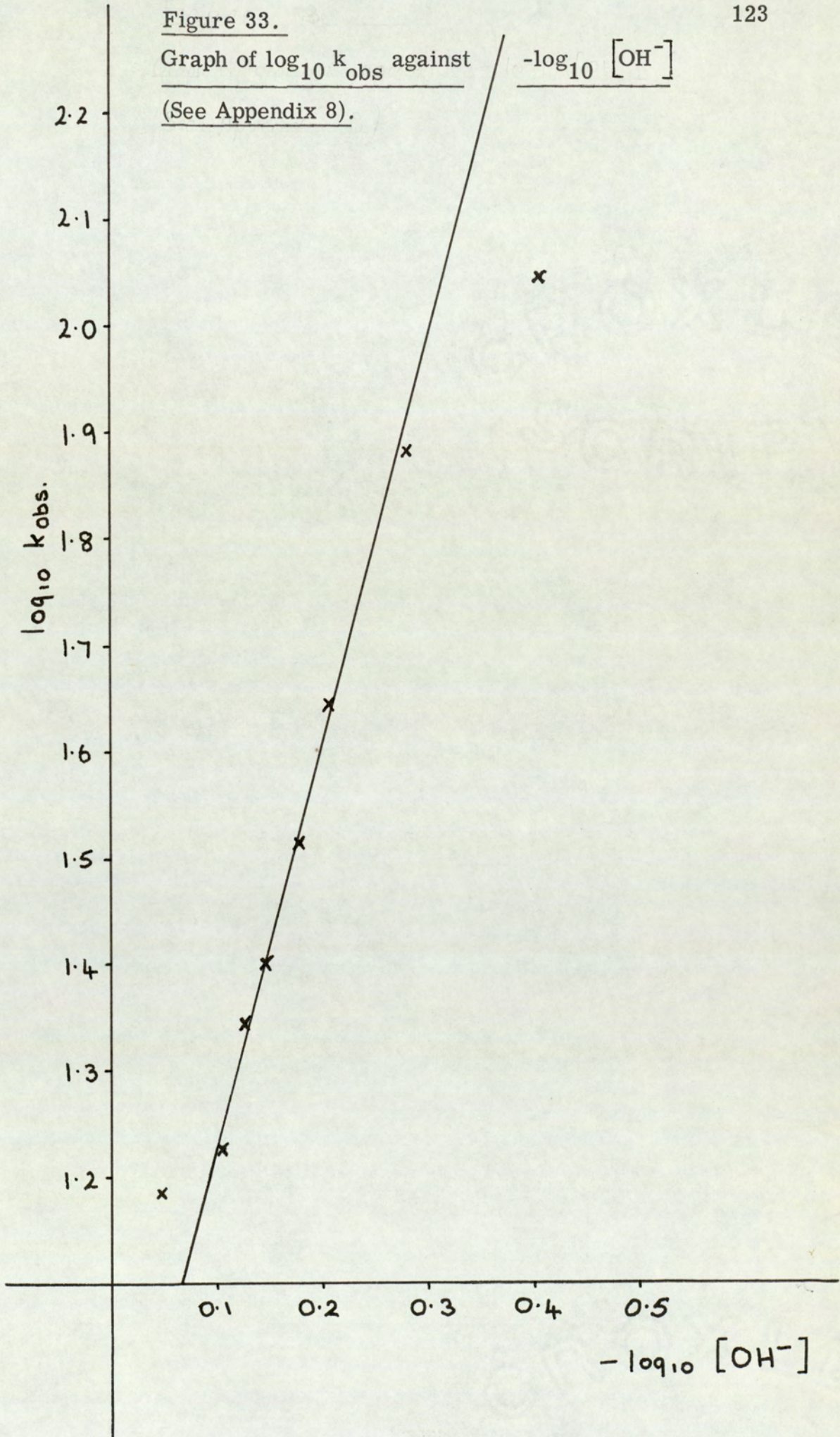


Investigation of the hydroxide dependence of the reaction showed that no reaction occurred until the ratio of hydroxide to  $\text{H} \left[ \text{Rh}^{\text{III}}(\text{DMG})_2\text{Cl}_2 \right]$  exceeded 1 : 1. Thus, using a  $2.98 \times 10^{-3} \text{M}$  rhodium (III) solution and  $2.98 \times 10^{-3} \text{M}$  hydroxide, (measured  $\text{pH} = 7.0$ ) no reaction occurred. A mixture containing  $2.98 \times 10^{-3} \text{M}$  rhodium (III) and  $4.95 \times 10^{-3} \text{M}$  hydroxide reacted slowly at  $50^\circ\text{C}$  to give a brown precipitate whereas mixtures containing a two-fold excess of hydroxide reacted immediately forming first a dark purple solution and finally a black precipitate in a green solution. This complex was isolated. Analytical data are consistent with a formula of  $\text{H} \left[ \text{Rh}^{\text{I}}(\text{DMG})_2 \right]$ . It is definitely not metallic rhodium as reported in reference 159. The complex is soluble in solutions containing greater than a five-fold excess of hydroxide and in organic basic solvents.

The required ratio of  $\text{Rh}^{\text{III}} : \text{OH}^-$  of greater than 1 : 1 is presumably due to the non reactivity of  $\text{H} \left[ \text{Rh}^{\text{III}}(\text{DMG})_2\text{Cl}_2 \right]$ . The strongly acidic proton must first be removed to form the  $\left[ \text{Rh}^{\text{III}}(\text{DMG})_2\text{Cl}_2 \right]^-$  active species.

The reaction rate showed a systematic inverse dependence on the fourth power of the hydroxide concentration in the range 0.526 to 0.787M (see Figure 33). At concentrations below 0.393 M the reaction was extremely fast, reaching completion in fifteen minutes, and the experimental technique became unsatisfactory. At concentrations of 0.901 M hydroxide and greater, the reaction was very slow, lengthy induction periods during which slight oxygen leakage into the apparatus occurred, were observed.

The reaction rate showed no dependence on the concentration of chloride ion in the range 0 to 1.25 M chloride and constant ionic strength  $\mu = 1.5$  (maintained by A. R. sodium nitrate). Values of  $k_{\text{obs}}$  were constant at  $45.7 \mp 4.0 \text{ litre mole}^{-1} \text{ minutes}^{-1}$  within the limits of experimental error.



Effect of  $[\text{Cl}^-]$  on the Reaction Rate at  $50^\circ\text{C}$ , 1 Atmosphere of Nitrogen Pressure  $[\text{OH}^-] = 0.623 \text{ M}$ ,  $[\text{Rh}_\text{O}^{\text{III}}] = 2.98 \times 10^{-3} \text{ M}$   
 in 25% Ethanol / Water  $\mu = 1.5$  (maintained by A.R. sodium nitrate).

$[\text{Cl}^-]$ (M)	$k_{\text{obs}}$ (litre mole <sup>-1</sup> minutes <sup>-1</sup> )
0	47.8
0.30	45.4
0.45	53.3
0.60	41.2
0.75	38.9
0.90	55.5
1.25	37.9

Addition of dimethylglyoxime showed a pronounced inhibitory effect on the reaction rate (see below).

Effect of Dimethylglyoxime Concentration on the Reaction Rate at  $50^\circ\text{C}$ , 1 Atmosphere of Nitrogen Pressure  $[\text{OH}^-] = 0.623 \text{ M}$   $[\text{Rh}_\text{O}^{\text{III}}] = 2.98 \times 10^{-3} \text{ M}$  in 25% Ethanol / Water  $\mu = 1.5$  (maintained by A. R. sodium nitrate.)

$[\text{DMG}] \times 10^2$ (M)	$k_{\text{obs}}$ (litre mole <sup>-1</sup> minutes <sup>-1</sup> )
0	46.5
1.50	21.0
2.46	10.1
6.47	8.77
8.62	6.27

It was not possible to deduce the dependence of reaction rate on concentration of added dimethylglyoxime owing to the irreproducibility of the results.

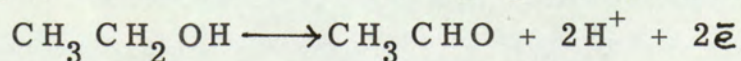
The reaction was found to have an absolute requirement for ethanol

as no reaction occurred in purely aqueous alkaline media. The ethanol dependence of the reaction rate was not investigated owing to the difficulty in interpreting results when the reaction medium is altered.

From these experimental observations, the following deductions were made. Since reactions showing a rate depending on the concentration of end product should theoretically never start, the reaction mechanism must either involve build up of the autocatalytic rhodium (I) species by a slow reduction process in the induction period, ethanol or hydroxide ion could be acting as the reducing agent, or the rhodium (III) samples must all contain some degree of rhodium (I) contamination. The induction period is followed by a faster autocatalytic reaction involving one mole of a rhodium (III) complex and one of a rhodium (I) complex in the rate-determining step.

In view of the necessity of having hydroxide present in greater than equimolar concentration relative to  $\text{H} \left[ \text{Rh}^{\text{III}}(\text{DMG})_2\text{Cl}_2 \right]$ , the protonated species  $\text{H} \left[ \text{Rh}^{\text{III}}(\text{DMG})_2\text{Cl}_2 \right]$  must be non-reactive. Removal of the strongly acidic proton is necessary to generate the active rhodium (III) and rhodium (I) anionic species involved in the rate-determining step. The observed inverse dependence on the fourth power of the hydroxide concentration is thought to result from equilibria existing between singly deprotonated rhodium (III) and rhodium (I) species involved in the rate-determining step and the complexes from which both the two acidic hydrogen-bonding protons have been removed. The latter complexes do not react.

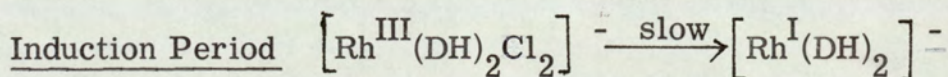
The absence of a chloride dependence of the reaction indicates that rhodium-chloride bonds are either broken after the slow step or in irreversible reactions. The fact that a hydrogen atmosphere is not necessary for reaction to occur shows that ethanol is probably acting as the two electron reducing agent in the autocatalytic reaction.



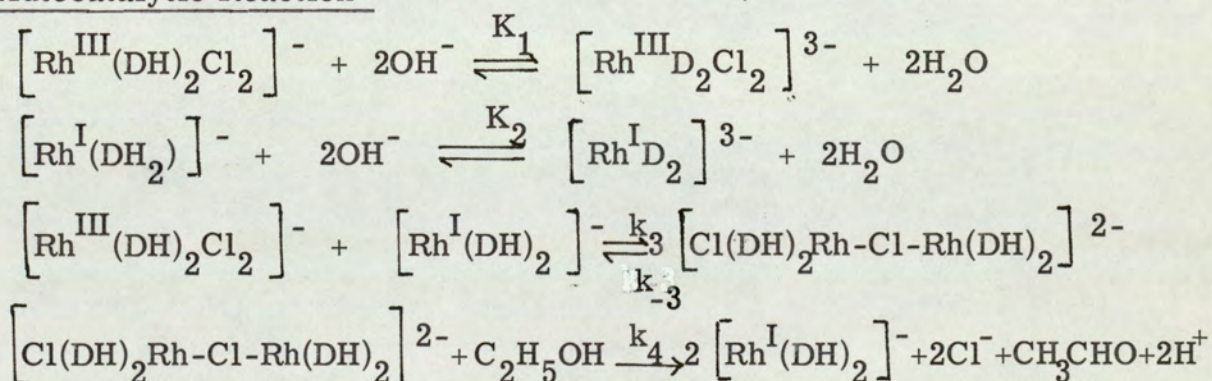
If hydroxide ion were acting as reducing agent, decomposition of the hydrogen peroxide end product would almost certainly cause an equilibrium to be set up between the rhodium (I) species and dissolved oxygen. This was not observed since all reactions went to completion.

Thus the reactions occurring in the initiation sequence and autocatalytic reduction of  $\text{H} \left[ \text{Rh}^{\text{III}}(\text{DMG})_2\text{Cl}_2 \right]^-$  are probably the same as those occurring in the induction period of  $\left[ \text{Rh}^{\text{III}}(\text{bipy})_2\text{Cl}_2 \right]^+$  reduction which also occurs under a nitrogen atmosphere.

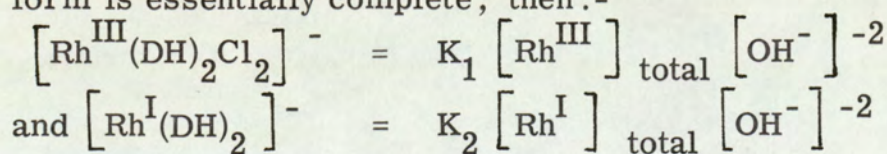
Inhibition by added dimethylglyoxime may result from coordination to the active rhodium(I) species, thereby blocking off the active site. On the basis of the experimental observations the following reaction mechanism is postulated where DH represents the dimethylglyoxime monoanion and D represents the dimethylglyoxime dianion.



Autocatalytic Reaction



If, in alkaline media, the deprotonation of ligands to the dianion form is essentially complete, then:-



On applying the steady state hypothesis to the intermediate dimer, this reaction scheme yields, as the rate equation,

$$\frac{d}{dt} [\text{Rh}^{\text{I}}]_{\text{total}} = \frac{K_1 K_2 k_3 k_4}{(k_{-3} + k_4)} [\text{Rh}^{\text{III}}]_{\text{total}} [\text{Rh}^{\text{I}}]_{\text{total}} [\text{OH}^-]^{-4}$$

The symbol  $k_4$  is used to represent the product of the rate constant  $k_4$  and whatever other reagents are involved in this step. These reagents will be at effectively constant concentrations.

The difference in the reducing agent in the autocatalytic reaction, that is, ethanol for trans- $[\text{Rh}^{\text{III}}(\text{DMG})_2\text{Cl}_2]^-$  and the more powerful reductant hydrogen gas for cis- $[\text{Rh}^{\text{III}}(\text{bipy})_2\text{Cl}_2]^+$ , probably arises from the less favourable  $E^0$  value for the latter complex.

This agrees with the previous report (147) that halogen interchange in trans- $[\text{Rh}^{\text{III}}(\text{py})_4\text{X}_2]^+$  ( $\text{X} = \text{Cl}$  or  $\text{Br}$ ) is catalysed by both primary and secondary alcohols whereas, in the case of trans- $[\text{Rh}^{\text{III}}(\text{en})_2\text{X}_2]^+$ , where the  $E^0$  value for reduction is less favourable, catalytic halogen interchanges are only induced by the presence of stronger reducing agents, for example,  $[\text{Rh}(\text{en})_2\text{H}(\text{OH})]^+$ . The mechanisms of these catalytic reactions are also thought to involve rhodium (I) species formed via a Rh(III) - H intermediate as the active catalyst.

Gillard, Heaton and Vaughan (147) report an unexpected result when halogen interchange in cis- $[\text{Rh}^{\text{III}}(\text{trien})\text{Cl}_2]^+$  was studied. From the  $E^0$  value (174) this complex is expected to undergo halogen exchange catalysed by ethanol. However, bromide interchange to form cis- $[\text{Rh}(\text{trien})\text{Br}_2]^+$  is not catalysed by ethanol. They attribute this fact to the  $E^0$  value being less positive than previously calculated or to the inability of the reduced species to catalyse cis-substitution at Rh<sup>III</sup> centres.

The results of Chapter V show that the latter suggestion is probably incorrect. However, the different mechanisms postulated for the

reduction of trans -  $[\text{Rh}(\text{DMG})_2\text{Cl}_2]^-$  and cis-  $[\text{Rh}(\text{bipy})_2\text{Cl}_2]^+$  on the basis of the experimental kinetic data, do suggest the importance of the stereochemistry of the oxidised form in the mechanism of autocatalytic reduction by the rhodium (I) species. A kinetic study on the reduction of cis-  $[\text{Rh}(\text{DMG})_2\text{Cl}_2]^-$  reported by Dwyer and Nyholm (171) would be of interest in this context.

## Chapter VII .

### Conclusion.

In the design of apparatus for the study of the reaction kinetics of transition metal complexes with gases in solution, the following considerations are important.

Firstly, it is essential to have good contact between the gaseous and solution phase. This is borne out in the study of oxygen uptake by cobaltous ion and diamino ethane, shaken under an atmosphere of the gas, and the hydrogen uptake by rhodium (I) bipyridyl species when the solutions were magnetically stirred. In both cases, diffusion control operated. In the former case, the problem could not be surmounted by increased shaking speeds. A stopped flow apparatus in which both cobaltous and diamino-ethane solutions are pre-saturated with oxygen, then mixed, is needed. The mixture is kept saturated with oxygen throughout the experiment and the reaction followed spectrophotometrically. In the latter case, the rate at which hydrogen dissolved in the reaction medium became non rate-determining if the less efficient vortex mixing was replaced by shaking the flask and contents. This method of agitation was satisfactory for the spectrophotometric runs under the initial concentrations of rhodium (III) and other reactants used. However, for the study of the rate of gas uptake, flask shaking is less satisfactory as the vibration causes considerable fluctuation of the butyl phthalate limbs of the apparatus. The accuracy in burette readings falls to  $\pm 0.5$  ml. More efficient mechanical stirring might be more satisfactory.

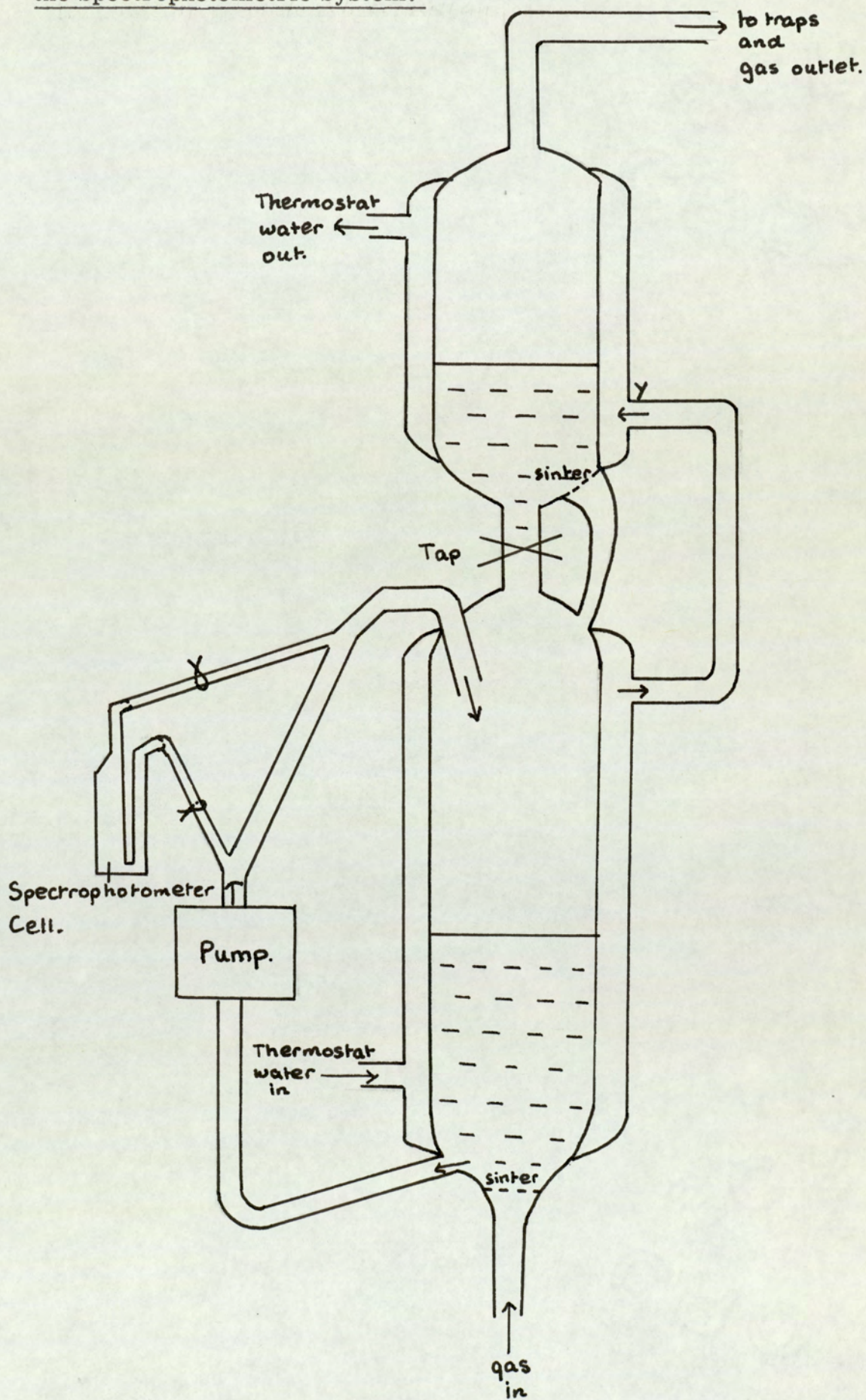
In the reduction of  $\text{H} \left[ \text{Rh}^{\text{III}}(\text{DMG})_2\text{Cl}_2 \right]$ , using the apparatus in Figure 8, a build up of the autocatalytic rhodium(I) species often occurred in the reaction vessel stem. This could be obviated by

circulating the reaction mixture by pump (see Figure 34). The mixture could be allowed to fall as a fine spray through an atmosphere of the gas maintained by a movable reservoir system (inlet Y at the top of the upper compartment) or gas could be passed through the solutions in the upper and lower compartments via sinters.

Secondly, in view of the extreme sensitivity of many reduced complexes to air for example  $[\text{Mn}(\text{salpn})\text{H}_2\text{O}]$ ,  $[\text{Rh}^{\text{I}}(\text{bipy})_2]\text{Cl}$  and  $\text{H}[\text{Rh}^{\text{I}}(\text{DMG})_2]$  it is essential to have an efficient means of degassing the reaction medium and apparatus and filling it with the required pressure of uncontaminated reactant gas. The simple method used was unsatisfactory as loss of solvent occurred on evacuation so that the initial reactant concentrations were not accurately known. In the gas uptake apparatus, (see Figure 4) distilled solvent condensing into the gas burette and limbs of the butyl phthalate manometer sometimes gave erroneous results. In the spectrophotometric system, during the rhodium / dimethylglyoxime complex runs, solvent passing from the lower to the upper compartment sometimes carried enough reactant to initiate reaction in the upper compartment before degassing was complete. In both cases, the variable lengths of the induction period suggested differing degrees of oxygen contamination due to inefficient degassing.

An improved method of degassing the apparatus would be to freeze the reaction medium by circulating coolant round the water jackets and to apply a high vacuum. If the reaction vessel is then sealed off from the vacuum, the solvent melted by circulating water at reaction temperature through the water jacket, occluded air would bubble out of the solvent with minimum solvent loss. Repetition of this cycle (175) flushing with the reactant gas in the freezing stage would ensure removal of air and an atmosphere of uncontaminated reactant gas.

Figure 34. Improved Reaction Vessel for  
the Spectrophotometric System.



In general, less volatile solvents are better as the reaction medium, particularly for the study of reactions at elevated temperatures since less solvent loss occurs in this process. The correction due to the partial pressure of the solvent vapour is less so that the actual partial pressure of the reactant gas is more accurately known.

A third requirement for the investigation of the reaction kinetics of transition metal complexes with gases in solution is an accurate method of initiating the reaction. In the gas uptake system, the magnetic cup method is satisfactory provided the reagent solid is readily soluble in the solvent, is not sensitive to the reactant gas and no solvent condenses on the solid before degassing is complete. A drop in mercury level and the left hand side limb of the butyl phthalate manometer occurs if the reactant gas is less soluble in the solvent and complex than in the solvent itself and owing to displacement by the magnetic cup itself. Addition of a small volume of fluid from the upper compartment to the lower compartment (see Figure 7) to generate the active species is less satisfactory as considerable drops in mercury manometer level result. For the spectrophotometric runs where volume changes are less important, initiation of the reaction by turning the tap to mix the two reaction components is satisfactory providing no pre-mixing has occurred in the degassing process. In the  $\left[ \text{Rh}^{\text{III}}(\text{bipy})_2\text{Cl}_2 \right]^+$  case, induction periods always preceded the reaction; the time of mixing the reaction components was arbitrary and did not need to be known accurately.

Fourthly, in both systems, an improved temperature control is needed. In the gas uptake apparatus, thermostating the gas burette, butyl phthalate manometer as well as the reaction vessels would improve accuracy, (176, 177) by eliminating the 'dead space'. In the spectrophotometric system the reaction vessel stem was not

thermostatted. This problem is eliminated in the apparatus in Figure 34. The Townson-Mercer water bath gave poor temperature control at 60°C ( $\pm 0.5^\circ\text{C}$ ) and above. Water should be replaced by oil for temperature control above this value.

Both systems need considerable modification to determine the dependence of reaction rate on the partial pressure of the reactant gas. In the gas uptake system, measurement of the actual gas pressure becomes increasingly difficult at pressures lower than atmospheric, particularly at elevated temperatures. An accurate correction for the solvent vapour pressure cannot be made in the case of many solvents for example 25% ethanol water at 60°C. This solvent mixture is not ideal and Raoult's Law cannot be used (a rough estimate gives a vapour pressure of 200mm mercury). As the pressure of gas admitted is decreased, the inaccuracy in the vapour pressure of the solvent produces greater inaccuracy in the corrected gas partial pressure. An improvement would be to use a known partial pressure of reactant gas in a gas / nitrogen mixture at atmospheric pressure. This would have the added advantage of no change in the total volume of gas absorbed as the partial pressure of reactant gas is altered.

In the spectrophotometric system, the greatest inaccuracy results from transfer of the reaction mixture from vessel to spectrophotometer cell. Contact of the reaction mixture with air can re-oxidise the rhodium (I) species to rhodium (III). Aerial oxidation is minimised by surrounding the reaction vessel with a polythene 'skirt'. A nitrogen stream enters at the top and emanates at bench level. The delay between sample removal and optical density measurement introduces another systematic error. This delay could be eliminated by circulating the reaction mixture through a special spectrophotometer cell fitted with glass inlet and outlet tubes. These glass tubes would be connected via flexible tubing passing through light-tight holes in

the cell compartment lid so that movement of the sample into the light beam of the S.P. 500 would still be possible. Alternatively, a double beam spectrophotometer, for example the Perkin Elmer model 137 ultra violet spectrophotometer and a stationary reaction vessel could be used. With this system, (see Figure 34) the dependence of the reaction rate on gas partial pressure could be investigated since sample is not removed from the reaction vessel. Both systems could be made more accurate and kinetic studies less time consuming by using an automatic method of gas absorption (176, 177, 178) or optical density measurement.

An important recurring feature of this work is the extreme reactivity of many of the starting materials and end products. For example  $[\text{Mn}(\text{salpn})]$ ,  $[\text{Mn}(\text{salpn})\text{H}_2\text{O}]$ ,  $[\text{Rh}^{\text{I}}(\text{bipy})_2]\text{Cl}$  and  $\text{H}[\text{Rh}^{\text{I}}(\text{DMG})_2]$  showed great sensitivity to oxygen even in the solid state. Oxygen uptake by  $[\text{Co}(\text{en})_2(\text{H}_2\text{O})_2]^{2+}$  is complete in the order of milliseconds. The apparatus in Figure 10, though rather cumbersome, was always successful in the isolation of pure air sensitive products. De-oxygenation of the gases by passage over red hot copper turnings at  $500^\circ$  to  $600^\circ\text{C}$  or over activated B.T.S. catalyst was also satisfactory. To study the reactions of several complexes, it was necessary to generate them in situ. For example, the complex  $[(\text{en})_2\text{Co}\mu\text{O}_2\mu\text{enCo}(\text{en})_2]^{4+}$  which equilibrates with the  $\mu$ -hydroxy species within forty minutes of its generation. The solid  $[\text{Mn}(\text{salpn})]$  was transferred to the oxygen uptake apparatus immediately after drying and pyridine removal was complete.

A second noticeable factor in the four kinetic studies undertaken is the preponderance of dimeric and polymeric species. For example the  $[(\text{en})_2\text{Co}\mu\text{O}_2\mu\text{enCo}(\text{en})_2]^{5+}$ ,  $[(\text{en})_2\text{Co}\mu\text{O}_2\mu\text{enCo}(\text{en})_2]^{4+}$ ,  $[(\text{en})_2\text{Co}\mu\text{O}_2\mu\text{OHCo}(\text{en})_2]^{3+}$  species, the dimeric  $[\text{Mn}(\text{salpn})\text{O}(\text{Py})]_2$  and polymeric  $[\text{Mn}(\text{salpn})\text{O}_2]_n$  or  $[\text{Mn}(\text{salpn})\text{O}]_n$  species,

the postulated dimeric  $\text{Rh}^{\text{I}} \dots \text{Cl} \dots \text{Rh}^{\text{III}}$  and trimeric intermediates in the reduction of  $[\text{Rh}^{\text{III}}(\text{bipy})_2\text{Cl}_2]^+$  by hydrogen and the dimeric  $\text{Rh}^{\text{I}} \dots \text{Cl} \dots \text{Rh}^{\text{III}}$  species in the reduction of  $\text{H} [\text{Rh}^{\text{III}}(\text{DMG})_2\text{Cl}_2]$  by ethanol. This is a consequence of the use of two electron oxidants such as oxygen gas or two electron reductants such as hydrogen gas or ethanol. Polymeric intermediates and products would be less predominant if one electron oxidant or reductant gases for example nitric oxide (124) had been used.

A suggestion for further work is a study of the kinetics of carbon dioxide uptake by  $[(\text{en})_2\text{Co}\mu\text{O}_2\mu\text{enCo}(\text{en})_2]^{4+}$  and  $[(\text{en})_2\text{Co}\mu\text{O}_2\mu\text{OHCo}(\text{en})_2]^{3+}$ . These complexes react causing the conversion of carbon dioxide to carbonate ion by molecular oxygen. The mechanism of carbon dioxide uptake is clearly different from that observed previously in sulphur dioxide and selenium dioxide uptake reactions. The above two complexes are however inactive in catalysing the reaction  $\text{N}_2\text{O} + \text{O}_2 \rightleftharpoons 2\text{NO}$ .

In view of the intractable nature of the  $[\text{Mn}(\text{salpn})]$  complexes and their oxygen adducts, preparation of manganese (II) complexes with other Schiff base ligands could prove more rewarding. The tendency to hydrolytic cleavage of the Schiff base imine group could be reduced by using less basic Schiff base ligands. That is the use of benzoylacetone instead of acetylacetone and 1, 2 diamino propane  $\text{pK}_a$  7.11 or diaminoethane  $\text{pK}_a$  7.22 in preference to the more basic 1, 3 - diamino propane  $\text{pK}_a$  8.88 (179). In general, ketone Schiff base complexes are more stable than aldehyde Schiff base complexes and 6, 5, 6 ring systems more stable than 6, 6, 6 systems (180). Therefore, a better choice of ligand would be the Schiff base of benzoylacetone or 2 hydroxy-acetophenone with 1, 2 diamino-propane or diamino-ethane. Electron withdrawing substituents at the 4 and to a lesser extent 6 positions on the benzene rings should render the Schiff base even less susceptible to hydrolysis(124).

Since the two rhodium(I) species  $[\text{Rh}^{\text{I}}(\text{bipy})_2] \text{Cl}$  and  $\text{H} [\text{Rh}^{\text{I}}(\text{DMG})_2]$  are easily generated by hydrogen and / or ethanol in alkaline medium as the reducing agent without the addition of borohydride, both should be screened as catalysts for the hydrogenation of alkynes and alkenes (70, 151, 157, 158), their carbonylation and subsequent reduction by hydrogen (151) (hydroformylation) the hydrogenation of aromatic nitro compounds (26, 163) aliphatic (158, 181) and aromatic nitriles (154) the reduction of benzoyl and acetyl chlorides (151), the polymerisation of acrylonitrile (160) and the isomerisation of olefins (16). A more quantitative study of the hydrogenation of maleic acid, quinones, benzonitrile and 1-decene thought to be catalysed by  $[\text{Rh}^{\text{I}}(\text{bipy})_2] \text{Cl}$  would also be of interest.

In the rhodoxime field there is great scope for further investigation. It would be interesting to compare the rates of reduction of complexes with substituted glyoxime or salicylaloxime equatorial ligands and different axial ligands. The kinetics of oxygen uptake by rhodoxime (II) complexes has not been investigated. Investigation of the kinetics of methylation of rhodoxime (I) complexes for example  $\text{H} [\text{Rh}^{\text{I}}(\text{DMG})_2]$  with varying axial, equatorial and alkyl groups would be of biochemical interest. Methane evolution from methyl rhodoxime (III) complexes by photolysis (62) or in the presence of A.T.P. vitamin  $\text{B}_{12\text{r}}$  and hydrogen (170) could be studied by the apparatus of Figure 4.

Appendix 1.

Conductivity Data.

$\sqrt{c}$  is the square root of the concentration (mole<sup>1/2</sup> ml<sup>-1/2</sup>)

$\Lambda$  is the molar conductivity (cm<sup>2</sup> ohm<sup>-1</sup> mole<sup>-1</sup>)

Temperature 21°C

Electrolytes used as Standards.

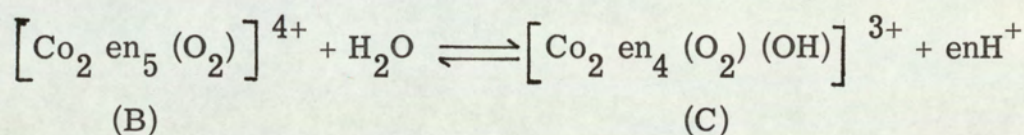
Electrolyte Type	1 : 3	1 : 4
Complex	$[\text{Co}(\text{NH}_3)_6] \text{Cl}_3$	$[\text{Co}_2(\text{NH}_3)_8(\text{OH})_2] 4\text{ClO}_4$
	$\sqrt{c} \times 10^3 \Lambda$	$\sqrt{c} \times 10^3 \Lambda$
	2.27      376	2.37      385
	1.01      446	1.06      409
	0.452     508	0.474     447

Electrolytes of Unknown Type.

Probable Electrolyte Type	1 : 3	1 : 4	1 : 5
Complex	$[\text{Co}_2(\text{en})_4\text{O}_2\text{OH}] 3\text{ClO}_4$	$[\text{Co}_2(\text{en})_5\text{O}_2] 4\text{ClO}_4$	$[\text{Co}_2(\text{en})_5\text{O}_2] 5\text{NO}_3$
	$\sqrt{c} \times 10^3 \Lambda$	$\sqrt{c} \times 10^3 \Lambda$	$\sqrt{c} \times 10^3 \Lambda$
	2.44      275	2.54      360	2.22      481
	1.09      318	1.14      432	0.992     574
	0.772     329	0.803     452	0.701     586

Appendix 2.

Rate Data for the Kinetics of the Conversion of (B) to (C).



pH<sub>0</sub> is the pH of the mixture containing (B) at zero time which is maintained throughout the reaction.

B<sub>0</sub> is the concentration of (B) at zero time.

B<sub>t</sub> is the concentration of (B) at time t.

K is the equilibrium constant for the reaction.

Run 1      Temperature = 25.8°C

pH<sub>0</sub> = 8.2

ml HClO <sub>4</sub>	en H <sup>+</sup> (M × 10 <sup>3</sup> )	B <sub>t</sub> (M × 10 <sup>2</sup> )	log <sub>10</sub> $\left\{ \frac{1}{\left(1+K\right)\frac{B_t}{B_0} - 1} \right\}$	time	
				mins.	secs.
0	0	2.38	0.370	0	00
1.07	1.74	2.21	0.492	3	10
1.78	2.89	2.10	0.597	7	10
2.43	3.95	1.99	0.719	10	35
2.90	4.71	1.91	0.839	15	00
3.30	5.36	1.85	0.975	19	20
3.67	5.96	1.79	1.15	23	50
3.95	6.42	1.74	1.38	31	30
4.39					∞

## Appendix 2 (contd.).

Run 2. Temperature =  $22.2 \pm 0.8^\circ\text{C}$ 

pHo = 8.2

ml HClO <sub>4</sub>	enH <sup>+</sup> (M × 10 <sup>3</sup> )	B <sub>t</sub> (M × 10 <sup>2</sup> )	$\log_{10} \left\{ \frac{1}{(1+K)\frac{B_t}{B_0} - 1} \right\}$	time	
				mins.	secs.
0	0	2.38	0.357	0	00
0.88	1.43	2.24	0.452	3	45
1.65	2.68	2.12	0.559	6	00
2.72	4.42	1.94	0.765	11	20
3.09	5.02	1.88	0.867	13	50
3.59	5.83	1.80	1.06	19	10
3.91	6.35	1.75	1.26	24	30
4.15	6.74	1.71	1.49	35	20
4.48				∞	

Run 3. Temperature =  $23.7^\circ\text{C}$ 

pHo = 8.27

ml HClO <sub>4</sub>	enH <sup>+</sup> (M × 10 <sup>3</sup> )	B <sub>t</sub> (M × 10 <sup>2</sup> )	$\log_{10} \left\{ \frac{1}{(1+K)\frac{B_t}{B_0} - 1} \right\}$	time	
				mins.	secs.
0	0	2.39	0.443	0	00
0.60	0.975	2.29	0.516	4	30
1.36	2.21	2.16	0.631	7	30
1.80	2.92	2.09	0.714	11	10
2.24	3.64	2.02	0.815	14	00
2.52	4.10	1.98	0.896	18	00
2.89	4.70	1.92	1.04	21	55
3.26	5.30	1.86	1.23	28	10
3.52	5.72	1.81	1.47	41	10
3.89				∞	

Appendix 3.

Temperature Dependence of the Rate of Reduction of  
cis - Dichlorobis - (bipyridyl) Rhodium (III) Nitrate Dihydrate  
in 25% Ethanol / Water.

1 Atmosphere of Hydrogen Pressure

$$\begin{aligned} [\text{OH}^-] &= 0.194 \text{ (M)} \\ [\text{Rh}^{\text{III}}]_0 &= 5.63 \times 10^{-4} \text{ (M)} \end{aligned}$$

T in °A

 $k_{\text{obs}}$  in litre<sup>2</sup> mole<sup>-2</sup>  
minutes<sup>-1</sup>

<u>1/T (× 10<sup>3</sup>)</u>	<u>log<sub>10</sub> k<sub>obs</sub></u>
2.91	6.7485
2.96	6.5206
3.00	6.4116
3.04	6.1202
3.10	5.9988
3.20	5.5335

These runs were done in duplicate and the average value of  $k_{\text{obs}}$  was calculated. Experimental error < 9%.

Appendix 4.

Hydroxide Dependence of the Rate of Reduction of  
cis - Dichlorobis - (bipyridyl) Rhodium (III) Nitrate Dihydrate  
in 25% Ethanol / Water.

1 Atmosphere of Hydrogen Pressure

Temperature = 60°C

$$[\text{Rh}^{\text{III}}]_0 = 5.63 \times 10^{-4} \text{ (M)}$$

$$k_{\text{obs}} \text{ litre}^2 \text{ mole}^{-2} \text{ minutes}^{-1}$$

$[\text{OH}^-] \text{ (M)}$	$\frac{[\text{OH}^-]}{k_{\text{obs}}} (\times 10^7)$
0.992	2.14
0.741	1.58
0.555	1.19
0.314	0.701
0.195	0.389
0.0213	0.583

These runs were done in duplicate and the average value of  $k_{\text{obs}}$  was calculated. Experimental error < 9%.

Appendix 5.

Ionic Strength Dependence of the Rate of Reduction of  
cis - Dichlorobis - (bipyridyl) Rhodium (III) Nitrate Dihydrate  
in 25% Ethanol / Water.

1 Atmosphere of Hydrogen Pressure

Temperature = 60°C

$$[\text{OH}^-] = 0.316 \text{ (M)}$$

$$[\text{Rh}^{\text{III}}]_0 = 5.63 \times 10^{-4} \text{ (M)}$$

$\sqrt{I}$  is the square root  
of the ionic strength  
 $k_{\text{obs}}$  in litre<sup>2</sup> mole<sup>-2</sup> minutes<sup>-1</sup>

$\sqrt{I}$	$\log_{10} k_{\text{obs}}$
0.584	6.5139
0.601	6.4422
0.637	6.3367
0.670	6.2739
0.701	6.2193
0.723	6.1942
0.746	5.9820

Appendix 6.Ethanol Dependence of the Rate of Reduction of  
cis - Dichlorobis - (bipyridyl) Rhodium (III) Nitrate Dihydrate

1 Atmosphere of Hydrogen Pressure

 $k_{\text{obs}}$  in litre<sup>2</sup> mole<sup>-2</sup> minutes<sup>-1</sup>

Temperature = 60°C

$$[\text{OH}^-] = 0.187 \text{ (M)}$$

$$[\text{Rh}^{\text{III}}]_0 = 5.63 \times 10^{-4} \text{ (M)}$$

<u>log<sub>10</sub> [EtOH]</u>	<u>log<sub>10</sub> k<sub>obs</sub></u>
0.1553	6.4007
0.4089	6.2292
0.5343	6.1810
0.6317	6.1149
0.8833	5.9705
1.0483	5.8968

Appendix 7.

Temperature Dependence of the Rate of Reduction of Monohydrogen  
trans - Dichlorobis (dimethylglyoximato) Rhodium (III)  
in 25% Ethanol / Water.

1 Atmosphere of Hydrogen Pressure

$$[\text{OH}^-] = 0.623 \text{ (M)}$$

$$[\text{Rh}^{\text{III}}]_0 = 2.98 \times 10^{-3} \text{ (M)}$$

$$\mu = 1.5 \text{ (NaNO}_3\text{)}$$

T in  $^{\circ}\text{A}$

$k_{\text{obs}}$  in litre mole<sup>-1</sup> minutes<sup>-1</sup>

<u><math>1/T (\times 10^3)</math></u>	<u><math>\log_{10} k_{\text{obs}}</math></u>
3.25	1.4011
3.15	1.6133
3.10	1.6677
2.96	1.9848
2.92	2.0447

Appendix 8.

Hydroxide Dependence of the Rate of Reduction of Monohydrogen  
trans - Dichlorobis (dimethylglyoximato) Rhodium (III)  
in 25% Ethanol / Water.

1 Atmosphere of Hydrogen Pressure  $k_{\text{obs}}$  in litre mole<sup>-1</sup> minutes<sup>-1</sup>  
 Temperature = 50°C  
 $[\text{Rh}^{\text{III}}]_0 = 2.98 \times 10^{-3}$  (M)  
 $\mu = 1.5$  (NaNO<sub>3</sub>)

<u><math>-\log_{10} [\text{OH}^-]</math></u>	<u><math>\log_{10} k_{\text{obs}}</math></u>
0.0453	1.1854
0.1042	1.2262
0.1250	1.3416
0.1469	1.4006
0.1754	1.5020
0.2059	1.6456
0.2792	1.8835
0.4056	2.0475

These runs were done in duplicate and the average value of  $k_{\text{obs}}$  was calculated. Experimental error  $< 10\%$

## APPENDIX 9.

```

DOC RHSIMPLIFY
'BEGIN' 'COMMENT' CHSTF083 ZRHSIMPLIFY FDO ;
'INTEGER' I,N,R ; 'REAL' C,D,E ;
'REAL' 'ARRAY' A[1:50], T,X,G[1:25], F[1:4] ;
'SWITCH' S:=ONE,TWO,THREE,FOUR ; SELECT OUTPUT(0) ;
N:=READ ; 'FOR' I:=1 'STEP' 1 'UNTIL' N 'DO' A[I]:=READ ;
ONE: R:=READ ; 'IF' R=-1 'THEN' 'GOTO' FOUR ;
C:=A[R-59] ;
WRITETEXT('('('2C')'RUN')') ; PRINT(R,2,0) ; NEWLINE(2) ;
N:=0 ;
TWO: D:=READ ; 'IF' D=-1 'THEN' 'GOTO' THREE ; E:=READ ;
T[N+1]:=D+E/60 ; D:=READ ; X[N+1]:=D-(0.0078)*(C-D) ; N:=N+1 ;
'GOTO' TWO ;
THREE: 'FOR' I:=1 'STEP' 1 'UNTIL' 4 'DO' F[I]:=0 ;
'FOR' I:=1 'STEP' 1 'UNTIL' N 'DO' 'BEGIN' D:=C-X[I] ;
G[I]:=1/(C*D) - LN(D/X[I])/(C*C) ; F[1]:=F[1] + T[I]*G[I] ;
F[2]:=F[2] + T[I] ; F[3]:=F[3] + G[I]*G[I] ; F[4]:=F[4] + G[I] ;
'END' ;
D:=(F[1]*N - F[2]*F[4])/(F[3]*N - F[4]*F[4]) ; E:=(F[2]-D*F[4])/N ;
WRITETEXT('('K('2S')'ZERO('1S')'TIME('2S')'ARE('2C')'')') ;
PRINT(1/D,0,4) ; PRINT(E,0,4) ;
WRITETEXT('('('2C')'X('2S')'TIME('2S')'CALC('1S')'TIME'
('2C')'')') ; 'FOR' I:=1 'STEP' 1 'UNTIL' N 'DO'
'BEGIN' PRINT(X[I],0,4) ; PRINT(T[I],0,4) ;
PRINT((D*G[I]+E),0,4) ;
NEWLINE(1) ; 'END' ; 'GOTO' ONE ;
FOUR: 'END' ; 'END' ;
****

```

## DOC RHKINETICS

```

'BEGIN' 'COMMENT' CHSTF083 ZRHKINETICS FDO ;
'INTEGER' I,J,K,N,Q,R ; 'REAL' M, P,U,V,W,Y,Z ;
'REAL' 'ARRAY' A,E,G[1:3], B,D,H,L,T,X[1:25], C,O[1:75], F[1:9] ;
'SWITCH' S:=ONE,TWO,THREE,FOUR,FIVE,SIX,SEVEN,EIGHT,NINE,TEN ;
SELECT OUTPUT(0) ;
N:=READ; 'FOR' I:=1 'STEP' 1 'UNTIL' N 'DO' O[I]:= READ;
ONE: R:=READ; 'IF' R=-1 'THEN' 'GOTO' TEN;
A[2]:=O[R-26]; U:=A[2]; WRITETEXT('('('2C')'RUN')');
PRINT(R,2,0) ; NEWLINE(2) ; N:=0 ; Q:=0 ;
TWO: M:=READ ; 'IF' M=-1 'THEN' 'GOTO' THREE ; P:=READ ;
T[N+1]:=M+P/60; P:=READ; X[N+1]:=P-(0.0078)*(A[2]-P);
N:=N+1 ; 'GOTO' TWO;
THREE: 'IF' X[N]'GE'U 'THEN' 'GOTO' EIGHT ;
'IF' ABS((U-A[2])/U) 'GE' 0.3 'THEN' 'GOTO' EIGHT ;
Q:=Q+1 ; 'FOR' I:=1 'STEP' 1 'UNTIL' 3 'DO' 'BEGIN' E[I]:=0 ;
'FOR' J:=0 'STEP' 1 'UNTIL' 2 'DO' F[3*J+I]:=0 ; 'END' ;
'FOR' I:=1 'STEP' 1 'UNTIL' N 'DO' 'BEGIN' H[I]:=A[2]-X[I] ;
B[I]:=1/(A[2]*H[I]) ; L[I]:= LN(H[I]/X[I])/(A[2]*A[2]) ;
C[I]:=B[I]-L[I] ; 'END' ; 'IF' Q=1 'THEN' 'GOTO' FOUR ;
'IF' O 'GE' A[1] 'THEN' 'GOTO' SEVEN ;
'IF' Q=10 'THEN' 'GOTO' SIX;
FOUR: Z:=0 ; Y:=0 ; W:=0 ; V:=0 ;
'FOR' I:= 1 'STEP' 1 'UNTIL' N 'DO' 'BEGIN'
Z:=Z +T[I]*C[I]; Y:=Y+T[I]; V:=V+ C[I];
W:=W+C[I]*C[I]; 'END';
A[3]:=(Z*V-Y*W)/(V*V-N*W); A[1]:=(Z-A[3]*V)/W;
FIVE: 'FOR' I:=1 'STEP' 1 'UNTIL' N 'DO' 'BEGIN' C[2*N+I]:=1 ;
C[N+I]:=-A[1]*(2*C[I]/A[2]+B[I]/H[I]) ;
D[I]:=T[I]-A[1]*C[I]-A[3] ;
'FOR' J:=0 'STEP' 1 'UNTIL' 2 'DO' 'BEGIN'
E[J+1]:=E[J+1]+D[I]*C[J*N+I];
'FOR' K:=0 'STEP' 1 'UNTIL' 2 'DO'
F[3*J+K+1]:=F[3*J+K+1] + C[J*N+I]*C[K*N+I] ; 'END' ; 'END' ;
Z:=E[1]*F[6]-E[2]*F[3];
Y:=F[2]*F[9]-F[3]*F[8];W:=F[2]*F[6]-F[3]*F[5] ;
'IF' W=0 'THEN' 'GOTO' NINE ; V:=F[1]*F[6]-F[3]*F[4] ;
M:= V*Y-W*(F[1]*F[9]-F[3]*F[7]) ; 'IF' M=0 'THEN' 'GOTO' NINE ;
G[1]:=(Z*Y-W*(E[1]*F[9]-E[3]*F[3]))/M ; G[2]:=(Z-V*G[1])/W ;
G[3]:=(E[1]-F[1]*G[1]-F[2]*G[2])/F[3];
'FOR' I:=1 'STEP' 1 'UNTIL' 3 'DO'
A[I]:=A[I]+G[I] ; 'GOTO' THREE ; SIX: WRITETEXT('('K'('2S')'
X'('1S')'INFINITY'('2S')'ZERO'('1S')'TIME'('2S')'ARE'('2C')')') ;
PRINT(1/A[1],0,4) ;
PRINT(A[2],0,4) ; PRINT(A[3],0,4) ;
WRITETEXT('('('2C')'DATA'('2S')'AS'('2S')'X'('2S')'TIME '('2S')
'CALC'('1S')'TIME'('2C')')') ; 'FOR' I:=1 'STEP' 1 'UNTIL'
N 'DO' 'BEGIN' PRINT(X[I],0,4) ; PRINT(T[I],0,4) ;
PRINT((A[1]*C[I]+A[3]),0,4) ;
NEWLINE(1) ; 'END' ; 'GOTO' ONE ;
SEVEN: WRITETEXT('('NEGATIVE'('2S')'RATE'('2S')'CONSTANT')') ;
'GOTO' ONE;
EIGHT: WRITETEXT('('X'('1S')'INFINITY'('2S')'POOR'('2S')')') ;
PRINT(A[2],0,4) ; 'GOTO' ONE ;
NINE: WRITETEXT('('CUTOUT')') ; 'GOTO' ONE ;
TEN: 'END' ; 'END' ;
****

```

Bibliography.

- (1) Halpern, J., Chem. Eng. News., 1966, 44, 68.
- (2) Ochiai, E-I., Coordin. Chem. Rev., 1968, 3, 49.
- (3) Kwiatek, J., Catalysis Rev., 1967, 1, 37.
- (4) Rose, D., Gilbert, J. D., Richardson, R. P., Wilkinson, G.,  
J. Chem. Soc. (A), 1969, 2610.
- (5) Kwiatek, J., Mador, I. L., Seyler, J. K., Adv. Chem. Ser.,  
1963, 37, 201.
- (6) Osborn, J. A., Jardine, F. H., Young, J. F., Wilkinson, G.,  
J. Chem. Soc. (A), 1966, 1711.
- (7) Giustiniani, M., Dolcetti, G., Nicolini, M., Belluco, U.,  
J. Chem. Soc. (A), 1969, 1961.
- (8) Bailar, J. C., Itatani, H., J. Amer. Chem. Soc., 1967, 89, 1592.
- (9) Yagupsky, G., Brown, C. K., Wilkinson, G.,  
J. Chem. Soc. (A), 1970, 1392.
- (10) Takegami, Y., Watanabe, Y., Masada, H.,  
Bull. Chem. Soc. Japan., 1967, 40, 1459.
- (11) Schrauzer, G. N., Adv. Organomet. Chem., 1964, 2, 1.
- (12) Cramer, R., J. Amer. Chem. Soc., 1965, 87, 4717.
- (13) Yamamoto, A., Morifuji, K., Ikeda, S., Saito, T., Uchida, Y.,  
Misono, A., J. Amer. Chem. Soc., 1968, 90, 1878.
- (14) Yamamoto, A., Morifuji, K., Ikeda, S., Saito, T., Uchida, Y.,  
Misono, A., J. Amer. Chem. Soc., 1965, 87, 4652.
- (15) Rinehart, R. E., Smith, H. P., Witt, H. S., Romeyn, H. Jr.,  
J. Amer. Chem. Soc., 1961, 83, 4864.
- (16) Yagupsky, M., Wilkinson, G., J. Chem. Soc. (A), 1970, 941.
- (17) Cramer, R., J. Amer. Chem. Soc., 1966, 88, 2272.
- (18) Harrod, J. F., Chalk, A. J., J. Amer. Chem. Soc., 1966, 88, 3491.
- (19) Roos, L., Orchin, M., J. Amer. Chem. Soc., 1965, 87, 5502.
- (20) Tayim, A. H., Bailar, J. C., Jr., J. Amer. Chem. Soc., 1967, 89, 3420.
- (21) Henry, P. M., Adv. Chem. Ser., 1968, 70, 126.
- (22) Schultz, R. G., Gross, D. E., Adv. Chem. Ser., 1968, 70, 97.
- (23) Halpern, J., James, B. R., Kemp, A. L. W.,  
J. Amer. Chem. Soc., 1961, 83, 4097.

- (24) James, B. R., Rempel, G. L., *J. Amer. Chem. Soc.*, 1969, 91, 863.
- (25) Otsuka, S., Nakamura, A., Tatsuno, Y.,  
*J. Amer. Chem. Soc.*, 1969, 91, 6994.
- (26) Brearley, A. E., Gott, H., Hill, H. A. O., O'Riordan, M., Pratt, J. M.,  
Williams, R. J. P., *J. Chem. Soc. (A)*, 1971, 612.
- (27) McWhinnie, W. R., Miller, J. D., Watts, J. B., Waddan, D. Y.,  
*Chem. Comm.*, 1971, 629.
- (28) Calderazzo, F., Noack, K., *Coordin. Chem. Rev.*, 1966, 1, 118.
- (29) Butler, I. S., Basolo, F., Pearson, R. G., *Inorg. Chem.*, 1967, 6, 2074.
- (30) Vogt, L. H., Jr., Faigenbaum, H. M., Wiberley, S. E.,  
*Chem. Rev.*, 1963, 63, 269.
- (31) Basolo, F., Pearson, R. G., "Mechanisms of Inorganic Reactions,"  
John Wiley, New York, 1967, 2nd. edn., p. 641.
- (32) Sykes, A. G., Weil, J. A., *Prog. inorg. Chem.*, 1970, 13, 1.
- (33) Martell, A. E., Calvin, M., "Chemistry of the Metal Chelate  
Compounds," Prentice-Hall Inc., New York, 1952.
- (34) Vaska, L., *Science*, 1963, 140, 809.
- (35) Ezerskaya, N. A., Solovykh, T. P., *Zhur. neorg. Khim.*, 1966, 11, 781.
- (36) Fallab, S., *Angew. Chem. Internat. Edn.*, 1967, 6, 496.
- (37) McGinety, J. A., Payne, N. C., Ibers, J. A.,  
*J. Amer. Chem. Soc.*, 1969, 23, 6301.
- (38) Chatt, J., *Proc. Roy. Soc., B*, 1969, 172, 327.
- (39) Murray, R., Smith, D. C., *Coordin. Chem. Rev.*, 1968, 3, 429.
- (40) Vol'pin, M. E., Chapovskaya, N. K., Shur, V. B.,  
*Izv. Akad. Nauk. S. S. S. R.*, 1966, 1033.
- (41) Maskill, R., Pratt, J. M., *J. Chem. Soc. (A)*, 1968, 1914.
- (42) Tamelen, E. E. van., Seeley, D., Schneller, S., Rudler, H., Cretney, W.,  
*J. Amer. Chem. Soc.*, 1970, 92, 5251.
- (43) Henrici-Olivé, G., Olivé, S., *Angew. Chem. Internat. Edn.*, 1969, 8, 650.
- (44) Allen, A. D., Senoff, C. V., *Chem. Comm.*, 1965, 621.
- (45) Sacco, A., Rossi, M., *Inorg. Chim. Acta.*, 1968, 2, 127.
- (46) Chatt, J., Melville, D. P., Richards, R. L.,  
*J. Chem. Soc. (A)*, 1969, 2841.

- (47) Bancroft, G. M., Mays, M. J., Prater, B. E., Stefanini, F. P.,  
J. Chem. Soc. (A), 1970, 2146.
- (48) Hidai, M., Tominari, K., Uchida, Y., Misono, A., Chem.  
Comm., 1969, 1392.
- (49) Chatt, J., Dilworth, J. R., Richards, R. L., Sanders, J. R.,  
Nature, 1969, 224, 1201.
- (50) Atkinson, L. K., Mawby, A. H., Smith, D. C., Chem. Comm., 1971, 157.
- (51) Schrauzer, G. N., Accounts Chem. Res., 1968, 1, 97.
- (52) Weber, J. H., Schrauzer, G. N., J. Amer. Chem. Soc., 1970, 92, 726.
- (53) Hill, H. A. O., Pratt, J. M., Williams, R. J. P.,  
Chem. Brit., 1969, 5, 156.
- (54) Das, P. K., Hill, H. A. O., Pratt, J. M., Williams, R. J. P.,  
J. Chem. Soc. (A), 1968, 1261.
- (55) Caulton, K. G., Cotton, F. A., J. Amer. Chem. Soc., 1969, 91, 6517.
- (56) Schrauzer, G. N., Lee, L. P., J. Amer. Chem. Soc., 1970, 92, 1551.
- (57) Bayston, J. H., King, N. K., Looney, F. D., Winfield, M. E.,  
J. Amer. Chem. Soc., 1969, 91, 2775.
- (58) Schneider, P. W., Phelan, P. F., Halpern, J.,  
J. Amer. Chem. Soc., 1969, 91, 77.
- (59) Schrauzer, G. N., Deutsch, E., J. Amer. Chem. Soc., 1969, 91, 3341.
- (60) Schrauzer, G. N., Windgassen, R. J.,  
J. Amer. Chem. Soc., 1967, 89, 1999.
- (61) Schrauzer, G. N., Lee, L. P., Sibert, J. W.,  
J. Amer. Chem. Soc., 1970, 92, 2997.
- (62) Pratt, J. M., Whitear, B. R. D., J. Chem. Soc. (A), 1971, 252.
- (63) Firth, R. A., Hill, H. A. O., Pratt, J. M., Thorp, R. G., Williams, R. J. P.,  
Chem. Comm. 1967, 400.
- (64) Hill, H. A. O., Mann, B. E., Pratt, J. M., Williams, R. J. P.,  
J. Chem. Soc. (A), 1968, 564.
- (65) Costa, G., Mestroni, G., Puxeddu, A., Reisenhofer, E.,  
J. Chem. Soc. (A), 1970, 2871.
- (66) Bigotto, A., Costa, G., Mestroni, G., Pellizer, G., Puxeddu, A.,  
Reisenhofer, E., Stefani, L., Tauzher, G.,  
Inorg. Chim. Acta Rev., 1970, 4, 41.

- (67) Sibert, J.W., Schrauzer, G.N., *J. Amer. Chem. Soc.*, 1970, 92, 1421.
- (68) Panov, V.B., Khidekel, M.L., Shchepinov, S.A.,  
*Izv. Akad. Nauk S.S.S.R.*, 1968, 2397.
- (69) Rogachev, B.G., Khidekel, M.L.,  
*Izv. Akad. Nauk S.S.S.R.*, 1969, 141.
- (70) Hui, B.C., Rempel, G.L., *Chem. Comm.*, 1970, 1195.
- (71) Harle, O.L., Calvin, M., *J. Amer. Chem. Soc.*, 1946, 68, 2612.
- (72) Lewis, J., Wilkins, R.G., "Modern Coordination Chemistry,"  
Interscience, New York, 1960.
- (73) Robinson, R.A., Stokes, R.H., "Electrolyte Solutions,"  
Butterworths, London., 1959, 2nd. edn..
- (74) Vogel, A.I., "A Text - book of Practical Organic Chemistry,"  
Longmans, 1956, 3rd. edn., p. 176.
- (75) Mori, M., Weil, J.A., Ishiguro, M., *J. Amer. Chem. Soc.*, 1968, 90, 615.
- (76) Thompson, R.L., Wilmarth, W.K., *J. Phys. Chem.*, 1952, 56, 5.
- (77) Mann, F.G., Saunders, B.C., "Practical Organic Chemistry,"  
Longmans, 1960, 4th. edn., p. 228.
- (78) Johnson, G.L., Beveridge, W.D., *Inorg. Nucl. Chem. Letters*,  
1967, 3, 323.
- (79) Yarino, T., Matsushita, T., Masuda, I., Shinra, K.,  
*Chem. Comm.*, 1970, 1317.
- (80) Belcher, R., Nutten, A.J., "Quantitative Inorganic Analysis,"  
Butterworths, London, 1960, 2nd. edn., p. 329.
- (81) Vogel, A.I., "A Text - book of Quantitative Inorganic Analysis,"  
Longmans, 1961, 3rd. edn., p. 536.
- (82) Calderazzo, F., Floriani, C., Henzi, R., L'Eplattenier, F.,  
*J. Chem. Soc. (A)*, 1969, 1378.
- (83) Martell, A.E., Linn Belford, R., Calvin, M.,  
*J. Inorg. Nucl. Chem.*, 1958, 5, 170.
- (84) Gillard, R.D., Osborn, J.A., Wilkinson, G., *J. Chem. Soc. (A)*, 1965, 1965,  
1951.
- (85) McKenzie, E.D., Plowman, R.A., *J. Inorg. Nucl. Chem.*,  
1970, 1, 199.

- (86) Snell, F.D., Snell, C. T., "Colorimetric Methods of Analysis,"  
Van Nostrand Inc., Princeton (N. J.), 1954, 3rd. edn., p. 523.
- (87) Martin, B., McWhinnie, W. R., Waing, G. M.,  
J. Inorg. Nucl. Chem., 1961, 23, 207 .
- (88) Dwyer, F. P., Nyholm, R. S., J. Proc. Roy. Soc. N. S. Wales,  
1944, 78, 266.
- (89) Schrauzer, G. N., Holland, R. J., J. Amer. Chem. Soc., 1971,  
93, 1505 .
- (90) Powell, P., J. Chem. Soc. (A), 1969, 2418 .
- (91) Mori, M., Weil, J. A., J. Amer. Chem. Soc., 1967, 89, 3732.
- (92) Garbett, K., Gillard, R. D., J. Chem. Soc. (A), 1968, 1725.
- (93) Sykes, A. G., Mast, R. D., J. Chem. Soc. (A), 1967, 784.
- (94) Hoffman, B. M., Diemente, D. L., Basolo, F.,  
J. Amer. Chem. Soc., 1970, 92, 61.
- (95) Crumbliss, A. L., Basolo, F., Science, 1969, 164, 1168.
- (96) Simplicio, J., Wilkins, R. G., J. Amer. Chem. Soc., 1969, 91, 1325.
- (97) Miller, F., Simplicio, J., Wilkins, R. G.,  
J. Amer. Chem. Soc., 1969, 91, 1962.
- (98) Holtzclaw, H. F., Sheetz, D. P., McCarthy, B. D.,  
Inorg. Synth., 1953, 4, 176.
- (99) Bailar, J. C., Inorg. Synth., 1946, 2, 222.
- (100) Miller, F., Wilkins, R. G., J. Amer. Chem. Soc., 1970, 92, 2687.
- (101) Simplicio, J., Wilkins, R. G., J. Amer. Chem. Soc., 1967, 89, 6092.
- (102) Feltham, R. D., Hayter, R. G., J. Chem. Soc., 1964, 4587.
- (103) Schlessinger, G. G., "Inorganic Laboratory Preparations,"  
Chemical Publishing, New York, 1962.
- (104) Harkins, W. D., Hall, R. E., Roberts, W. A.,  
J. Amer. Chem. Soc., 1916, 38, 2643.
- (105) Ebsworth, E. A. V., Weil, J. A., J. Phys. Chem., 1959, 63, 1890.
- (106) Bernal, I., Ebsworth, E. A. V., Weil, J. A.,  
Proc. Chem. Soc., 1959, 57.
- (107) Selwood, P. W., "Magnetochemistry," Interscience, New York,  
1956, 2nd. edn. .

- (108) Michailidis, M. S., Martin, R. B., *J. Amer. Chem. Soc.*, 1969, 91, 4683.
- (109) Ballhausen, C. J., Gray, H. B., *Inorg. Chem.*, 1962, 1, 111.
- (110) "Inorganic Reaction Mechanisms," 1971, 1, 90. *Period. Rep. Chem. Soc. (London)*, ed. Burgess, J., Hague, D. N., Kemmitt, R. D. W., McAuley, A.
- (111) Alexander, M. D., Spillert, C. A., *Inorg. Chem.* 1970, 9, 2344.
- (112) Kaden, T., Sigel, H., *Helv. Chim. Acta*, 1968, 51, 947.
- (113) Floriani, C., Calderazzo, F., *J. Chem. Soc. (A)*, 1969, 946.
- (114) Floriani, C., Calderazzo, F., *Prog. Coordin. Chem.*, ed., Cais, M., Elsevier, Amsterdam, 1968, p. 196.
- (115) Engelsma, G., Yamamoto, A., Markham, E., Calvin, M., *J. Phys. Chem.* 1962, 66, 2517.
- (116) Manassen, J., *Inorg. Chem.*, 1970, 9, 966.
- (117) Hariharan, M., Urbach, F. L., *Inorg. Chem.*, 1969, 8, 556.
- (118) Hoyt, W. C., Everett, G. W., Jr., *Inorg. Chem.*, 1969, 8, 2013.
- (119) Mathew, M., Carty, A. J., Palenik, G. J., *J. Amer. Chem. Soc.*, 1970, 92, 3197.
- (120) Earnshaw, A., Hewlett, P. C., King, E. A., Larkworthy, L. F., *J. Chem. Soc. (A)*, 1968, 241.
- (121) Gerloch, M., Mabbs, F. E., *J. Chem. Soc. (A)*, 1967, 1598.
- (122) Buckley, A. N., Rumbold, B. D., Wilson, G. V. H., Murray, K. S., *J. Chem. Soc. (A)*, 1970, 2298.
- (123) Hobday, M. D., Smith, T. D., *J. Chem. Soc. (A)*, 1970, 1085.
- (124) Earnshaw, A., Hewlett, P. C., Larkworthy, L. F., *J. Chem. Soc.*, 1965, 4718.
- (125) Baker, E. N., Hall, D., Waters, T. N., *J. Chem. Soc. (A)*, 1970, 400.
- (126) Calligaris, M., Nardin, G., Randaccio, L., Ripamonti, A., *J. Chem. Soc. (A)*, 1970, 1069.
- (127) West, B. O., in "New Pathways in Inorganic Chemistry," ed., Ebsworth, E. A. V., Maddock, A. G., Sharpe, A. G., Cambridge U. P., 1968, p. 303.
- (128) Holm, R. H., Everett, G. W., Jr., Chakravorty, A., *Prog. inorg. Chem.*, 1966., 7, 83.

- (129) Earnshaw, A., King, E. A., Larkworthy, L. F.,  
J. Chem. Soc. (A), 1968, 1048.
- (130) Lewis, J., Mabbs, F. E., Weigold, H., J. Chem. Soc. (A), 1968, 1699.
- (131) Asmussen, R. W., Soling, H., Acta Chem. Scand., 1957, 11, 1331.
- (132) Calligaris, M., Minichelli, D., Nardin, G., Randaccio, L.,  
J. Chem. Soc. (A), 1970, 2411.
- (133) Calligaris, M., Nardin, G., Randaccio, L., Chem. Comm. 1970, 1079.
- (134) Connor, J. A., Ebsworth, E. A. V.,  
Adv. Inorg. Chem. Radiochem., 1964, 6, 279.
- (135) Ueno, K., Martell, A. E., J. Phys. Chem., 1956, 60, 1270.
- (136) James, B. R., Rempel, G. L., J. Chem. Soc. (A), 1969, 78.
- (137) James, B. R., Rempel, G. L., Ng, F. T. T.,  
J. Chem. Soc. (A), 1969, 2454.
- (138) James, B. R., Rempel, G. L., Canad. J. Chem., 1966, 44, 233.
- (139) James, B. R., Rempel, G. L., Canad. J. Chem., 1968, 46, 571.
- (140) Basolo, F., Morris, M. L., Pearson, R. G.,  
Discuss. Faraday Soc., 1960, 29, 80.
- (141) Josephsen, J., Schaffer, C. E., Chem. Comm. 1970, 61.
- (142) Panunzi, A., Basolo, F., Inorg. Chim. Acta, 1967, 1, 223.
- (143) Burgess, J., Ann. Reports Chem. Soc. (A), 1967, 64, 365.
- (144) Rund, J. V., Inorg. Chem., 1968, 7, 24.
- (145) Rund, J. V., Basolo, F., Pearson, R. G., Inorg. Chem. 1964, 3, 658.
- (146) Baker, D. J., Gillard, R. D., Chem. Comm., 1967, 520.
- (147) Gillard, R. D., Heaton, B. T., Vaughan, D. H.,  
J. Chem. Soc. (A), 1971, 1840.
- (148) James, B. R., Ng, F. T. T., Chem. Comm. 1979, 908.
- (149) Hughes, W. B., Chem. Comm. 1969, 1126.
- (150) Chatt, J., Butter, S. A., Chem. Comm. 1967, 501.
- (151) Baird, M. C., Mague, J. T., Osborn, J. A., Wilkinson, G.,  
J. Chem. Soc. (A), 1967, 8, 1347.
- (152) Porri, L., Lionetti, A., Allegra, G., Immirzi, A.,  
Chem. Comm. 1965, 336.
- (153) Uguagliati, P., Deganello, G., Busetto, L., Belluco, U.,  
Inorg. Chem. 1969, 8, 1625.

- (154) Ugo, R., Bonati, F., Fiore, M., *Inorg. Chim. Acta*, 1968, 2, 463.
- (155) Douek, I. C., Wilkinson, G., *J. Chem. Soc. (A)*, 1969, 2604.
- (156) Collman, J. P., Hoffman, N. W., Harris, D. E.,  
*J. Amer. Chem. Soc.*, 1969, 91, 5659.
- (157) Osborn, J. A., Jardine, F. H., Young, J. F., Wilkinson, G.,  
*J. Chem. Soc. (A)*, 1966, 1711.
- (158) Shapley, J. R., Schrock, R. R., Osborn, J. A.,  
*J. Amer. Chem. Soc.*, 1969, 91, 2816.
- (159) Gillard, R. D., Wilkinson, G., *J. Chem. Soc.*, 1963, 3594.
- (160) Dewhurst, K. C., *Inorg. Chem.* 1966, 5, 319.
- (161) Syamal, A., Johnson, R. C., *Inorg. Chem.* 1970, 9, 265.
- (162) Battino, R., Clever, L. H., *Chem. Rev.*, 1966, 66, 395.
- (163) Griffith, W. P., Wilkinson, G., *J. Chem. Soc.*, 1959, 2757.
- (164) Green, M. L. H., Jones, D. J., *Adv. Inorg. Chem. Radiochem.*,  
1965, 7, 115.
- (165) McWhinnie, W. R., Miller, J. D.,  
*Adv. Inorg. Chem. Radiochem.*, 1969, 12, 135.
- (166) Brandt, W. W., Dwyer, F. P., Gyarfas, E. C.,  
*Chem. Rev.* 1954, 54, 959.
- (167) James, B. R., Rempel, G. L., *Discuss. Faraday Soc.*, 1968, 46, 48.
- (168) Shchepinov, S. A., Sal'nikova, E. N., Khidekel, M. L.,  
*Izv. Akad. Nauk S. S. S. R.*, 1967, 2128.
- (169) Schrauzer, G. N., Sibert, J. W., Windgassen, R. J.,  
*J. Amer. Chem. Soc.*, 1968, 90, 6681.
- (170) McBride, B. C., Wood, J. M., Sibert, J. W., Schrauzer, G. N.,  
*J. Amer. Chem. Soc.*, 1968, 90, 5276.
- (171) Collman, J. P., Holtzclaw, H. F., Jr.,  
*J. Amer. Chem. Soc.*, 1958, 80, 2054.
- (172) Gillard, R. D., Wilkinson, G., *J. Chem. Soc.*, 1963, 6041.
- (173) Green, M., Mawby, R. J., Swinden, G., *Chem. Comm.* 1967, 127.
- (174) Gillard, R. D., Wilkinson, G., *J. Chem. Soc.*, 1965, 4107.
- (175) Chalk, A. J., Halpern, J., *J. Amer. Chem. Soc.*, 1959, 81, 5846.
- (176) Scanlan, J., Dunn, J. R., *J. Sci. Instr.*, 1961, 38, 28.

- (177) Bell, C. L., *J. Sci. Instr.*, 1961, 38, 27.
- (178) Bolland, J. L., *Proc. Roy. Soc., A*, 1946, 186, 218.
- (179) Hovey, R. J., O'Connell, J. J., Martell, A. E.,  
*J. Amer. Chem. Soc.*, 1959, 81, 3189.
- (180) Nakao, Y., Nonagase, N., Nakahara, A.,  
*Bull. Chem. Soc. Japan*, 1969, 42, 452.
- (181) Catsikis, B. D., Good, M. L., *Inorg. Chem.*, 1969, 8, 1095.
- (182) Gill, N. S., Nuttall, R. H., Scaife, D. E., Sharp, D. W. A.,  
*J. Inorg. Nucl. Chem.*, 1961, 18, 79.